Theses and Dissertations

2017

Development of Brain Functional Connectivity and Its Relation To Infant Sustained Attention In The First Year Of Life

Wanze Xie
University of South Carolina

Follow this and additional works at: https://scholarcommons.sc.edu/etd

Part of the Experimental Analysis of Behavior Commons

DEVELOPMENT OF BRAIN FUNCTIONAL CONNECTIVITY AND ITS RELATION TO
INFANT SUSTAINED ATTENTION IN THE FIRST YEAR OF LIFE

by

Wanze Xie

Bachelor of Science
East Tennessee State University, 2012

_____

Submitted in Partial Fulfillment of the Requirements

For the Degree of Doctor of Philosophy in

Experimental Psychology

College of Arts and Sciences

University of South Carolina

2017

Accepted by:

John E. Richards, Major Professor

Jessica Green, Committee Member

Jeff Schatz, Committee Member

Troy Herter, Committee Member

Cheryl L. Addy, Vice Provost and Dean of the Graduate School

DEDICATION

This dissertation is dedicated to my family, Xiuping Lyu, Kecheng Xu, and Penny Song for their support in the past five years. The support from my parents, especially the support and soul massage from my mother, Xiuping Lyu, prevents me from quitting the program. The "push" from my fiancé Penny ensures that I finish my PhD in five years not eight years. This dissertation is also dedicated to my mentor, John E. Richards, for all the efforts he has made to keep me on the right track. His passion for research sets a standard for me. I am sure I would not have as many accomplishments as I have now as a graduate student without his negative comments and his emails after midnight. Finally, I would like to dedicate this dissertation to myself for my hard work and my optimism after those insomnia nights.

ABSTRACT

This dissertation project studies the development of infant sustained attention and its relation to brain functional connectivity from 6 to 12 months of age. Chapter 1 is a general introduction of the dissertation project. Chapter 2 is a review of the existing literature on the development of infant sustained attention. This chapter includes theories on infant sustained attention and findings from studies using behavioral and psychophysiological measurements. Chapter 3 is a review of the recent advances made in the study of the development of functional connectivity in brain networks. This chapter covers some empirical evidence for the development of functional networks using EEG and fMRI techniques. In Chapter 4 I introduce an experiment that examined the potential relation between infant sustained attention and distinct patterns of brain functional connectivity suggested by the literature reviewed in Chapter 2 and 3. The sample of the experiment consisted of 59 participants aged from 6 to 12 months. Infant sustained attention and inattention were defined by measuring infant heart rate changes. Functional connectivity was estimated with high-density EEG recordings from the electrodes on the scalp and with the reconstructed cortical source activities in brain regions. Graph theory measures were applied to give a broader view of the architecture of brain functional networks. It was found that infant sustained attention was accompanied by attenuated functional connectivity in the dorsal attention and default mode networks in the alpha band. Graph theory analyses showed that there was an increase in path length and a decrease in clustering coefficient during infant sustained attention. The functional

connectivity in brain networks and the graph theory measures of path length and clustering coefficient were found to increase with age. The small-worldness was found for infants at 6 and 8 months in the alpha and beta bands. These findings lend support to the hypothesis of the relation between the distinct patterns of brain functional connectivity and infant sustained attention. The current findings also provide convergent evidence for the rapid development of functional connectivity in brain networks during infancy.

TABLE OF CONTENTS

LIST OF TABLES

LIST OF FIGURES

CHAPTER 1

GENERAL INTRODUCTION

Infant sustained attention is a type of endogenous attention that represents the arousal state of infants (Colombo, 2001; Richards, 1989a, 1989b). Both behavioral and psychophysiological methods have been employed in the study of infant sustained attention (Mallin & Richards, 2012; Xie, Mallin, & Richards, 2017). Infant sustained attention emerges at around 2 months of age and develops substantially during the first year of life (Colombo, 2001; Richards, 2008). There is empirical evidence showing that infant sustained attention is important for infants' information processing and attention allocation (Xie & Richards, 2016a, b), which in turn affects the development of other high-level cognitive processes, such as memory encoding and learning (Richards, 2009, 2010). A recent study by Xie, Mallin, and Richards (2017) sheds light on the neural mechanisms underlying infant sustained attention by showing its relation to electroencephalography (EEG) oscillatory activity in the theta and alpha rhythms. The existing literature suggests that the effects of infant sustained attention may result from or be associated with distinct pattern(s) of communications inside the brain.

The application of network analysis provides an illuminating perspective on the dynamic interregional communications or connectivity inside the brain. A functional brain network is defined as the correlated dynamic physiological activities in various brain regions (Chu-Shore, Kramer, Bianchi, Caviness, & Cash, 2011; Goldenburg & Galván, 2015). Recent research has focused on the development of brain functional

connectivity over childhood and adolescence (Power et al., 2010). Studies with EEG measures have shown that the integration and segregation of information processing in brain networks develop dramatically from childhood to adolescence (Bathelt et al., 2013; Boersma et al., 2011). However, the empirical evidence for the development of functional networks during infancy is primarily obtained from fMRI research with sleeping or sedated infants. It has been found that brain networks with functional significance, such as the default mode network (DMN), start to emerge during the first two years of life (Fair et al., 2007; Gao et al., 2009, 2011).

The progress made in the field of network analysis expanded the means to examine the relationship between infant sustained attention and brain functional connectivity. The fundamental goal of the dissertation project was to study whether infant sustained attention is associated with distinct brain functional connectivity and how this relation might change in the first year of life. A second goal of the dissertation was to examine the development of brain functional connectivity in brain networks from 6 to 12 months of age with EEG recordings. This age range was chosen because it has been shown as a key period for the development of infant sustained attention and brain functional networks (Richards, 2008, 2009; Gao et al., 2009). High-density EEG recordings, cortical source analysis, functional connectivity analysis, and graph theory analysis were applied to achieve these goals

CHAPTER 2

INFANT SUSTAINED ATTENTION

2.1 Richards' Model on Infant Sustained Attention

Infant sustained attention has been predominantly studied by Richards and colleagues using the measure of heart rate (HR) derived from electrocardiogram (ECG) recordings. The HR model of infant sustained attention is shown in Figure 2.1. Infant sustained attention is the third of the four attention phases defined by HR changes during infants' looking (Reynolds & Richards, 2008). The two attention phases preceding sustained attention are automatic interrupt and stimulus orienting. Infants are involved in detecting transient changes in the environmental stimulation during automatic interrupt. Stimulus orienting is the second phase that lasts for 3 – 5s. Infants decide whether to allocate additional mental sources to stimulus presentation based on its intrinsic properties (e.g., novelty and variety) during stimulus orienting. Infant HR during the phases of automatic interrupt and stimulus orienting starts to fluctuate, but is not significantly distinguished from the prestimulus baseline. Automatic interrupt and stimulus orienting are both involved in the orienting and preprocessing of a stimulus. Because of this, these two phases have been combined and named as "pre-attention" or stimulus orienting in some recent studies (e.g., Guy, Zieber, & Richards, 2016; Xie & Richards, 2016a, b; Xie, Mallin, & Richards, 2017).

Sustained attention is the distinct phase that follows stimulus orienting. Infant HR decelerates significantly and remains at a lower level than the prestimulus baseline during
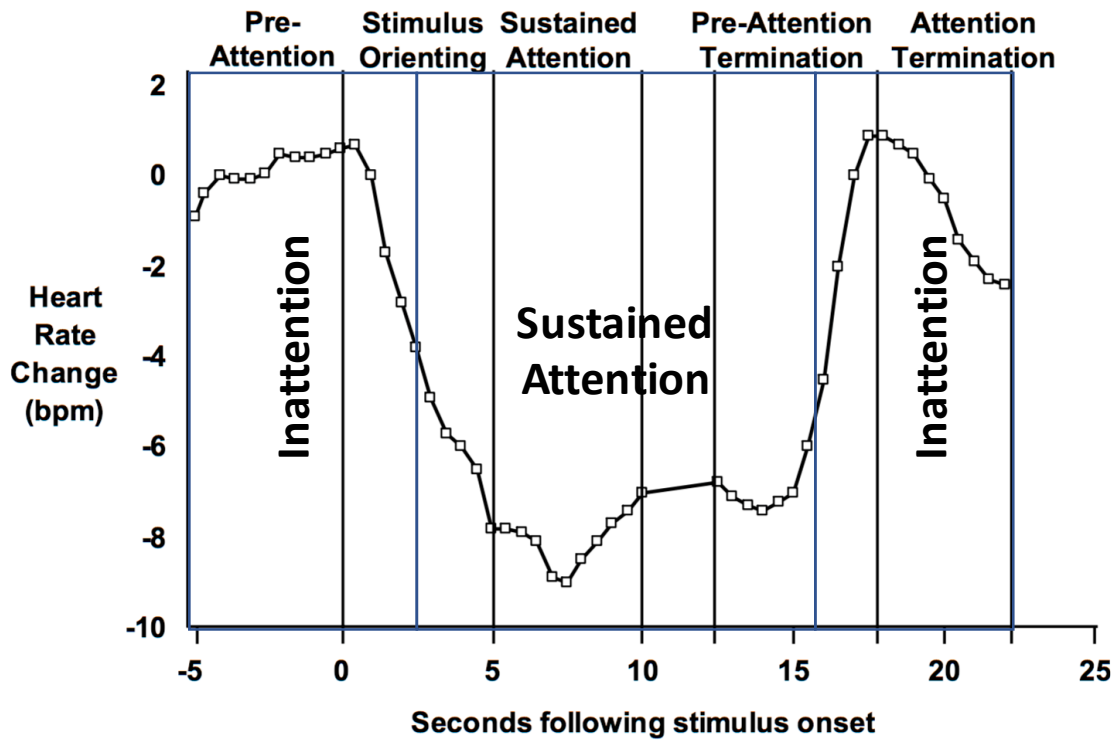
Figure 2.1 Richards' heart rate model of infant sustained attention.

sustained attention. The criterion for a significant HR deceleration has been typically set as the inter-beat intervals (IBIs) of five successive beats being longer than the median IBI of the five preceding beats (Reynolds & Richards, 2008). The IBI has an inverse association with HR. The lengthening of IBI corresponds to the deceleration of HR, and the shortening of IBI corresponds to the acceleration of HR. Sustained attention begins at 4 - 5 seconds following the stimulus onset and lasts from 2 - 3 seconds to about 20 seconds. It has been argued that the deceleration of HR during sustained attention results from the interactions between the frontal and the brainstem portions of the infant alerting network (Richards & Casey, 1991; Richards, 2008). The cortico-subcortical communication within the alerting network leads to various autonomic effects including the cardiac and respiratory changes (Reynolds & Richards, 2008).

The attention phase that follows sustained attention is attention termination. Attention termination is accompanied by a significant HR acceleration. The criterion for a significant HR acceleration has been set as the IBIs of five successive beats being shorter than the median IBI of the five proceeding beats (Reynolds & Richards, 2008). Attention termination lasts for about 5 -6 seconds when HR returns to the prestimulus level. Attention termination also has been termed as attention disengagement because infants are more likely to shift their visual fixation elsewhere during this phase (Colombo, 2002). Attention termination, together with automatic disrupt and stimulus orienting, are typically categorized as *inattention* in empirical research (e.g., Guy et al., 2016; Reynolds & Richards, 2005; Richards, 2003).

2.2 The Development of HR Defined Infant Sustained Attention

Infant sustained attention as defined by HR develops substantially in the first year of life. Infant HR deceleration has not been found in infants younger than 6 weeks of age (Berg & Berg, 1979; Jackson, Kantowit, & Graham, 1971). The absence of sustained attention before 6 weeks suggests that the cortico-subcortical communication inside the alerting network may not be established in the first few weeks of life. Evidence of infant sustained attention has been obtained in infants as young as 8 weeks (Richards, 1989b). Richards (1989b) presented 8-week-old infants with varying and complex patterns of stimuli on a TV monitor. Infants' HR was measured and analyzed when they were looking at the stimulus presentation. Richards found that 8-week-old infants started to show different patterns of HR changes during looking, such as the HR deceleration (sustained attention) and HR acceleration (attention termination). A similar paradigm has been used in a following longitudinal study with infants tested at 14, 20, and 26 weeks (Richards, 1989a). The duration of sustained attention and the amount of HR variability were found to increase dramatically from 14 to 26 weeks (i.e., 3 to 6 months) of age. The finding from Richards (1989a) suggests that there are substantial changes in the amount, depth, and frequency of sustained attention from 3 to 6 months. Infant sustained attention continues to develop in the second half of the first year (Lansink, Mintz, Richards, 2000). Its development lasts even into the second and third years of life (Richards & Cronise, 2000; Ruff & Lawson, 1990) but with a much slower pace.

2.3 Effects of Infant Sustained Attention on Attention Allocation and Orienting

Infants show distinct patterns of visual fixation during sustained attention. Studies have consistently found that infant sustained attention is associated with

6

maintaining fixation on a focal stimulus in the presence of a peripheral distracting

stimulus (Casey & Richards, 1988; Pérez-Edgar et al., 2010; Richards, 1989a, 1989b;

Richards & Hunter, 1997; Richards & Turner, 2001). In these studies, a central stimulus

was presented to attract infants' fixation. A secondary stimulus was presented on a side

monitor within the infants' field of vision after they looked toward the central stimulus.

This secondary stimulus was presented either during sustained attention or inattention.

The infants were found to be less likely to be distracted by the secondary stimulus during

sustained attention than during inattention. The improvement of engagement in the

stimulus presentation has been argued as the result of the enhancement of general arousal

and attention allocation during sustained attention (Richards, 2008, 2009). Researchers

also have studied infant sustained attention during toy play (Lansink & Richards, 1997;

Oakes, Madole, & Cohen, 1991; Oakes & Tellinghuisen, 1994; Ruff, 1986). The period

when infants showed visual fixation on an object/toy has been named as *focused attention*

and regarded as the behavioral marker of sustained attention (Ruff, 1986). Oakes and her

colleagues found that focused attention during object manipulation was normally

combined with turning the object or touching it with fingers with an intent facial

expression (Oakes et al., 1991; Oakes & Tellinghuisen, 1994). This distinct pattern of

visual fixation that infants showed during stimulus presentation and toy play indicates

that visual fixation is an important behavioral index of infant sustained attention.

Sustained attention has been found to benefit the saccadic localization of a

peripheral stimulus. The localization of a saccade to a peripheral stimulus is a process

involving attention orienting and saccade planning. A few studies by Richards and

colleagues have examined the effect of infant sustained attention on the localization of a

peripheral stimulus in infants aged between 5 weeks and 6 months (Hicks & Richards, 1998; Hunter & Richards, 2003; Mallin & Richards, 2012; Richards & Hunter, 1997). For example, Mallin and Richards (2012) tested whether the latency of the localization of a peripheral stimulus would be facilitated by sustained attention in 3-, 4.5, and 6-month-old infants. The authors employed a continuous presentation paradigm in which the experimental trials (e.g., images, videos) were presented continuously without an interstimulus gap (Pempek et al., 2010; Reynolds, Courage, & Richards, 2010). The continuous presentation paradigm was expected to elicit and extend sustained attention. Mallin and Richards (2012) presented the infants with a moving character at the center of the screen, and a peripheral moving character was presented once the infants' fixation was judged to be on the center stimulus. The localization of the moving character in the peripheral location was faster during sustained attention than inattention. This finding indicates that sustained attention enhances infants' ability to allocate their spatial attention and facilitates the early visual processing involved in the detection of a peripheral stimulus.

Infants' behavioral performance in a spatial cueing paradigm improves during sustained attention. Richards (2004) examined whether infants' reaction time (RT) to the target in a special cueing paradigm would be faster during sustained attention than during inattention. Infants from 3 to 6 months were first presented with a central stimulus to attract their attention. A peripheral cue was presented either simultaneously with the central stimulus, after a 2s delay, or until a significant deceleration in HR occurred. Results from the "2s delay" trials replicated previous findings that the validity effect emerged from 3 months and the inhibition of return (IOR) effect did not show until 4.5 to

6 months (Richards, 2000, 2001). The simultaneous presentation of the central stimulus and peripheral cue resulted in no difference in RT among the valid, invalid, and neutral trials. When the cue was presented contingent on the occurrence of a HR deceleration, the IOR effect was found in 3-month-olds. Richards (2004) argued that infants' behavioral responses associated with covert orienting were improved while attention engagement was well underway. The effect of infant sustained attention on the behaviors associated with covert orienting indicates that the neural mechanisms in the orienting network underlying these behavioral signatures may be energized during sustained attention.

Distinct patterns of smooth pursuit have been shown in infants during sustained attention. Smooth pursuit refers to the continuous and smooth eye movement that occurs while tracking or following a moving object. Richards and Holley (1999) measured the effect of sustained attention on the development of smooth pursuit in infants from 2 to 6 months of age. The infants were presented with a small rectangle moving in a sinusoidal pattern at various speeds while their eye movements were recorded. The authors found an overall increase in infants' smooth pursuit performance and their compensatory saccade amplitude at faster tracking speeds in all the ages. A more intriguing finding was that infants showed different patterns of stimulus tracking between the states of sustained attention and inattention when the stimulus speed increased to the highest velocity. The infants showed a tendency to shift from smooth pursuit to saccadic tracking during sustained attention but not during inattention.

2.4 Effects of Infant Sustained Attention on Information Processing and Memory

Sustained attention plays an important role in gathering and processing information. The increased brain arousal during infant sustained attention enhances the

efficiency of information processing (Colombo, 2001; Richards, 2008; Richards & Casey, 1992). The improved attention engagement, allocation and orienting during sustained attention also benefit the selection and processing of the presented stimuli (Guy et al., 2016; Xie & Richards, 2016a, b). Therefore, the majority of infants' information processing takes place during sustained attention (Colombo, 2001).

The facilitation effect of infant sustained attention on information processing leads to the close relation between sustained attention and recognition memory. Infants demonstrated better memory for the events they were exposed to during sustained attention compared to the events they were exposed to during inattention (Frick & Richards, 2001; Reynolds & Richards, 2005; Richards, 1997). Richards (1997) tested the effect of sustained attention on infant recognition memory in 3- to 6-month-olds with two experiments. In the first experiment, infants were exposed to stimulus presentations ranging in duration from 2.5 to 20s in the familiarization procedure under indeterminate states of attention. It was found that the stimuli presented for 2.5 to 5s resulted in longer looking period to them (i.e., familiarity preference) in the following paired-comparison procedure, in which a familiar and a novel stimulus were presented side by side. The stimuli presented for 10 to 20s resulted in longer looking period to the novel stimulus (i.e., novelty preference) in the following paired-comparison procedure. In the second experiment, the same participants were presented with visual stimuli for 2.5 to 5s either during sustained attention or during inattention. It was found that the stimuli presented for around 5s during sustained attention resulted in the novelty preference in the following paired-comparison procedure, which was similar to the effect shown after a 20s familiarization in the first experiment. The duration of stimulus exposure in sustained

attention was also positively correlated with the possibility of the novelty preference in the paired-comparison procedure. The findings from Richards (1997) suggest that infant sustained attention and recognition memory are closely related and most of the information processing occurs during sustained attention.

Infant sustained attention not only impacts the familiarization of stimulus presentation but also influences the recognition process. Infants were observed to show increased recognition performance if the recognition process occurred in sustained attention (Richards & Casey, 1992). The paradigm used by Richards and Casey (1992) resembled the one used by Richards (1997); however, the attention states were analyzed during the recognition process instead of the familiarization process. Richards and Casey found that 3- to 6- month-old infants spent 12 seconds on average in sustained attention in the paired-comparison procedure (i.e., recognition process). The infants spent about 7.5 s looking at the novel stimuli and about 4.5 s looking at the familiar stimuli in the paired-comparison procedure during sustained attention. Alternatively, the infants spent equal amount of time between looking at the novel and the familiar stimuli during inattention. The exhibition of recognition memory and novelty performance in the paired-comparison procedure indicates infants' attempt to acquire new information from the previously unseen stimulus during sustained attention.

2.5 The Model of the Development of Infant Attention Networks

The effect of infant sustained attention on the orienting network and high-level cognitive functions (e.g., information processing and memory encoding) has been summarized by a previous study (Xie, 2016, Comprehensive exam paper). Figure 2.2 illustrates the model of the development of infant attention networks (Xie, 2016). This

The Alerting Network

    Alert state

    Sustained attention

The Orienting Network

    Smooth pursuit

    Disengagement

    Anticipatory saccade

    Covert orienting

    Inhibition of return

Some High-order Cognitive Functions Discussed in this Article

    Memory encoding

    Visual short-term memory

    Perception of eye gaze

    Perception of hand gestures

    Perceptual narrowing

0 1 2 3 4 5 6 7 8 9 10 11 12

Postnatal Age (Month)

Figure 2.2 The model of the development of attention networks during infancy.

model includes the aforementioned impact of infant sustained attention, a major component of the infant alerting network, on infants' spatial orienting and information processing. The unfilled vertical arrows/lines in the model indicate the relations between the networks and the cognitive functions. The back of an arrow means the source (or mechanism) of an effect. The front of an arrow means the site (or consequence) of an effect. The front of an arrow means the site (or consequence) of an effect. The filled horizontal arrows/lines demonstrate the developmental courses of the various components. The back of an arrow indicates the proximate emergence of a component supported by empirical evidence. The gradual change of the darkness indicates the development (i.e., relative degree of maturity) of the component. The end of the horizontal arrows does not refer to the cease of the development of a component by the corresponding age. Instead, it means that the function of that component is well established and can be consistently measured by then.

2.6 The ERP Correlates of Infant Sustained Attention

There has been a growing interest in the usage of scalp-recorded event-related potentials (ERPs) as a measure of infant visual attention. The ERP reflects the EEG activity time-locked to the onset of a stimulus. The usage of EEG and ERPs provides non-invasive methods to examine infants and children's cortical activity and neural responses to different types of stimuli (de Haan, 2007).

The correspondence between the HR-defined sustained attention and ERP components in infants have recently been established. The negative central (Nc) component is the most commonly used ERP measure for infant sustained attention. The Nc comprises a negative deflection that is most prominent in the fronto-central electrodes

(Goldman, Shapiro, & Nelson, 2004). The amplitude of the Nc peaks at about 400 –

800ms after stimulus onset (Courchesne, Ganz, & Norcia, 1981) and increases with age

over the first year of life (Richards, 2003; Webb, Long, & Nelson, 2005). The

association of infant sustained attention with the Nc component was first addressed in

Richards (2003). The participants were tested at 4.5, 6, or 7.5 months of age and

presented with Sesame Street clips and static pictures. The Sesame Street videos were

used to elicit sustained attention and the brief stimuli were presented in a modified

oddball procedure (Nelson & Collins, 1991). The modified oddball procedure includes

frequent familiar (60%), infrequent familiar (20%), and infrequent novel (20%) stimuli

for presentation. It was found that the amplitude of the Nc did not differ with the stimulus

type; however, it was significantly larger during infant sustained attention than

inattention (Richards, 2003). The Nc amplitude also was found to increase with age. The

author argued that the Nc component might reflect the attention-getting properties of the

stimulus and the activation of a general arousal system (i.e., the alerting system) in the

brain.

The link between the Nc component and infant sustained attention and the

development of the Nc amplitude have been replicated by recent studies (e.g., Guy et al.,

2016; Reynolds et al., 2010; Reynolds & Richards, 2005; Xie & Richards, 2016a). For

example, Xie and Richards (2016a) found that using a presentation paradigm that

facilitated infant sustained attention and engagement elicited a greater Nc response to the

stimulus presentation. The authors examined the effects of the interstimulus interval (ISI)

in the stimulus presentation on infant attention. They compared an ISI (1,500 – 2,000ms)

that was typically used in infant EEG/ERP studies (e.g., Richards, 2003) with two shorter

durations (400 – 600ms, 600 – 1000ms). Using shorter ISIs was hypothesized to facilitate infant sustained attention because it would increase the presentation complexity and the amount of information presented in a certain period (Courage, Reynolds, & Richards, 2006). Xie and Richards (2016a) found that using shorter ISIs for stimulus presentation resulted in more visually fixated trials and reduced frequency of fixation disengagement per experimental block. Using shorter ISIs also elicited greater HR deceleration during sustained attention. The facilitation effects of using shorter ISIs on infant sustained attention enlarged infants' Nc amplitude in response to the stimulus presentation regardless of the stimulus type (Xie & Richards, 2016a).

The improved attention allocation and brain general arousal during sustained attention is thought to cause the enlarged cortical activation following a stimulus presentation (Reynolds & Romano, 2016; Richards, 2008). This argument has been supported by recent findings of the effects of infant sustained attention on ERPs components subserving different brain functional networks. Guy et al. (2016) examined infants' ERP responses to faces and toys during various attentional phases. Two face-sensitive infant ERPs, the N290 and the P400, were measured as neural correlates of infant face perception. Both the N290 and P400 responses were found to be larger during sustained attention than inattention. The N290 amplitude was greater to faces than toys during attention, but this effect was not shown during inattention. Infant sustained attention also has been found to enhance the P1 and N1 components that represent the early visual processing of a visual stimulus. Xie and Richards (2016b) studied 3- and 4.5-month-old infants' ERPs and cortical source activities in response to the visual targets in a spatial cueing paradigm. The amplitudes of infants' P1 and N1 components and their

15

corresponding cortical source activities were found to be enlarged during sustained attention than inattention in regardless of the cue-target validity.

2.7 Infant Sustained Attention and EEG Oscillations

The changes in infant behaviors and ERP components provide evidence for the consequences of infant sustained attention effects. Previous studies have linked the EEG oscillations in frequency bands (e.g., theta and alpha) to the sustained attention performance in infants (Xie et al., 2017) and adults (Sauseng et al., 2007). Therefore, the measuring EEG oscillatory properties in frequency rhythms should provide a way to understand the neural mechanisms underlying the effects of infant sustained attention. Two frequently studied infant EEG rhythms, theta and alpha rhythms, undergo substantial development during infancy. The frequency ranges used to define infant theta and alpha rhythms are about 2 to 6 Hz and 6 to 9 Hz respectively. The peak frequencies of infant theta and alpha rhythms show a developmental change during the first two years of life (Marshall et al., 2002). Marshall and colleagues found that infants did not show a clear pattern of alpha activity before 10 to 12 months of age, whereas infant theta activity emerged at younger ages. Infant alpha rhythm is more prominent over central and parietal than frontal electrodes; infant theta rhythm is more prominent over frontal and occipital than the central electrodes (Marshall et al., 2002; Orekhova, Stroganova, & Posikera, 2001).

A study by Xie and colleagues (2017) examined the relation between infant sustained attention and infant EEG oscillatory activities with infants at 6, 8, 10, and 12 months of age. The power spectral density (PSD) of the infant theta (2 – 6 Hz), alpha (6 – 9 Hz), and beta (9 – 14 Hz) rhythms was estimated and compared between sustained

16

attention and pre-attention and attention termination. An increase of the theta PSD was found over fontal pole and parietal electrodes during infant sustained attention for the 10- and 12-month-olds. An attenuation of the alpha PSD was found over frontal, central and parietal electrodes during sustained attention. This alpha effect started to emerge at 10 months and became well established by 12 months. No difference for the beta rhythm was found between different attention phases. Cortical source analysis was conducted with realistic infant MRI models to examine the potential generators of the effects found on the sensor level. The increased power in the theta band during sustained attention was localized to the orbital frontal, temporal pole, and ventral temporal areas. The alpha attenuation effect during sustained attention was localized to the brain regions composing the DMN including the medial prefrontal cortex, posterior cingulate cortex, precuneus, inferior parietal gyrus. The alpha effect also was localized to the pre- and post-central gyri.

The study by Xie and colleagues established a connection between infant sustained attention and EEG oscillatory activities. Their findings were compatible with previous infant and adult literature. Researchers have found an increase in the theta PSD that was referred to "theta synchronization" during infant anticipatory attention (Orekhova, Stroganova, & Posikera, 1999). They also have found an attenuation of the alpha PSD that was referred to as "alpha desynchronization" during infant attention to external stimulus (Orekhova, et al., 2001). These theta synchronization and alpha desynchronization effects are robust electrical indices of brain arousal and attention allocation in adulthood (Ergenoglu et al., 2004; Sauseng et al., 2005, 2007). Xie et al. (2017) sheds light on the developmental origin of this relation between EEG rhythmic

activities and attention allocation and brain arousal. The changes in the effects of attention on the theta and alpha activities with age suggest the intertwined development of infant sustained attention and EEG oscillations during the first year of life.

2.8 Suggestion for Future Research on Infant Sustained Attention

There may be distinct pattern(s) of brain functional connectivity in certain EEG frequency bands during infant sustained attention. Studies discussed in the previous sections have shown that infant sustained attention is accompanied by improved information processing efficiency, attention allocation and orienting capacity, and enhanced brain arousal. These effects suggest the communications or functional connections between brain regions be distinguished during infant sustained attention. The potential relation between sustained attention and functional connectivity in infants should be studied by future research. This would advance our understanding of the neural mechanisms in brain networks underlying infant sustained attention. Recent advances in the field of brain network analysis expand the means to explore the pattern of the communication and connectivity between brain regions or channels on the scalp. Chapter 3 gives an overview of the recently developed techniques for brain network analysis and the application of these techniques in the study of brain functional connectivity with children and adolescents.

CHAPTER 3

DEVELOPMENT OF BRAIN FUNCTIONAL NETWORKS

3.1 Introduction to Brain Functional Networks

The application of fMRI and EEG methods provides ways to investigate the

dynamic interregional communications inside the brain and their development over

childhood. Resting-state functional magnetic resonance imaging (fMRI) is a frequently

used method to study the development of functional brain networks (Goldenburg &

Galván, 2015). The resting-state means the participant is not engaged in any specific

experimental task (i.e., in a resting condition). High-density EEG recordings offer a

comparatively easy-to-use alternative to measure brain functional networks (Boersma et

al., 2011, 2013; Miskovic et al., 2015). The EEG recordings are more tolerant to young

children's movements compared to fMRI scanning, and thus using EEG makes it possible

to investigate infant brain networks while they are awake. Physiological signals recorded

from both methods have been recently analyzed with graph theory to model the topology

of functional networks (Vertes & Bullmore, 2015). Studies using various methods have

consistently shown that there is a shift from random organizations to more integrated

brain networks over the brain development from infancy to adolescence (Power et al.,

2010).

Construction of functional networks requires recording physiological signals from

multiple spatial locations that can be either brain regions of interest (ROIs) or channels of

EEG, functional near-infrared spectroscopy (fNRIS), or magnetoencephalography

(MEG). Correlated physiological activity inside a functional network is typically referred to as functional connectivity, which is estimated by analyzing the correlation between dynamic physiological signals recorded at multiple locations.

There are three widely used methods to define functional networks, component analyses, seed-based correlation maps, and graph theory. Component analyses, such as the independent and principle component analyses (ICA and PCA), highlight the brain networks (i.e., components) in the psychophysiological signals that share variance in the time series (Damoiseaux et al., 2006). Seed-based correlation maps are constituted of spatial locations (e.g., ROIs and voxels) where physiological signals (e.g., BOLD, EEG source activity) are correlated with the signals in a seed ROI or voxel (Lowe et al., 1998). A broader view of brain functional networks may not be obtained with the component analyses or a seed map (Power et al., 2010). Graph theory provides a common framework to model the dynamic processes in brain networks (Rubinov & Sporns, 2010). It has recently been used to characterize the overall architecture of brain networks (Bullmore & Sporns, 2009; Power et al., 2010; Vertes & Bullmore, 2015). These three types of methods have been used in the studies that are discussed in the following sections.

This chapter reviews recent studies that have advanced our understanding of the development of brain functional networks. The next section (3.2) introduces the methods that have been used to estimate the functional connectivity with EEG recordings. The following section (3.3) gives a brief overview of graph theory. The last section (3.4) reviews the study of the development of brain functional networks using graph theory measures based on EEG recordings. It should be noted that a large body of evidence for the development of brain functional networks originates from the fMRI research with

20

children. However, fMRI was not used in this dissertation because it is more practical to use EEG than fMRI to study infants' brain activation when they are awake. Therefore, the current article briefly mentions some findings from the fMRI research but emphasizes studies with EEG measures. A detailed review of fMRI research on the development of brain networks can be found elsewhere (e.g., Bullmore & Sporns, 2009; Power et al., 2010; Vertes & Bullmore, 2015; Xie, Comprehensive Exam Paper).

3.2 Measures of functional connectivity

A few methods have been developed and employed for the estimation of the functional connectivity with EEG and MEG signals. The current section introduces four methods that have been frequently employed in the literature. They are the coherence, imaginary part of the coherency (IC), weighted phase lag index (wPLI), and the correlation between cortical reconstructed source activities. The coherence, IC, and the wPLI are mathematical methods used to examine the similarity and synchrony between the oscillatory activities in two or more EEG channels or brain regions.

$$C_{xy}(f) = \frac{|G_{xy}(f)|}{\sqrt{G_{xx}(f) * G_{xx}(f)}}$$

The coherence (C_{xy}) between two signals x(t) and y(t) is defined by the equation above. The "t" refers to the time series. The "f" refers to the Fourier transformation of the signal in a certain time window (1s in the current project) obtained from the fast Fourier transform (FFT) analysis. The "Gxy" stands for the cross-spectral density (CSD) of the two signals "x" and "y" (e.g., two channels or brain regions) obtained from the frequency analysis. The "Gxx" and "Gyy" represent the power-spectral density (PSD) for the signal "x" and "y". It can be seen from the equation that the coherence is a measure of the

linear relationship between two signals. The coherence is an absolute value ranging between 0 and 1.

Coherence has been widely accepted as a method to estimate functional connectivity. The usage of this method to estimate the brain functional connections has been extended to research with pediatric populations (e.g., Cuevas, Swingler, Bell, Marcovitch, & Calkins, 2012; Thatcher, Walker, & Giudice, 1987). However, there is an important issue in the interpretation of the coherence found between EEG electrodes due to the volume conduction or field spread problem (Nolte et al., 2004; Nunez et al., 1997). The volume conduction represents the currents flowing in different types of brain tissues surrounding the neural generators. The distance between the generators and the EEG electrodes and the tissues that the currents need to flow in would lead to the mix of the currents generated by multiple sources. There is also spatial blurring effect of the skull on the distribution of the EEG signal on the scalp. Thus, a signal underlying neuronal source might be recorded at multiple EEG sensors, especially when they are close to each other. This issue would cause spurious correlation (coherence) between these EEG sensors (Bastos & Schoffelen, 2016).

$$\text{Coh}_{\text{xy}}(f) = \frac{G_{xy}(f)}{\sqrt{G_{xx}(f) * G_{xx}(f)}}$$

New methods have been developed to reduce the effects of volume conduction and field spread on the estimation of functional connectivity between EEG sensors. The IC is one method that estimates the functional connectivity between two signals using the imaginary part of the coherency. The coherency (Coh_{xy}) is defined by the equation above. It can be seen from the equation that coherence is the absolute value of the coherency. The coherency obtained from the Fourier transformation of time series x and y is a

22

complex quantity that includes a real part and an imaginary part. The imaginary part of the coherency is only sensitive to the synchronization between two signals that are time-lagged to each other, i.e., it discards the contributions of 0° phase difference between two signals to their connectivity (Nolte et al., 2004). The rhythmic activity generated by one source could be observed in two or more EEG electrodes due to the volume conduction issue discussed above. If this is the case there should be 0° phase difference (i.e., no time lag) between the spuriously correlated signals observed in the EEG electrodes given that the electrical transmission in the brain is instantaneous in regardless of the sample rate of the data. Thus, the IC method should outperform the coherence method in measuring the real interaction (connectivity) between two signals (Nolte et al., 2004). More details about the IC method and its comparison to the coherence method have been described in Nolte et al. (2004).

The wPLI is another recently developed method that is more resistant to the volume conduction problem than the measurement of coherence. The wPLI is an extension of the phase lag index (PLI) method. The PLI estimates to what extent the phase leads or lags between two signals based on the imaginary part of the CSD of the two signals (Stam, Nolte, & Daffertshofer, 2007). A problem associated with the PLI method is that its estimation of the phase leads and lags can be impacted by noise perturbations in the signals, such as the electrical signals from the eye and muscle movements and externally-generated artifacts (Vinck et al., 2011). These noise perturbations could possibly have near zero phase difference and lead to the detection of "false positive" connections. The wPLI method was designed to solve this issue by weighting the phase differences according to the magnitude of the leads and lags so that

23

phase differences around zero would only have a marginal contribution to the wPLI results (Vinck et al., 2011). It has been shown that the wPLI outperforms the PLI and the IC in terms of reduced sensitivity to uncorrelated noise and increased power to detect changes in the phase synchronization between signals (Vinck et al., 2011).

The effects of volume conduction on spurious connectivity are much alleviated when analyzing the correlations between reconstructed cortical source activities (Schoffelen & Gross, 2009). Although there are also issues associated with estimating cortical source activities, such as the uncertainty about the inverse solution, a detailed discussion about these issues is out of the scope of this article. the Cortical source analysis with realistic MRI models provides an alternative way to study cortical activation during the awake state (Michel et al., 2004; Michel & Murray, 2012). Functional connectivity between brain ROIs can be estimated after the cortical reconstruction of the time-series on the scalp. For example, Bathelt et al. (2013) calculated the cross-correlations between the cortical reconstructed time-series in brain ROIs. In another study, Hillebrand, Barnes, Bosboom, Berendse, and Stam (2012) measured the coherence and the PLI between the cortical reconstructed time-series in brain ROIs. The results from these studies were described in the following sections.

The outputs from the estimation of the functional connectivity with the aforementioned methods can be used to generate the *adjacency matrix*. The adjacency matrix is a N X N matrix that represents the overall functional network with Nx(N-1)/2 unique connections. The "N" is the number of electrodes or brain ROIs. Each element represents the connectivity between a pair of electrodes or brain ROIs. The seed-based functional connectivity between EEG electrodes or brain ROIs can be extracted from the

adjacency matrix. The architecture of the overall functional network (i.e., the topology) represented by the adjacency matrix can be studied with graph theory measures. The graph theory measures are described in the following section.

3.3 Graph theory

Functional networks can be described as graphs that are composed of *nodes* and *edges*. The nodes stand for the components and the edges stand for the pairwise correlations between the nodes in a functional network (i.e., graph; see Bullmore & Sporns, 2009, for review). Nodes can be ROIs, voxels, or collection of voxels in fMRI research. They can also be channels in EEG, fNIRS, and MEG research. Edges can be correlations between the BOLD signals in different ROIs or between the EEG oscillations in various EEG channels. The structure of a graph is typically described as a list of nodes and edges (between nodes). This structure can be conveniently organized as a matrix termed as an *adjacency matrix*. Each node has a column and a row in this matrix. The adjacency matrix illustrates the pairwise correlations (i.e., edges) between nodes.

There are measures in graph theory to qualify and quantify the connectivity in a network. For example, the *path length* is the minimum number of edges traversed to go from any given node to another one in the network (Bullmore & Sporns, 2009). Two nodes in a binary network (matrix) may not directly connecting to each other because the connectivity value between them might be zero. Thus, the minimum number of edges/connections between them would be larger than one because one node needs to go through other nodes to reach the target node. In a weighted network, the inverse of the correlation between each pair of the nodes is calculated to represent the "path" between them. The shortest path length is then calculated as the minimum value for the sum of

25

connections between these two nodes, i.e., the inverse of the strongest correlations between two nodes. The *clustering coefficient* of a node is the number of connections that exist between the nearest neighbors of a node, expressed as a proportion of the maximum number of possible connections between the nearest neighbors of the node (Bullmore & Sporns, 2009). For example, if there are four nodes surrounding the target node and two of the neighbors are connected the clustering coefficient would be 0.167 (1 connection divided by 6 potential connections). The path length and the clustering coefficient represent the global and local network efficiency respectively (Bullmore & Sporns, 2009). It is because path length reflects how fast or efficient the information can be transmitted between distant nodes, and clustering coefficient reflects how efficient the information can be transmitted between nodes closed to each other. Measures of path length and clustering coefficient confer properties of the network as a whole instead of on individual nodes. One measure of the centrality of a node is the sum of all edges connected to a node. This is called the *degree centrality* or the *degree* of a node (Bullmore & Sporns, 2009). High-degree nodes that play important roles in the network structure and dynamics are called *hubs* (Power et al., 2010). A second measure of the centrality of a node is to calculate the fraction of all shortest paths in a network that cross over a given node. This property is called the *betweenness centrality* of a node, which is a useful measure of how much information might traverse certain parts (i.e., nodes, ROIs, voxels) of a network (Bullmore & Sporns, 2009). Nodes with high betweenness centrality may be crucial bridges for the communication between different parts of a network (Power et al, 2010).

The measure of *small-worldness*, which is based on the parameters of path length and clustering coefficient indicates the efficiency of local and global communication inside a network. The calculation of the small-worldness is described in Chapter 4. The fundamental insight of the *small-world* structure is that networks can possess both high clustering coefficients and short path lengths (Watts & Strogatz, 1998). These properties make the networks simultaneously efficient on local and global communications (Watts & Strogatz, 1998). More details about the measure of small-worldness in graph theory can been found in recent reviews (e.g., Bullmore & Sporns, 2009; Chu-Shore et al, 2011; Power et al., 2010; Rubinov & Sporns, 2010; Vertes & Bullmore, 2015).

3.4 Development of functional networks based on EEG Recordings

Examination of connectivity between EEG oscillations using graph theory has become an alternative of studying brain functional networks in developmental populations in addition to the usage of fMRI. There is growing interest in using EEG to examine the development of brain networks in pediatric populations because of the easy application of EEG and its tolerance to movement compared to fMRI (Boersma et al., 2011; Smit et al., 2011). Progress in this approach has recently been made by conducting cortical source analysis with age-specific children MRI templates so that brain networks can be constructed based on connectivity between neural substrates (Bathelt et al., 2013). Results from these EEG studies have shown consistent findings on the development of brain functional networks with those from the fMRI studies. Overall, there were changes in both integration and segregation of information processing in children's resting-state functional networks measured with EEG recordings. The current section reviews some existing EEG studies on the development of resting-state functional networks during

resting state. It also discusses and summarizes some recently developed methods based on EEG data that can be used to study functional connectivity and networks in the current project with infants.

The examination of connectivity between EEG oscillations using graph theory provides insights into the changes in the electrophysiological dynamics within functional networks. A longitudinal study conducted by Boersma and colleagues (2011) recorded resting-state eye-closed EEG oscillations from children at 5 and 7 years of age. Synchronization likelihood (SL) represents the co-oscillation between EEG signals. It has been used as a measure of functional connectivity between different scalp areas or brain regions in EEG studies. Boersma and colleagues (2011) calculated the SL in three frequency bands (theta: 4 – 6 Hz, alpha: 6 – 11 Hz, and beta: 11 – 25 Hz,) between each pair of electrodes to obtain SL-weighted graphs. The mean SL over all pairs of eletrodes was found to decrease from 5 to 7 years of age. Boersma et al. (2011) interpreted this finding as an overall decrease in functional connectivity that might reflect the pruning of unused synapses and the preservation of strong connections. The authors postulated that the process of synaptic pruning and the preservation of useful connections might result in more cost-effective networks. To test this hypothesis, the authors also calculated the mean normalized clustering coefficient and average path length to characterize network organization. They found that the average clustering coefficient increased from 5 to 7 years of age in the alpha rhythm and the average path length increased during this age in all three frequency bands. These findings were interpreted as reflecting a shift from random to more organized functional networks during the development of human brain over childhood.

Convergent evidence came from large cross-sectional studies that investigated the development of brain functional connectivity throughout the lifespan (Smit et al., 2011, 2012). For example, Smit et al. (2012) utilized graph theory to examine the connectivity patterns between EEG electrodes in resting-state networks constructed with EEG oscillations and SL values. EEG recordings were digitally filtered in three frequency bands of interest: alpha (6-13 Hz), beta (15-25 Hz), and theta (3-5.6 Hz). Participants were aged from 5 to 71 years. The analyses in Smit et al. (2012) revealed a substantially increased average clustering coefficient and path length of the resting-state functional networks from childhood to adolescence. The increase of clustering and path length continued at a slower pace into adulthood peaking at around 50 years. These changes suggested decreases in network randomness and increases in order. The authors argued that the protracted increases in connectivity were consistent with white matter development curves that change from a relatively random to a more ordered organization found by research using diffusion tensor imaging (DTI) (Paus, 2010; Westlye et al., 2010). Although the findings of functional connectivity between signals in EEG electrodes have shed light on the development of brain functional networks, limited information about the connectivity between the underlying brain regions could be inferred from scalp recorded EEG data.

The functional connectivity in different EEG frequency rhythms has been measured with alternative methods. For example, Miskovic and colleagues (2015) examined the development of brain networks and functional connectivity computed with the IC (Nolte et al., 2004) between signals in EEG electrodes. They found that the average path length and strength homogeneity decreased from 7 to 11 years in the alpha

rhythm (7 – 14 Hz). Strength homogeneity reflects how evenly the connectivity is distributed among electrodes with higher value meaning more evenly distributed connectivity. The finding of a decrease of path length was inconsistent with previous EEG research discussed above. The inconsistency might be due to the different techniques used by these studies to compute EEG functional connectivity. There have been other techniques used to compute EEG and MEG functional connectivity in addition to the ones mentioned above, such as coherence (Cuevas et al., 2012), phase lag index (Stam et al., 2007), and weighted phase lag index (Vinck et al., 2011). The differences between these methods and their advantages and disadvantages have been discussed elsewhere (Bastos & Schoffelen, 2016).

Recent progress has been made in the study of the development of resting-state functional networks with EEG recordings. Bathelt and colleagues (2013) conducted cortical source analysis of EEG recordings with head models created from age-specific MRI templates, and then examined functional connectivity between localized activation in cortical regions using graph theory. In contrast to the previously reported channel-level analysis, the approach used by Bathelt and colleagues provided information about the cortical areas that are most likely to be involved in the functional networks (c.f., Babiloni et al., 2005; De Vico Fallani et al., 2007).

The methods used by Bathelt and colleagues could be summarized into five steps. First, the authors collected the EEG data from children aged between 2 to 6 years while the participants watched a video clip of calming scenes for 2 minutes. Second, EEG preprocessing was completed by segmenting the EEG recordings into 1s epochs, filtering the EEG data to 1 to 40 Hz, and conducting artifact detection and channel interpolation.

Preprocessed EEG recordings were filtered into different frequency bands (e.g., alpha, beta, theta). Third, cortical reconstruction of the EEG data was conducted with the current density reconstruction (CDR) technique, which resulted in current density amplitude in the brain. The brain was segmented into 68 cortical regions (i.e., ROIs), and thus the cortical reconstructions (current density amplitudes) were parcellated into these ROIs. Fourth, the time series of cortical ROIs derived from EEG segments were correlated in pairwise correlations, and a relative threshold for the correlation values was chosen to take the different noise levels of the recordings into consideration. The fourth step resulted in connectivity (adjacency) matrices that describe the connectivity between each pair of the ROIs, separately for different frequency rhythms. Finally, graph theory measures, such as node degree, clustering coefficient, and path length, were derived from the adjacency matrices.

The majority of the findings by Bathelt et al. (2013) were consistent with previous fMRI and EEG literature. The findings of the increase of the node degree, clustering coefficient, and betweenness centrality of the functional networks with age were comparable to previous literature (Boersma et al., 2011; Power et al., 2010; Smit et al., 2011, 2012). The average path length was found to decrease with age. This finding was inconsistent with the increase of path length throughout childhood shown by the channel-level analyses (Boersma et al., 2011; Smith et al., 2011, 2012). However, the decrease of path length found by Bathelt et al. (2013) was interpreted as being in alignment with the increase of functional integration observed in fMRI research (e.g., Fair et al., 2007, 2008, 2009; see Power et al., 2010, for review). Bathelt et al. (2013) also applied eigenvalue decomposition to obtain functional modules. Modules within networks are groups of

nodes (i.e., ROIs) that are richly connected with one another within the larger framework of the entire network (Power et al., 2010). Functional modules are networks comprising groups of nodes with similar functions. Bathelt et al. (2013) found several functional modules involving interconnected brain regions that were identifiable in different EEG frequency bands (alpha, beta, theta). The connections within these modules remain unchanged but the inter-hemispheric connections between modules increased between 2 and 6 years of age.

The methodological advances in the Bathelt et al. (2013) might result in the more comparable finding to the previous fMRI literature. Bathelt et al. (2013) conducted cortical source analysis to examine brain connectivity among cortical regions instead of only using scalp-recorded EEG signals. The volume conduction effect, as mentioned earlier, would lead to the mixing and spatial smearing of the source activity estimated from scalp-recorded EEG. Therefore, the connectivity patterns constructed with source activity in various cortical areas (Bathelt et al., 2013) might differentiate from those generated with EEG signals recorded from the scalp (Boersma et al., 2011; Smit et al., 2011, 2012).

Another progress made by Bathelt et al. (2013) was the use of age-specific average MRI templates to create a head model for their cortical source analysis. The templates were obtained from the Neurodevelopmental MRI Database (Richards, Sanchez, Phillips-Meek, & Xie, 2016; Richards & Xie, 2015). An accurate MRI model that describes the materials inside the head and their relative conductivity is beneficial for source analysis of EEG signals (Michel et al., 2004; Reynolds & Richards, 2009). Age-specific MRIs may be especially important for pediatric populations (e.g., infants and

young children) due to the neuroanatomical differences that would be a poor fit with an adult MRI template (Reynolds & Richards, 2009; Richards & Xie, 2015). A significant advance in cortical source analysis with infant and young child participants will be obtaining MRIs for individual participants who also are tested in the experimental procedures (Guy et al., 2016; Reynolds & Richards, 2009). However, it is difficult to obtain individual structural MRIs for such participants in a typical experiment. One alternative is to use MRI models from similarly aged infants or young children, such as MRIs from infants or young children with similar head shape and size (Reynolds et al., 2010) or an age-appropriate MRI average (Liao, Acar, Makeig, & Deak, 2015). Bathelt et al. (2013) created the head models for source analysis with age-appropriate MRI templates to minimize the errors that would be caused by the differences between the anatomical features of the participants' brain and head and the features of the average norm.

To sum up, results from different neuroimaging modalities (fMRI, EEG, cortical source analysis) converged on a substantial development of brain functional networks throughout childhood and adolescence. Studies using graph theory have shown that the characteristics of brain networks, such as clustering efficiency and path length, changed over development from childhood to adolescence. Some of the findings discussed above suggested an increase of local efficiency, as well as global integration during the brain development. Studies with EEG recordings provided insights into correlated neurophysiological dynamics between electrodes and cortical sources. Techniques based on EEG recordings made it practical to study the development of functional networks in infancy during awake state. Cortical source analysis of EEG recordings has been shown

as a reliable neuroimaging method to be used in the study of brain functional connectivity in children. Age-specific MRI templates (e.g., the Neurodevelopmental MRI Database, Richards et al., 2016) that provide accurate anatomical information about infants' brain can be used to facilitate the cortical reconstruction.

3.5 Brain Structural Development in the First Year of Life

Recent MRI research offers insights into the potential structural underpinnings of the development of brain functional connectivity during infancy. There are rapid increases of gray matter (GM) volume during the first year of life primarily due to the synaptogenesis process. For example, the total hemispheric volume of GM increases by 149% in the first year with regional difference in the developmental trajectory (Knickmeyer et al., 2008). The dramatic development of GM should drive the functional maturation in brain regions. White matter (WM) develops at a slower pace in the first year with a total hemispheric increase in volume of 11% (Knickmeyer et al., 2008; cf. Richards & Xie, 2015). Although WM volume develops at a slower pace, a recent study using diffusion tensor imaging (DTI) observed substantial development of WM fiber tracts connecting major brain regions from 6 to 12 months of age (Wolff et al., 2012). The changes in WM fiber tracts during the first year were quite visible in averaged MRI brain templates (Richards & Xie, 2015). The posterior limb of the internal capsule was well myelinated at 3 months; posterior regions of the hemispheres (e.g., occipital and temporal lobes) showed myelination at 9 months, and seemingly full coverage of myelination by about 12 months of age (Richards & Xie, 2015). The development of WM fiber tracts during the first year of life should improve structural connections and signal integration between brain areas, thus influencing functional connectivity analysis

at this age. The myelination does not occur at an equal rate throughout the brain (Giedd et al., 1999), which might have an impact on the functional connectivity involving different regions. For example, the functional connectivity involving the frontal regions might be delayed compared to the connectivity within the visual network.

CHAPTER 4

THE STUDY OF THE DEVELOPMENT OF INFANT
SUSTAINEDATTENTION AND BRAIN FUNCTIONAL
CONNECTIVITY DURING INFANCY

Introduction

The existing literature described in Chapter 2 and 3 suggests distinct pattern(s) of

brain functional connectivity during infant sustained attention. Distinguished functional

connectivity might underlie the effects of infant sustained attention on various cognitive

processes. This potential relation between functional connectivity and infant sustained

attention has not been examined, and its development during the first year of life is still

unclear.

The primary objective of this dissertation was to directly link infant sustained

attention to functional brain connectivity. Infant sustained attention and the phase of

inattention were defined based on infant HR changes while looking at stimulus

presentation (Reynolds & Richards, 2008; Xie et al., 2017). The weighted phase lag

index (wPLI; Vinck et al., 2011) between EEG oscillations in the theta, alpha, and beta

frequency bands were measured to represent the functional connectivity. The

connectivity was examined using both the sensor activities and the cortical source

activities in different brain regions. Cortical source reconstruction was conducted with

realistic head models created with age-appropriate average MRI templates (Richards et

al., 2015; Richards & Xie, 2015). Seed-based functional connectivity analysis was

conducted for five major brain networks suggested by an adult resting-state fMRI study (Yeo et al., 2011). These included the visual, somatomotor, dorsal attention, ventral attention, and default mode networks. The default mode, dorsal attention, and ventral attention networks were chosen because their function is related to attention as described in Chapters 1 and 2. The somatomotor network was chosen because a prior study has found the effect of infant sustained attention on the activity in the ROIs involved in this network (Xie et al., 2017). The visual network was chosen for comparison because Xie et al. (2017) found that the activities in the visual areas were not affected by infant sustained attention, although research with adults has shown the changes in the alpha band oscillations in the visual areas as a function of attention orienting (Sauseng et al., 2005). Graph theory measures of path length, clustering coefficient, and small-worldness were used to estimate the overall topology of brain functional networks. Functional connectivity during infant sustained attention was hypothesized to be attenuated in the alpha band and increased in the theta band within the five brain networks. This hypothesis was made based on previous EEG studies on infant attention that have found an opposite pattern of the changes in the power of the alpha and theta bands during sustained attention (e.g., Orekhova, Strognova, & Posikera, 1999, 2001; Xie et al., 2017). It was also hypothesized to find differences in the graph theory measures between infant sustained attention and inattention. However, no specific hypothesis was made for how the patterns would be different between the two attention phases because no study has been conducted to examine infant attention with graph theory measures.

The development of functional connectivity in brain networks before the age of two has not been studied with high-density EEG recordings. Therefore, it is an open

question whether the development of brain functional connectivity during infancy measured with EEG recordings would converge on the previous findings reported from fMRI research (e.g., Cao et al., 2017; Fair et al., 2007; Gao et al., 2009, 2011).

A second goal of the dissertation project was to investigate the development of brain functional connectivity with high-density EEG recordings for infants aged between 6 and 12 months. The same functional connectivity and graph theory measures were used to accomplish the second goal. One hypothesis was that infants would show a decrease of path length and an increase of clustering coefficient and small-worldness during this age period. A second hypothesis was that the functional connectivity in the five major brain networks would increase from 6 to 12 months of age for all three frequency bands. These hypotheses were made based on the aforementioned EEG and fMRI studies on the development of brain functional connectivity over infancy and childhood, as well as the anatomical changes found in the first year of life.

Method

Participants

The final sample had 59 participants and contained the following numbers of participants for each age group: 6 ($N = 15$, $M = 184.4$ days, $SD = 15.51$), 8 ($N = 17$, $M = 239.4$, $SD = 15.02$), 10 ($N = 14$, $M = 289.3$, $SD = 14.53$), and 12 ($N = 13$, $M = 350.6$, $SD = 13.77$) months. The gender information for two subjects were missing. There were 25 (43.86%) females in the rest of the 57 subjects. An additional eight participants were tested but they became fussy before the end of the data collection. Two participants did not finish the experiment due to equipment failure (e.g., programs crashed). Another nine participants were excluded from analyses due to excessive artifacts (e.g., eye or body

movements and noise) in their data. Thus, sixty-eight participants were tested in total ranging in age from 6 to 12 months. The number of participants recruited for each group was listed as follow: 6 ($N = 18$), 8 ($N = 17$,), 10 ($N = 16$), or 12 ($N = 17$) months of age.

Apparatus and Stimuli

A color monitor, two cameras, and computers were used for stimulus presentation and video recording. Microsoft Visual C ++ programs were used for presentation and experimental control. The stimuli included seven Sesame Street dancing and singing sequences made from the movie, "Sesame Street's 25th Anniversary". The character in a scene might talk (or sing) at one location, disappear from the scene, move from one location to another on the screen, or disappear as it was moving across the screen. These characters were placed over a static background in order to improve infants' engagement in the presentation (Mallin & Richards, 2012). These Sesame Street characters have been consistently used to elicit different attention phases during infants' looking (Courage, Reynolds, & Richards, 2006; Guy et al., 2016; Richards, 2010).

Procedure

One randomly selected Sesame Street movie sequence was presented at the beginning of each experimental block. When the infant looked toward this movie, a randomly selected Sesame Street character was presented on the left or the right side of the monitor. The character stayed at that location singing or dancing for 8 – 12 s. The character then moved to the other side of the monitor and stayed there for 8 – 12 s. The character moved back to the original side for an additional 8 – 12 s. The character might also disappear, i.e., hide behind the scene for a few seconds. However, the data collected during the disappearance of the character were excluded from further analyses. A new

character was then introduced with these procedures. One experimental block lasted until two minutes had elapsed. It was repeated with a new Sesame Street movie and character sequences.

Judgment of Visual Fixation

Participants' looking was judged based on the review of the video recordings. A single experimenter determined if the participant was looking toward the video presentation. Looking away from the presentation was marked by the experimenter. Data were only used for further analyses when a participant looked toward the presentation.

ECG Recording and HR Defined Attention Phases

The ECG data were recorded with two Ag-AgCL electrodes placed on each infant's chest. The R-R interval is the latency period between the R waves of two heartbeats, and it was used to compute the inter-beat-interval (IBI). The IBI has an inverse association with HR, such that HR deceleration corresponds to lengthening of the IBI and HR acceleration corresponds to shortening of the IBI.

Attention phases were defined based on HR (IBI) changes during infants' looking. The phase of sustained attention was defined as the time when there was a significant deceleration of HR compared to the prestimulus level and the HR remaining at the lowered level. The phase of inattention consisted of the phase of pre-attention (stimulus orienting) and attention termination. The pre-attention phase was defined as the period between the onset of a look and a significant HR deceleration. The phase of attention termination was defined as the period that HR returned to the prestimulus level. More details about the criteria used to define these phases could be found elsewhere (Reynolds & Richards, 2008; Xie et al., 2016a, b).

EEG Recording and Preprocessing

EEG was recorded simultaneously with the ECG. The Electrical Geodesics Incorporated (EGI, Eugene, OR) EEG system was used for EEG recording. The data of 34 participants were recorded with the 128-channel "Geodesic Sensor Net (GSN)". The data for the rest 25 participants were recorded with the 128-channel "HydroCel Geodesic Sensor Net (HGSN)". EEG was measured from 124 channels in the electrode net. The other four channels were left for the Ag-AgCl electrodes used to measure ECG and electrooculogram (EOG). The EEG was recorded with 20 K amplification at a 250 Hz sampling rate with band-pass filters set from 0.1 – 100 Hz. The channel impedance was measured and accepted if it was below 100 kΩ. The EEG recording was referenced to the vertex and then algebraically recomputed to an average reference.

The EEG recordings were preprocessed using the EEGLAB toolbox (Delorme & Makeig, 2004) in MATLAB (R2015b, the Mathworks, Inc.). Preprocessing included filtering, segmentation, inspection for artifacts, channel interpolation, and data filtering. The continuous EEG data was filtered with band-pass filters set from 1 – 50 Hz. The filtered data was then segmented into 1s epochs (Bathelt et al., 2013). The EEG epochs were inspected for artifacts (ΔEEG > 200 µV or ΔEEG > 100 µV within 50 ms). Independent component analysis (ICA) was conducted using the "runica" program in MATLAB to remove components of eye movements. Channel interpolation was conducted using the five closest channels if there were fewer than 12 channels that were missing or had bad data. Each attention phase must have at least 10 clean trials for the data to be included for further analyses (DeBoer, Scott, & Nelson, 2007). The details of the preprocessing for the EEG data have been described in Xie et al. (2017).

Cortical Source Reconstruction

Figure 4.1 demonstrates the pipeline for source-space functional connectivity analysis from the step of cortical source reconstruction. It illustrates the procedures and the outputs for the methods described in the following sections including cortical source reconstruction, parcellation of cortical reconstructions into brain ROIs, and functional connectivity analysis with the wPLI method.

The cortical source reconstruction of EEG recordings for different frequency bands was conducted with the Fieldtrip (Oostenveld et al., 2011) toolbox. The steps of source analysis included the selection of anatomical MRI, construction of realistic head models, distributed source reconstruction, and segmenting source activity of the whole brain into ROIs. Details about each step have been described by Xie and Richards (2016b) and Xie et al. (2017). These steps were also compatible with those employed by Bathelt et al. (2013) and Hillebrand et al. (2012) with older children and young adults.

An age-related average MRI template was selected for each age group from the Neurodevelopmental MRI Database (Richards et al., 2016; Richards & Xie, 2015). These MRI templates were used to create the realistic head models. Anatomical MRIs were segmented into component materials with the GM and eyes being used as source volumes. Finite Element Method (FEM) model with 5 mm spatial resolution were created. A forward model was created for each MRI template with the FEM model, source volumes, and an electrode placement map (Richards, Boswell, Stevens, & Vendemia, 2015). The forward model was then used to estimate the lead field matrix and the spatial filter matrix (inverse of the lead field matrix).
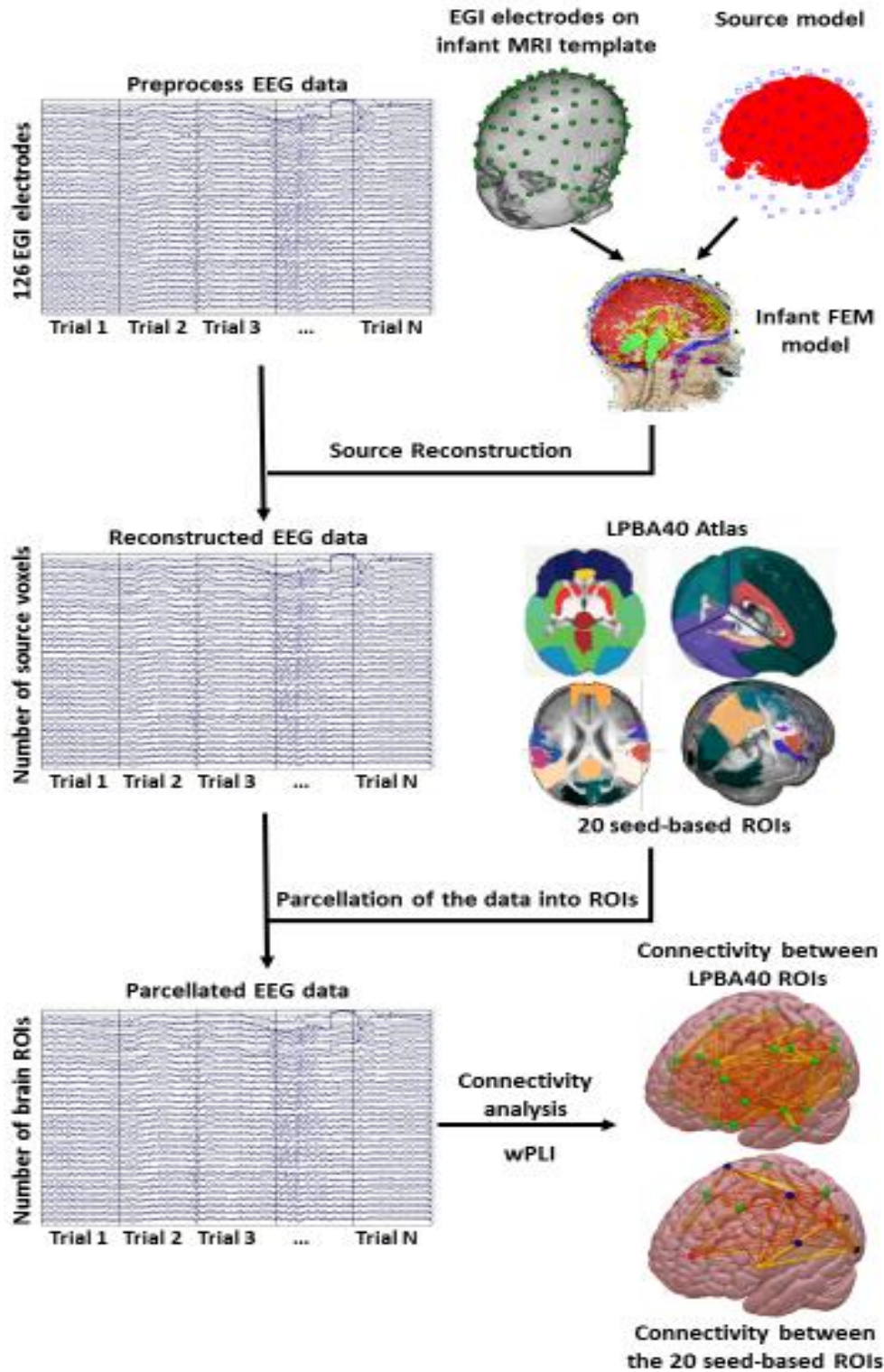
Figure 4.1 Pipeline for the functional connectivity analysis in the source space.

Cortical source reconstruction was conducted using the current density reconstruction (CDR) technique with the head models, lead field matrix, and the spatial filter matrix. Distributed source reconstruction of the EEG time-series in each epoch was conducted with the exact-LORETA (eLORETA; Pascual-Marqui, et al., 2011) as the constraint. This process resulted in source activities in three moments (directions) for each source voxel. The dimension that explains the most variance of the source activities in a voxel was used to represent its activation (Bathelt et al., 2013; Hillebrand et al., 2012). The details of the procedures for source analysis have been described by Xie and Richards (2016b).

Parcellation of Cortical Source Activity into ROIs

The reconstructed cortical time-series in GM voxels were parcellated into brain ROIs. Anatomical brain MRIs were segmented into ROIs using the LPBA brain atlas (Shattuck et al., 2008). This resulted in 48 cortical ROIs. The reconstructed time-series in the source voxels were averaged for each brain ROI (Bathelt et al., 2013; Dai et al., 2017). The reconstructed time-series also were parcellated into 20 cortical areas that are the major components of five brain networks defined by Yeo and colleagues (2011). The five networks included the visual, somatomotor, dorsal attention, ventral attention, and the DMN networks. The Yeo 7 and 17 networks (Yeo et al., 2011), Automatic Anatomical Labeling (AAL; Tzourio-Mazoyer et al., 2002), LPBA (Shattuck et al., 2008), and the Hammers (Hammers et al., 2003) atlases were used to define the 20 cortical ROIs (i.e., components) included in these networks. The ROIs for the five brain networks were illustrated in Figure 4.2. The atlases and the procedures used to construct the ROIs are described in Table 1.

Functional Connectivity Analysis

The first step in functional connectivity analysis was to assess the power spectral density (PSD) and the cross-spectral density (CSD) with frequency analysis in the Fieldtrip toolbox. The EEG time-series were filtered with different cutoffs before frequency analysis: infant theta (2 – 6 Hz), alpha (6 – 9 Hz), and beta (9 – 13 Hz) bands. The Fast Fourier Transform (FFT) was applied on the EEG time-series with a 1s-width Hanning window and 50% overlap (i.e., Welch's method, Welch, 1967). The PSD and the CSD were calculated separately for the three frequency rhythms. This frequency analysis was conducted for the data in the electrodes, as well as the reconstructed source activities in brain ROIs.

Functional connectivity analysis was then conducted separately for the three frequency bands in the Fieldtrip toolbox using the PSD and CSD. The weighted phase lag index (wPLI) was calculated to estimate the functional connectivity between the 126 EEG electrodes, the 20 ROIs for the five brain networks, as well as the 48 cortical ROIs defined by the LPBA atlas. The functional connectivity analysis generated N x N adjacency matrices where N stands for the number of electrodes or brain ROIs. Each value or element in these adjacency matrices represented the wPLI value between a pair of electrodes or brain ROIs. There were N x (N – 1) / 2 unique connections in these N x N matrices. The Fisher's r-to-z transformation was applied to these "correlation" values in the adjacency matrices to improve the normality of their distribution.

The adjacency matrices for the functional connectivity between the EEG electrodes were reorganized into virtual electrode clusters. There were 10 clusters that were the frontal pole, left frontal, right frontal, left temporal, right temporal, left central,
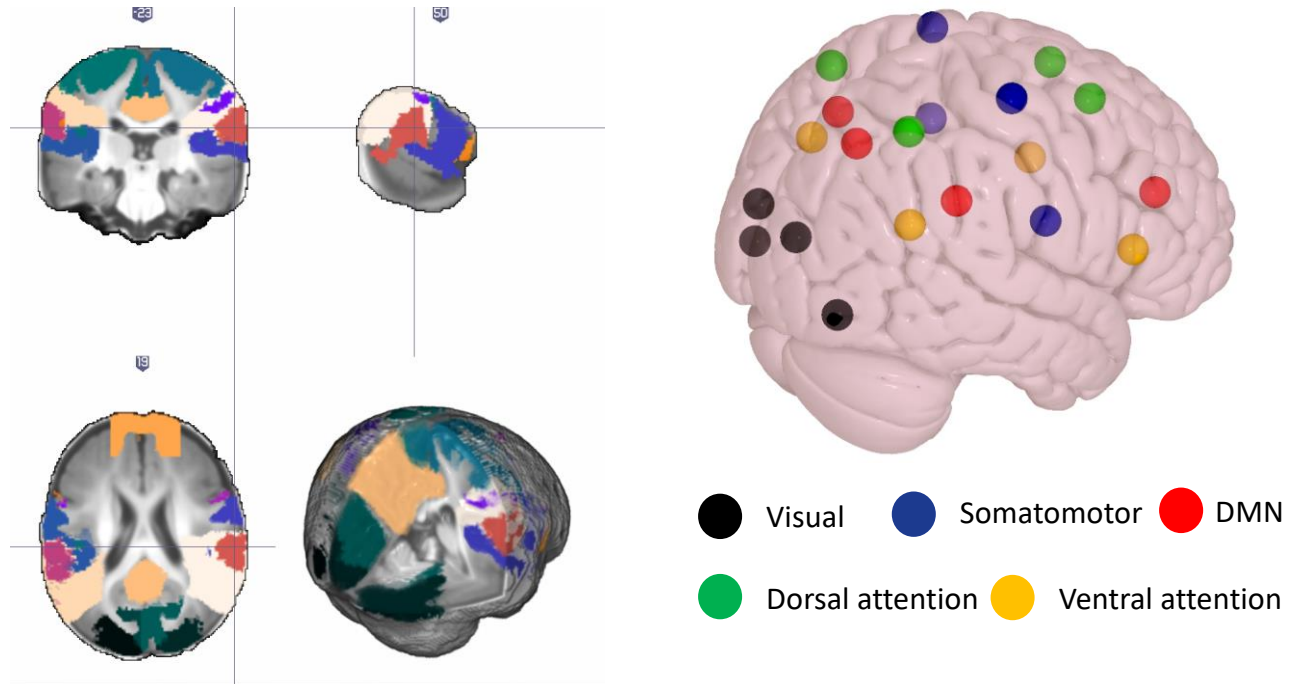
Figure 4.2 The 20 ROIs included in the five brain networks displayed in an infant brain MRI and a 3D brain surface image.

Table 4.1 *Five Brain networks used for the functional connectivity analysis, the 20 cortical ROIs included in the networks, and the atlases used to make these ROIs. The atlases included the Yeo atlases for 7 and 17 networks (Yeo et al., 2011), the AAL (Tzourio-Mazoyer et al., 2002) LPBA (Shattuck et al., 2008), Hammers (Hammers et al., 2003), and Harvard-Oxford (Smith et al., 2004) atlases.*

Brain Networks	ROIs	Atlases
Visual	Peripheral visuaROI (left and right) Central visual ROI (left and right)	Yeo 17 Networks
Somatomotor	Dorsal somatomotor ROI (left and right) Ventral somatomotor ROI (left and right)	Yeo 17 Networks
Dorsal Attention	Superior parietal gyrus (SPG[1]) and Intraparietal sulcus (IPS[1]) (left and right) Frontal eye field (FEF[2]) (left and right)	Yeo 7 Networks AAL
Ventral Attention	Temporal parietal junction (TPJ[3]; left and right) Ventral frontal cortex (VFC[4]; left and right)	Yeo 7 Networks AAL
Default Mode[5]	Medial prefrontal cortex Precuneus/Posterior cingulate cortex Inferior parietal lobule (left and right)	Yeo 7 Networks Hammers;LPBA Harvard-Oxford

Notes: [1]The SPG and IPS (i.e., the posterior part) of the dorsal attention network was made with the overlapping areas between the SPG and IPS in the AAL atlas and the Yeo dorsal attention network.
[2]The FEF ROI was generated by taking the overlapping area between the Yeo dorsal attention network and the middle, superior frontal, and the precentral gyri in the AAL atlas.
[3]The TPJ ROI was generated by taking the overlapping area between the Yeo ventral attention network and the supramarginal, superior and middle temporal gyri in the AAL atlas.
[4]The VFC ROI was generated by taking the overlapping area between the Yeo ventral attention network and the pars opercularis, Rolandic operculum, insula, superior temporal gyrus, and superior temporal pole in the AAL atlas.
[5]The DMN in the current study was generated by taking the overlapping area between the Yeo DMN and the DMN made in Xie et al. (2017).

right central, left parietal, right parietal, and the occipital-inion clusters. The GSN and HGSN electrodes used to make these clusters and the corresponding 10-10 positions are described in Table 2.

The current project used weighted adjacency matrices instead of binary (unweighted) matrices. The weighted matrices keep the original functional connectivity values in the matrices without dividing them into 0s and 1s using a threshold. A weighted matrix incorporates additional information on the strength of the functional connectivity and enables more comprehensive understanding of network organizations (Miskovic et al., 2015; Stam et al., 2009; Wang et al., 2011).

A range of sparsity thresholds was applied to the adjacency matrices to take the noise and spurious connectivity into account. A sparsity (cost) threshold was defined as a ratio of the number of actual connections or edges in a network to the maximum number of possible connections in a network. For example, a cost threshold of 0.1 means only 10% of the maximum potential number of the connections are regarded as real functional connectivity and kept in the matrix, and thus the rest of the connections are set to 0. There is currently no consensus regarding the standard of the threshold for an adjacency matrix created with brain functional data (Zhang et al., 2011). Therefore, a range of cost/sparsity thresholds ($0.1 \leq$ threshold ≤ 0.4, step $= 0.05$) was selected in the current study so that the findings would be less likely to be biased by the arbitrary selection of a threshold (Rubinov & Sporns, 2010; Wang et al., 2011).

Seed-based Functional Connectivity Analysis

Seed-based functional connectivity analysis was conducted in the source space. The wPLI value between each pair of the 20 ROIs was extracted from the adjacency

Table 4.2 *Virtual clusters and corresponding 10 – 10 positions and GSN (HGSN) electrodes.*

Clusters	10-10 Positions	GSN electrodes	HGSN electrode
Frontal Pole	Nz FPz N1 N2 FP1 FP2 AF9 AF10	8 9 14 15 17 18 22 23 26 125 126	8 9 14 15 17 21 22 25 126
Left Frontal	AFZ AF3 AF7 F1 F3 F5 F7 F9	16 19 20 24 25 27 28 33 34	16 18 19 23 24 26 27
Right Frontal	Fz AF4 AF8 F2 F4 F6 F8 F10	1 2 3 4 5 10 11 12 119 122 123 124	1 2 3 4 5 10 11 12 118 124
Left Temporal	FT7 T7 TP7 P7 FT9 T9 TP9 P9	39 40 44 45 46 47 49 50 51 56 57 58 63	33 38 39 43 44 45 48 56 57 58 63 64
Right Temporal	FT8 T8 TP8 P8 FT10 T10 TP10 P10	96 97 98 100 101 102 103 108 109 114 115 116 120 121	96 99 100 101 107 108 114 115 119 120 121
Left Central	FCz FC1 FC3 FC5 C1 C3 C5	6 13 21 29 30 31 35 36 37 41 42	6 13 2028 29 30 34 3 40 41
Right Central	Cz FC2 FC4 FC6 C2 C4 C6	7 32 81 104 105 106 107 110 111 112 113 117 118	7 31 80 103 104 105 109 110 111 112 116
Left Parietal	CPz CP1 CP3 CP5 P1 P3 P5 PO7 PO9	38 43 48 52 53 54 55 59 60 61 65 66 70	37 42 46 47 51 52 53 59 60 61 65 69
Right Parietal	Pz CP2 CP4 CP6 P2 P4 P6 PO8 PO10	62 79 80 87 88 90 91 92 93 94 99	62 78 79 85 86 87 89 92 93 95 97 98 10
Occipital-Inion	POz Oz Iz PO3 PO4 O1 O2 I1 I2	67 68 69 71 72 73 74 75 76 77 78 82 83 84 85 86 89 95	66 67 68 70 71 72 73 76 77 81 82 83 84 88

49

matrices. This allowed us to compare the connectivity between certain pairs of ROIs and to compare the averaged connectivity within a network (e.g., the DMN) between different conditions (e.g., sustained attention vs inattention).

Seed-based functional connectivity analysis also was conducted on the sensor level. The wPLI value between the 126 electrodes (seeds) was extracted from the adjacency matrices and grouped into the 10 visual clusters. The wPLI value between the electrodes in a virtual cluster was calculated.

Graph Theory Measurements

The brain network topology was estimated with graph theory measures. Graph theory measurements of the properties (e.g., path length, clustering coefficient) of functional networks were applied with the Brain Connectivity Toolbox (BCT; Rubinov & Sporns, 2010) and the GRETNA toolbox (Wang et al., 2015) in MATLAB (R2016a, the Mathworks, Inc.).

Graph theory measurements were examined in the source space and on the channel level. The nodes of a network were defined as the 126 electrodes or the 48 LPBA cortical ROIs. The edges were defined as the functional connections (wPLI values) between all pairs of the nodes. The clustering coefficient for a node was calculated as the proportion of its neighboring nodes that were connected to each other. The averaged clustering coefficient (Cp) that reflects the average level of local organization of a network was then calculated. The path length was defined as the inverse of the wPLI value. The shortest path length between two nodes was calculated as the lowest value among the sums of different path lengths between them. The averaged shortest path

length (Lp) of the entire network was then calculated to reflect the average level of global organization of the network.

A normalization process of the Lp and Cp was conducted to calculate the small-worldness (sigma). Two hundred randomized networks were generated with the same number of nodes and distribution of edges as the real functional networks (Maslov & Sneppen, 2002; Sporns & Zwi, 2004). The averaged path length (Lp-r) and clustering coefficient (Cp-r) of these randomized networks were calculated. The normalized path length (lambda) was defined as the ratio of Lp to Lp-r. The normalized clustering coefficient (gamma) was defined as the ratio of Cp to Cp-r. The sigma of a network was defined as the ratio of gamma to lambda, which represented the ratio of local organization efficiency to global organization efficiency for a network (Stam et al., 2009). A sigma value greater than 1 indicates a network having the property of small-worldness (Watts & Strogatz, 1998).

The area under the curve (AUC) was calculated for these graph theory measures given that a range of network intensities was employed. This was because a range of sparsity thresholds was applied to the adjacency matrices to obtain networks with different intensity. Each threshold ended up with a set of graph theory measures (the Lp, Cp, and sigma). The usage of the AUC value provided a summarized scalar for the graph theory measures in regardless of the network intensity (Zhang et al., 2011).

Figure 4.3 summarizes the procedures for the data analysis in the current study. It includes the major steps form the preprocessed EEG data to the seed-based connectivity and graph theory analysis. The procedures for the analyses on the sensor level and in the source space were covered in this figure.

Design for Statistical Analysis

Statistical analysis was performed with mixed-design ANOVAs using the Proc GLM function in SAS (SAS institute Inc, Cary, NC). The averaged wPLI value within a network was analyzed as the dependent variable in the seed-based connectivity analyses for the five brain networks. Post hoc tests (e.g., multiple comparisons) for the wPLI value between individual pair of ROIs were conducted with false discovery control (FDR, $p <$ 0.05). The AUC values for the path length (Lp), clustering coefficient (Cp), and small-worldness (sigma) were analyzed as the dependent variables in the graph theory analyses.
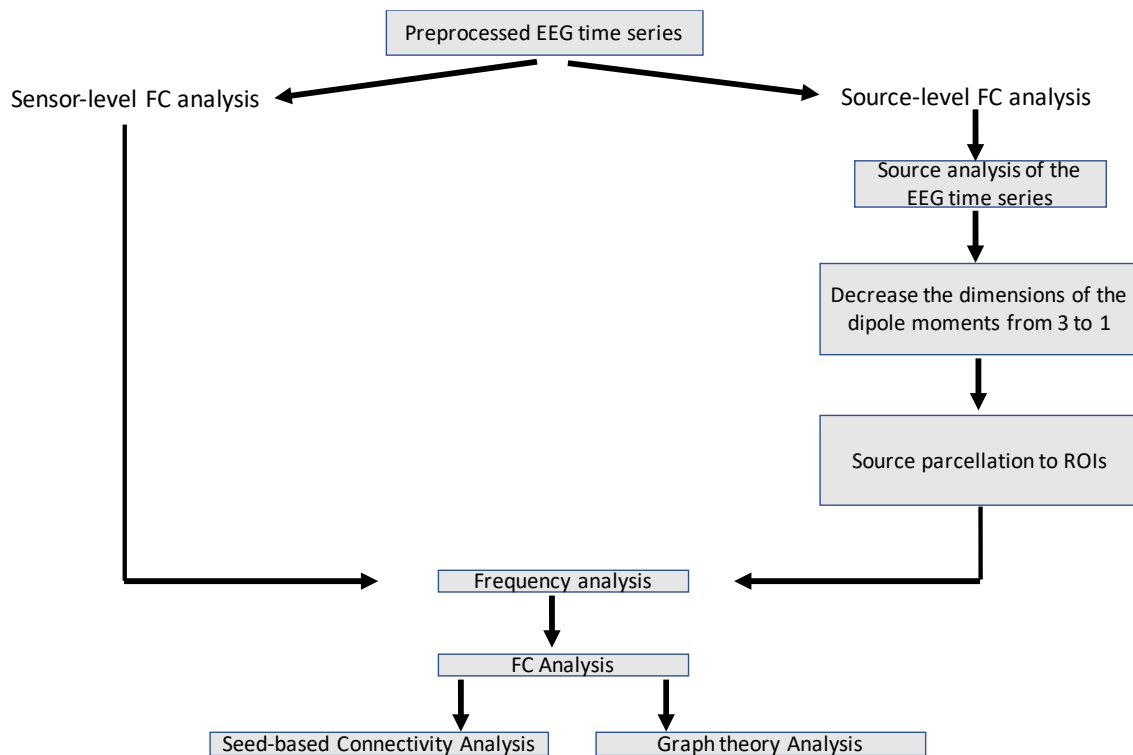

Figure 4.3. Summary of the procedures for data analysis in the current study.

The seed-based connectivity and graph theory analyses both included attention phase (2: attention and inattention) and frequency band (3: theta, alpha, and beta) as within-subject independent variables, and age (2: 9 and 12 months) as a between-subject independent variable. All significant tests were reported at $p < 0.05$.

It should be noted that the age was analyzed as a categorical variable in the ANOVAs. This was because the data were collected from participants at specific ages (e.g., 6, 8, 10, 12 months) instead of being collected continuously with a broader age range. Regression analysis with age as a continuous variable should be superior to the current ANOVAs in examining the linear or non-linear changes that might occur between different ages. However, the validity of this type of regression analysis relies on the number of data points over the age range (e.g., 6 to 12 months). It means that more data needs to be collected to cover the entire age range in order to obtain sufficient power for the analysis. In contrast, 10 – 12 subjects per age group should provide sufficient power to examine the difference between two ages according to previous infant EEG/ERPs studies (e.g., Xie & Richards, 2016a, b; Xie et al., 2017).

Results

Sufficient numbers of trials were obtained for the conditions of sustained attention and inattention. The number of trials obtained for sustained attention ($M = 174.49$, 95% CI [140.15 196.26]) was not significantly different than that for inattention ($M = 151.78$, 95% CI [117.39 186.17]). The numbers of trials for both conditions were much greater than the recommended minimum number of trials (10 ~ 20) per condition for infant EEG studies (DeBoer et al, 2007).

Graph Theory Analysis

Statistical analyses were performed to determine the effects of infant sustained attention and age on brain network topology in different frequency bands. The graph theory measures, path length (Lp), clustering coefficient (Cp), and small-worldness (sigma) were analyzed as a function of attention phase, age, and frequency bands. These analyses were conducted in the source space with 48 cortical ROIs, as well as on the channel level with 126 electrodes.

Sensor level analysis

This section includes the results from analyses for the path length, clustering coefficient, and small-worldness. They are reported separately in this section. A summary of the results for these measures is given at the end of the section.

Path length (Lp) on sensor level An analysis was conducted to determine the effect of attention and age on the global network efficiency in different frequency bands. The AUC value for Lp was analyzed as a function of attention phase, age, and frequency band with a mixed-design ANOVA. The analysis for the Lp showed a main effect of attention phase, $F(1, 55) = 7.95$, $p = 0.0067$. The AUC value for Lp was greater during sustained attention than inattention. There was no age or interaction between the three factors. Figure 4.4A shows the AUC value for Lp as a function of attention phase and age, separately for the three frequency bands. The AUC value for Lp appears to be greater during sustained attention than inattention in all three frequency bands. Figure 4.4B depicts the changes in the Lp value as a function of network intensity from 10% to 100%, separately for the attention phases, ages, and frequency bands. This figure shows that the
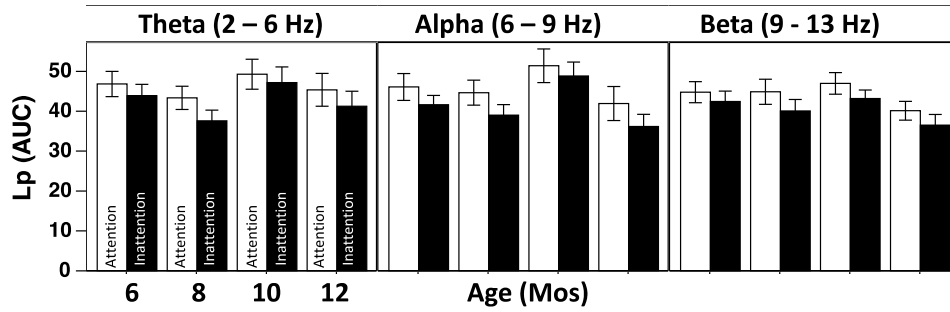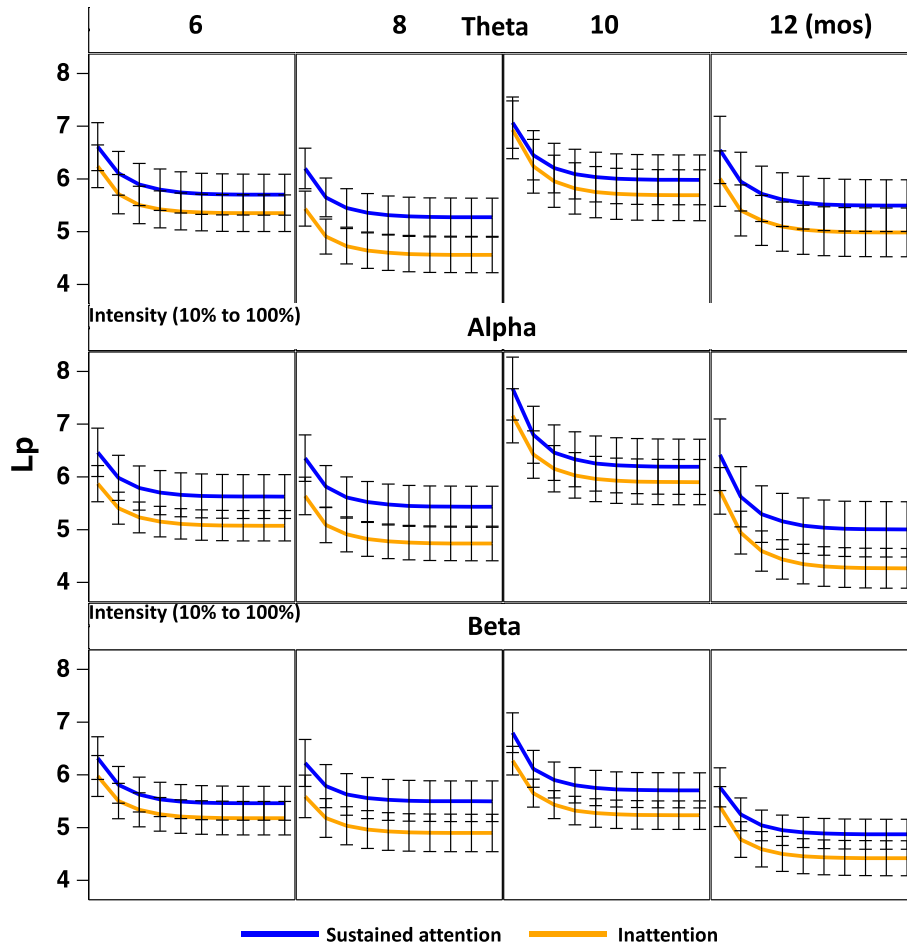
Figure 4.4 The changes of the path length (Lp) on the sensor level as a function of attention phase, and age, and frequency band. (A) Individual bars for the mean value of the Lp across conditions. Overall the AUC value for Lp appears to be greater during sustained attention than inattention. (B). The changes of Lp as a function of network intensity (i.e., threshold) from 10% to 100%, separately for different attention phases, ages, and frequency bands. In specific, there are 10 different intensities: 10%, 15%, 20%, 25%, 30%, 35%, 40%, 45%, 50%, and 100%.

difference between sustained attention and inattention was consistent across different network intensities.

Clustering coefficient (Cp) on sensor level The analysis for the Cp showed a main effect of attention phase, $F(1, 55) = 7.29$, $p = 0.0092$. The AUC value for Cp was greater during inattention than sustained attention. The interaction between age and frequency band was not significant, $F(6, 110) = 2.16$, $p = 0.0525$. Follow-up analyses showed that the age effect was significant for the alpha, $F(6, 110) = 9.79$, $p = 0.0010$ and beta, $F(6, 110) = 6.43$, $p = 0.0144$, bands. The AUC value for Cp was greater for the 12 months compared to the other three ages for the alpha and beta bands. Figure 4.5A shows the individual bars for the AUC value of Cp, separately for different attention phases, ages, and frequency bands. It can be seen that the Cp value increased with age in the alpha and beta bands, and it was greater during inattention than sustained attention. This information is also shown in Figure 4.5B that depicts the changes of Cp as a function of network intensity.

Small-worldness (sigma) on sensor level The analysis for the sigma value showed a significant interaction between age and frequency band, $F(6, 110) = 2.58$, $p = 0.0223$. A simple effect test showed that the AUC value for sigma decreased with age only for the alpha band, $F(3, 110) = 11.27$, $p < 0.00010$. Figure 4.6A shows the bars for the AUC value of sigma as a function of attention phase, age, and frequency band. It can be seen that this value decreased with age in the alpha band. Figure 4.6B also shows this decrease of sigma from 6 to 12 months of age. In addition, it shows that when the network intensity was low (e.g., 10%, 15%, and 20%) the sigma value was greater than 1 at 6 and 8 months in the alpha and beta bands.
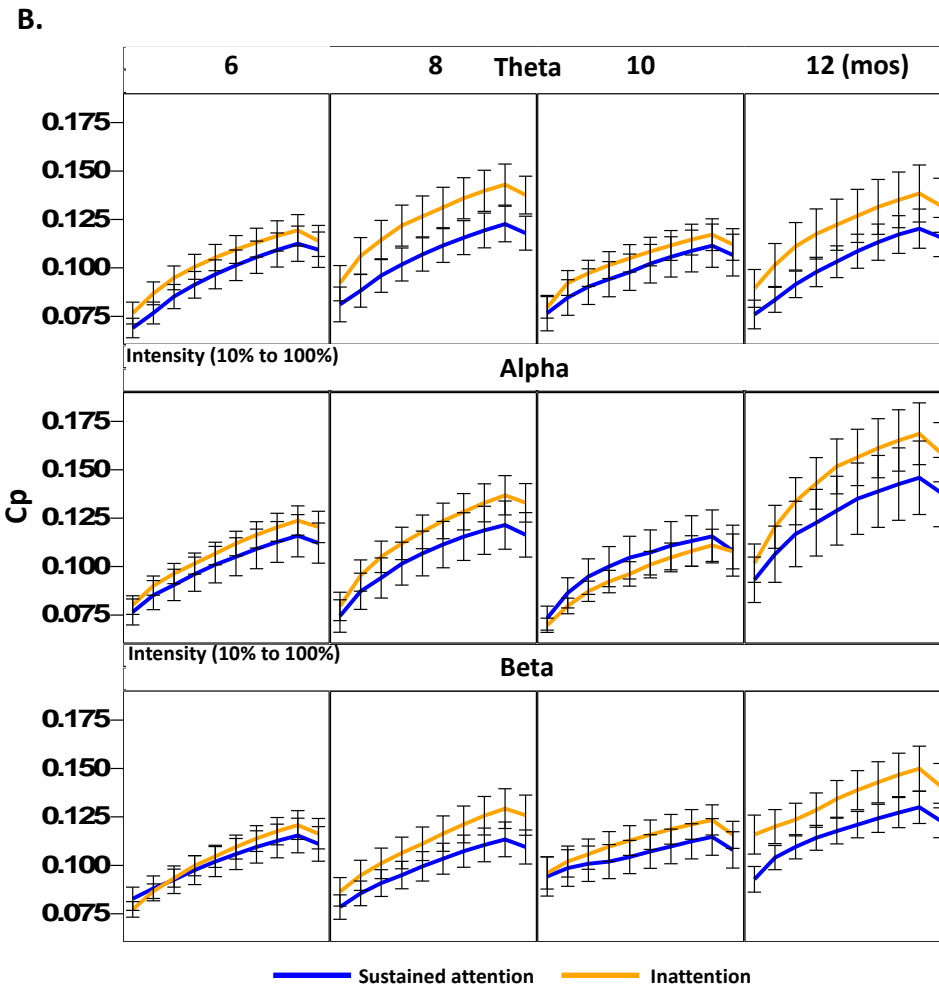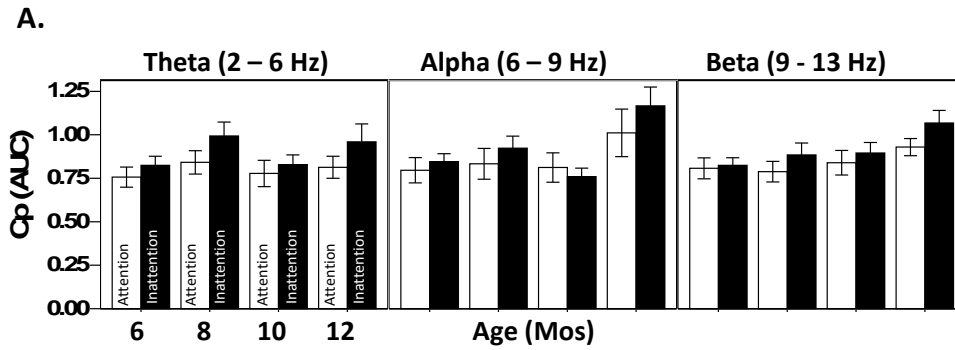
Figure 4.5 The changes of the clustering coefficient (Cp) on the sensor level as a function of attention phase, and age, and frequency band. (A) Individual bars for the mean value of the Cp across conditions. Overall the AUC value for Cp appears to be smaller during sustained attention than inattention and increases with age in the alpha and beta bands. (B) The changes of Cp as a function of network intensity (i.e., threshold) from 10% to 100%, separately for different attention phases, ages, and frequency bands.
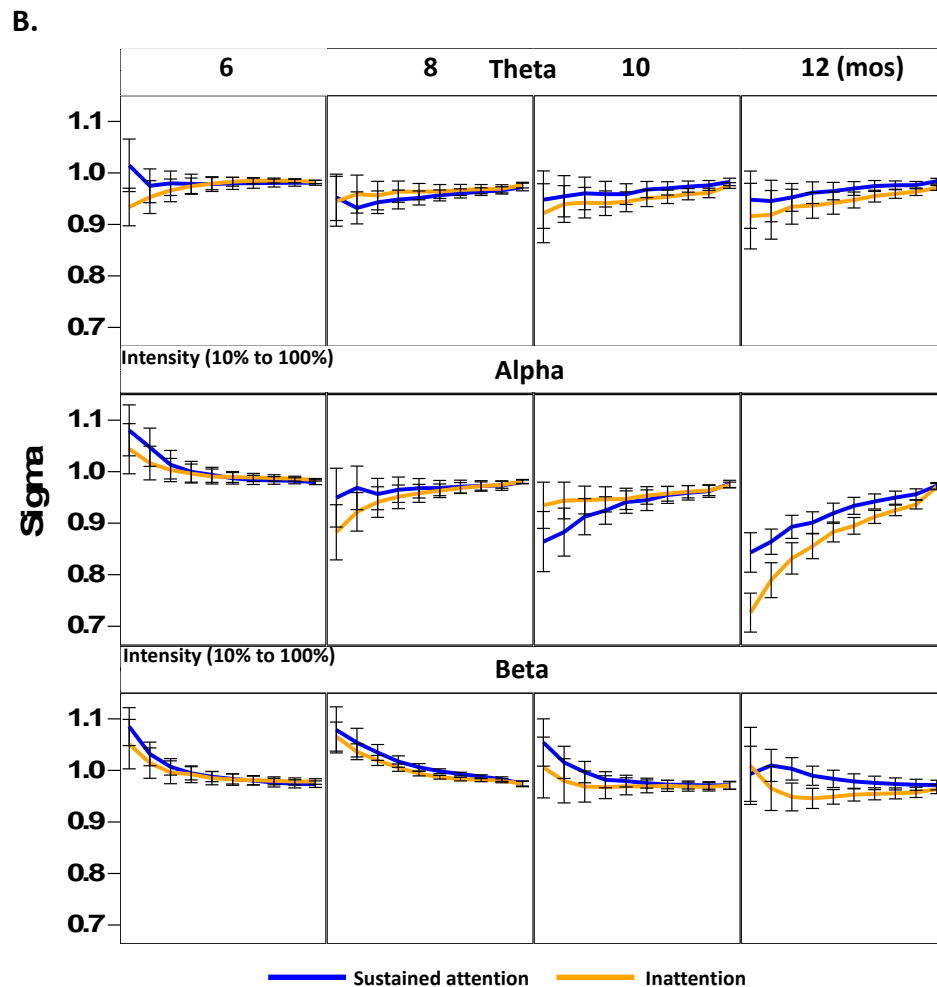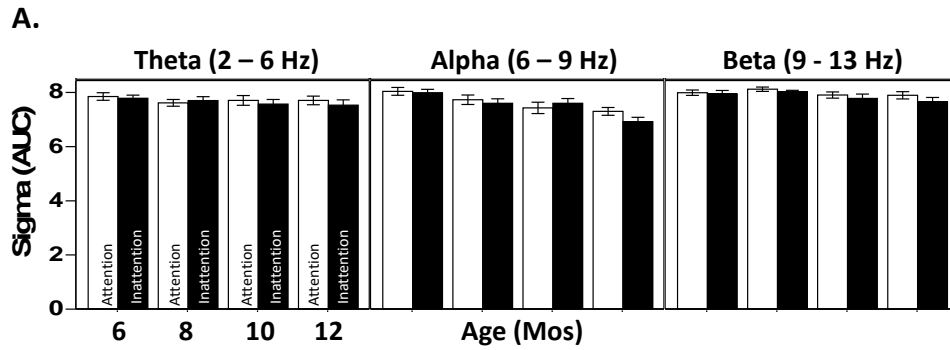
Figure 4.6 The changes of the small-worldness (Sigma) on the source level as a function of attention phase, and age, and frequency band. (A) Individual bars for the mean value of sigma across conditions. (B) The changes of sigma as a function of network intensity (i.e., threshold) from 10% to 100%, separately for different attention phases, ages, and frequency bands. The sigma appears to be greater than one at 6 months for the alpha band and at 6 and 8 months for the beta band when the intensity is low.

Summary of the results for the graph theory measures on the sensor level

The graph theory analyses with the adjacency matrices of the 126 electrodes showed that the network topology on the scalp changed with age and attention phase. The Lp was found to be greater and the Cp was found to be smaller during sustained attention than inattention. The Cp was found to increase with age in the alpha and beta bands. The small-worldness (sigma > 1) was shown for infants at 6 and 8 months with low network intensity. However, there was no sustained attention effect on the sigma value for all the ages. The details of the results are summarized in Table 3.

Source space analysis

The section includes the results from the analyses of the graph theory measures in the source space. The results for the path length, clustering coefficient, and small-worldness are reported separately in this section. They are followed by a summary of these results at the end of the section.

Path length (Lp) in source space An analysis was conducted to determine the effect of attention and age on the global network efficiency in different frequency bands. The AUC value for Lp was analyzed as a function of attention phase, age, and frequency band with a mixed-design ANOVA. There was a main effect of attention phase on the AUC value for Lp, $F (1, 55) = 8.96$, $p = 0.0041$. The AUC value was greater for sustained attention than inattention. The analysis on Lp also revealed an interaction between age and frequency band, $F (6, 110) = 3.39$, $p = 0.0042$. A simple effect test showed that the AUC value for Lp significantly decreased with age for the alpha, $F (3, 110) = 6.10$, $p = 0.00070$, and theta, $F (3, 110) = 7.45$, $p = 0.00010$ bands. Figure 4.7A

Table 4.3 *Summary of the major results from the graph theory analyses on the sensor level.*

Variables	Results	Figures
Sensor level		
Path length (Lp)	i). The Lp was smaller during inattention than sustained attention.	Figure 6
Clustering Coeffcient (Cp)	i). The Cp was greater during inattention than sustained attention in the alpha band.	Figure 7
	ii). The Cp increased with age in the alpha and beta bands.	Figure 7
Small-worldness (Sigma)	i). The sigma decreased with age in the alpha band.	Figure 8
	ii). When the network intensity is low the sigma was greater than 1 in the alpha and beta bands for the 6- and 8-month-olds.	Figure 8B

shows the AUC value for Lp as a function of attention phase and age, separately for the three frequency bands. Overall the AUC value for Lp appears to be greater during sustained attention than inattention and decreases with age in the theta and alpha bands. Figure 4.7B depicts the changes in the Lp value as a function of network intensity (i.e., threshold) from 10% to 100%, separately for the attention phases, ages, and frequency bands. It can be that the difference between sustained attention and inattention was consistent across different network intensities.

Clustering coefficient (Cp) in source space Another mixed-design ANOVA was conducted to determine the effect of attention and age on the local network efficiency in different frequency bands. The AUC value for Cp was analyzed as a function of the three variables. There was an interaction between attention phase and frequency band, F (2, 110) = 3.83, p = 0.025. This interaction was driven by the greater AUC value for Cp during inattention than sustained attention for the alpha, F (1, 110) = 28.78, p < 0.0001, but not for the theta and beta bands. There was also an interaction between age and frequency band, F (6, 110) = 4.61, p = 0.00030. A simple effect test showed that the AUC value for Cp increased with age for theta, F (3, 110) = 6.43, p = 0.00050, and alpha, F (3, 110) = 5.68, p = 0.0012, bands. Figure 4.8A shows the AUC value for Cp as a function of attention phase and age, separately for the three frequency bands. The AUC value for Cp appears to be smaller during sustained attention than inattention in the alpha band and increases with age in the theta and alpha bands. Figure 4.8B depicts the changes in the Cp value as a function of network intensity, separately for different attention phases, ages, and frequency bands. This figure also shows the difference between sustained attention and inattention primarily in the alpha band, as well as
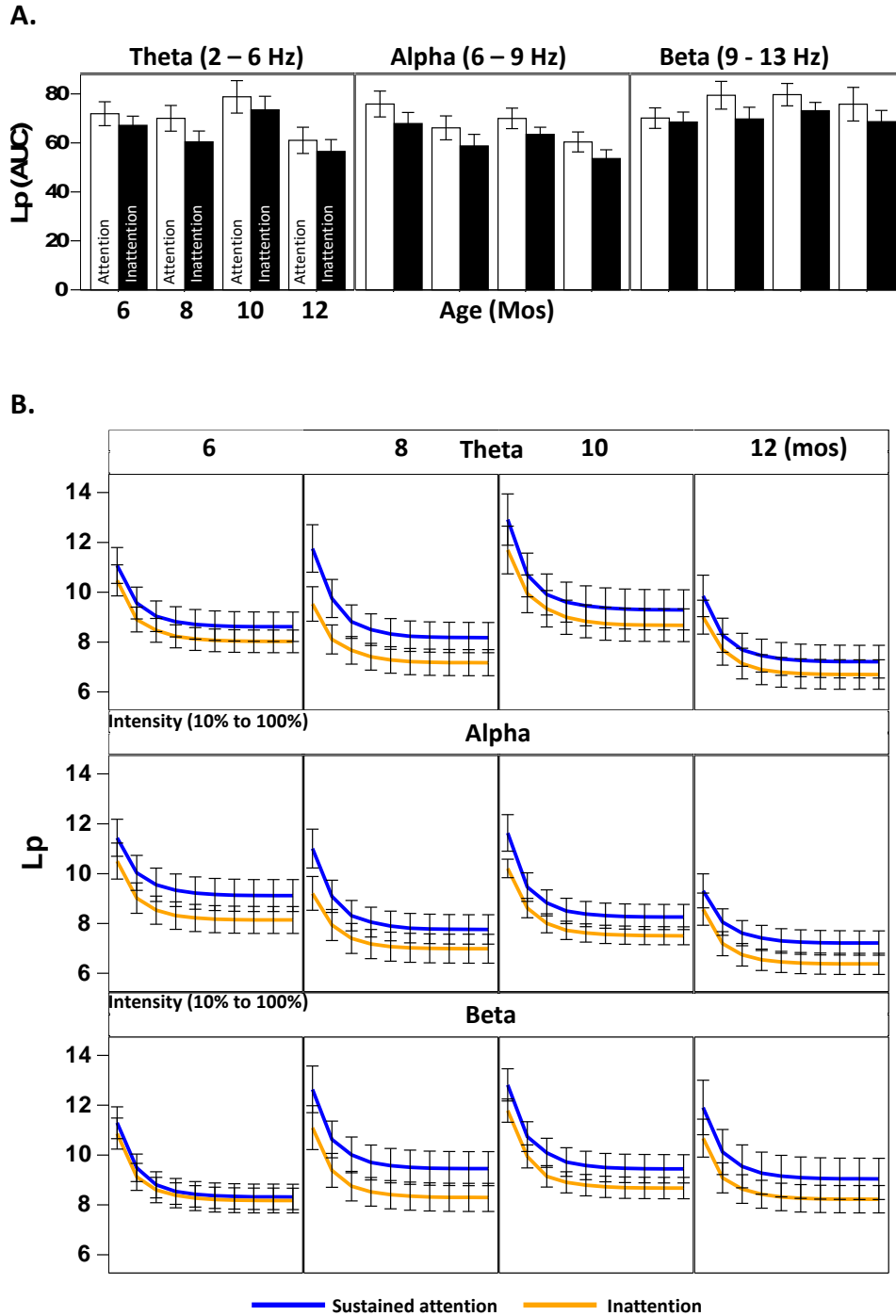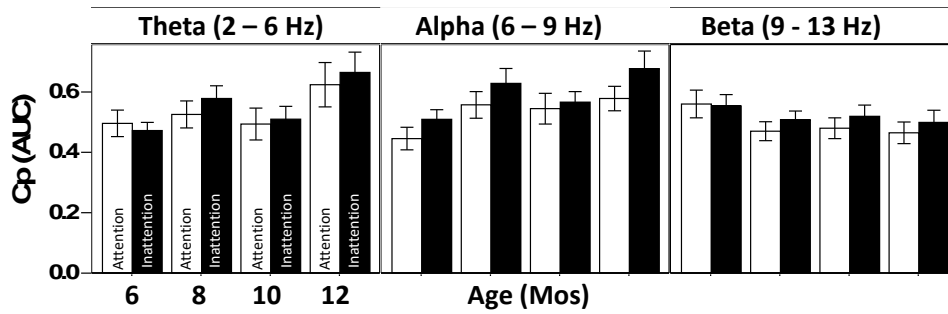
Figure 4.7 The changes of the path length (Lp) in the source space as a function of attention phase, age, and frequency band. (A) Individual bars for the mean value of the Lp across conditions. The error bars stand for the standard errors. Overall the AUC value for Lp appears to be greater during sustained attention than inattention and decreases with age. (B) The changes of Lp as a function of network intensity (i.e., threshold) from 10% to 100%, separately for different attention phases, ages, and frequency bands.
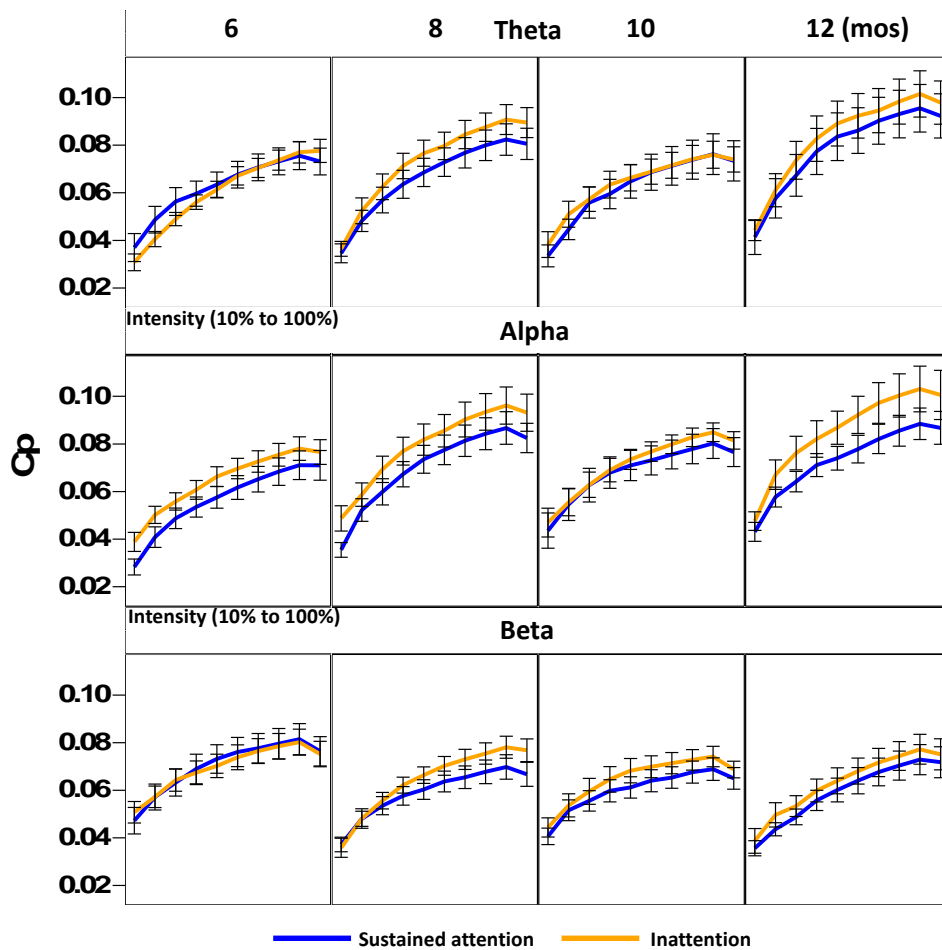
Figure 4.8 The changes of the clustering coefficient (Cp) in the source space as a function of attention phase, and age, and frequency band. (A) Individual bars for the mean value of the Cp across conditions. Overall the AUC value for Cp appears to be smaller during sustained attention than inattention and increases with age. (B) The changes of Cp as a function of network intensity (i.e., threshold) from 10% to 100%, separately for different attention phases, ages, and frequency bands.

changes of Cp with age in the alpha and theta bands.

Small-worldness (sigma) in source space The sigma value was analyzed to determine the effect of attention and age on the small-worldness in different frequency bands. The AUC value for sigma was analyzed as a function of attention phase, age, and frequency band. This analysis did not show a main effect of attention phase or age, or an interaction between them. Figure 4.9A shows individual bars representing the AUC value for sigma across different attention phases, ages, and frequency bands. It can be seen that there was no clear change in the AUC value for sigma with age or any difference between the two attention phases. Figure 4.6B depicts the changes in the sigma value across network intensities. There is no clear change of sigma value shown in the figure across ages. However, when the network intensity is low (10%, 15%, 20%, and 25%) the sigma value appears to be greater than 1 in the alpha (during inattention) and beta bands for the 6-month-olds (Figure 4.9B). The sigma value greater than 1 is a sign of showing small-worldness as mentioned earlier in the paper.

Summary of the results for the graph theory measures in the source space The same kinds of analyses were performed for the graph theory measures in the source level with the 48 brain ROIs. Overall, the results from the analyses on the sensor level were comparable to those with cortical ROIs. The Lp value was greater and the Cp value was smaller during sustained attention than during inattention. There was a decrease of Lp and an increase of Cp with age in the theta and alpha bands. The small-worldness was found at 6 and 8 months with low network intensity. There were also inconsistent results
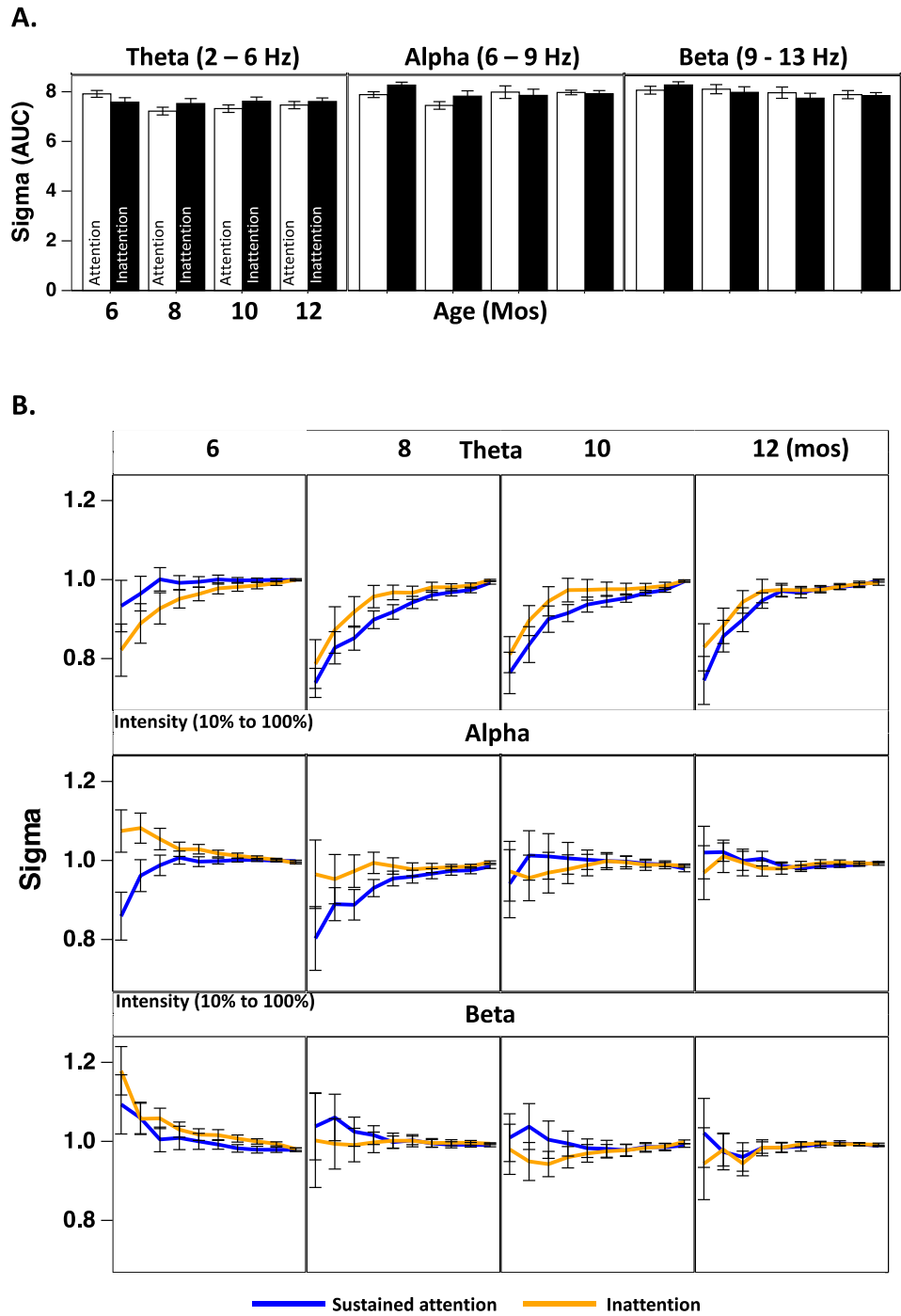
Figure 4.9 The changes of the small-worldness (Sigma) in the source space as a function of attention phase, and age, and frequency band. (A) Individual bars for the mean value of sigma across conditions. (B) The changes of sigma as a function of network intensity (i.e., threshold) from 10% to 100%, separately for different attention phases, ages, and frequency bands. The sigma appears to be greater than one at 6 months for the alpha (inattention) and beta bands when the intensity is low.

between the source space and sensor level analyses. There was a change of Lp with age found in the source space, but the age effect was not found by the analyses on the sensor level. There was no age effect on the sigma value according to the analyses in the source space, but it was found to decrease with age in the alpha band. The details of the results are summarized in Table 4.

Connectivity Analysis

The connectivity analysis was conducted for the 20 ROIs (seeds) in the five brain networks and the 126 electrodes on the scalp. Statistical analyses were performed for the seed-based connectivity analysis to determine the effects of infant sustained attention and age on the connectivity in the brain for different frequency bands. The averaged functional connectivity within a network was analyzed as a function of attention phase, age, and frequency band. This kind of analysis was conducted separately for the five brain networks that included the visual, somatomotor, dorsal attention, ventral attention, and the default model networks. The overall pattern for the connectivity between the 20 ROIs also was demonstrated following the analyses for the brain networks with circular maps and adjacency matrices. The connectivity analysis on the sensor level included the illustration of the adjacency matrices for the 126 electrodes grouped into the 10 virtual clusters. No statistical analysis was conducted, and no circular maps were made for the sensor level connectivity analysis. It was because the primary goal of the connectivity analysis in the current study was to examine the functional connectivity in brain networks as a function of attention and age. In addition, the number of electrodes (126) is much greater than the number of ROIs (20) in the seed-based connectivity analysis. Thus, the connections between the electrodes are displayed in a different fashion (i.e., in the raw

66

adjacency matrices) rather than the circular maps for the differences in the source space connectivity.

<u>Seed-based Connectivity Analysis for Brain Networks in the Source Space</u>

The seed-based functional connectivity between the ROIs in brain networks was analyzed to determine the effects of attention and age on brain functional connectivity and how these effects might differ with the frequency band. The mean wPLI value between ROIs within a network was analyzed as a function of age, attention phase, and frequency band with a mixed-design ANOVA for each network. When a significant effect of attention was found for a network post-hoc multiple comparisons between sustained attention and inattention were conducted for individual pairs of connections in a network with FDR control.

The results for the five brain networks are reported separately in this section. These are followed by a section for the connectivity between the 20 ROIs. A summary of the findings is given at the end of the section.

Visual network The mean wPLI value for the connections within the visual network was analyzed to determine whether there was difference between attention phases and ages in different frequency bands. The mean wPLI value was analyzed as a function of attention phase, age, and frequency band with a mixed-design ANOVA. This analysis revealed a significant interaction between age, attention phase, and frequency band, $F(6, 110) = 2.72$, $p = 0.017$. Following analyses showed that the interaction between age and attention phase was not significant for the alpha band, $F(3, 55) = 2.75$, $p = 0.051$. A simple effect test showed the mean wPLI value increased with age only during inattention, $F(3, 55) = 2.91$, $p = 0.042$. Figure 4.10A shows individual bars

67

Table 4.4 *Summary of the major results from the graph theory analyses in the source space.*

| Variables	Results	Figures
	Source space	
Path length (Lp)	i). The Lp was smaller during inattention than sustained attention.	Figure 9
	ii). The Lp decreased with age in the theta and alpha bands.	Figure 9
Clustering Coeffcient (Cp)	i). The Cp was greater during inattention than sustained attention in the alpha band.	Figure 10
	ii). The Cp increased with age in the theta and alpha bands.	Figure 10
Small-worldness (Sigma)	i). The Sigma did not change with age or attention phase.	Figure 11
	ii). When the network intensity is low the sigma was greater than 1 in the alpha and beta bands for the 6-month-olds.	Figure 11B

that represent the mean wPLI value within the visual network for different attention phases and ages, separately for the three frequency bands. The mean wPLI value was greater for 12 months than the other ages during inattention in the alpha band (Figure 4.10A).

The ANOVA for the visual network also revealed a significant main effect of attention phase, $F(1, 55) = 6.57$, $p = 0.0131$. The mean wPLI value was greater during inattention than sustained attention. Figure 4.10A shows that the mean wPLI value was overall greater during inattention than sustained attention. This effect appeared to be bigger with age in the alpha and beta bands. Post-hoc comparisons ($p < 0.05$, corrected by FDR) were then conducted to analyze the attention effect for the connectivity between individual pairs of ROIs within the visual network (e.g., left central and left peripheral visual areas) in the three frequency bands. There was no significant difference found between sustained attention and inattention for any pair of the ROIs.

Somatomotor network The mean wPLI value within the somatomotor network also was analyzed as a function of attention phase, age, and frequency band with a mixed-design ANOVA. This analysis showed that the age effect differed with frequency band. There was a significant interaction between age and frequency band, $F(6, 110) = 2.28$, $p = 0.041$. A simple effect test showed that the age effect was significant only for the alpha band, $F(3, 55) = 4.88$, $p = 0.0032$. The mean wPLI value increased with age. Figure 4.10B shows the changes in the mean wPLI value within the somatomotor network across attention phases, ages and frequency bands. It can be seen that the mean wPLI value network increases with age in the alpha band.
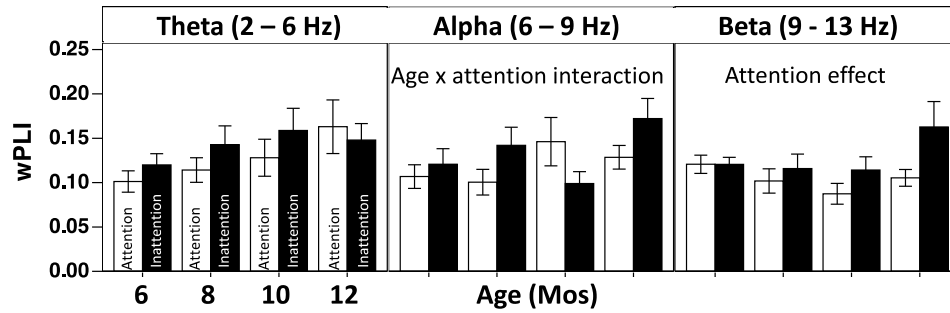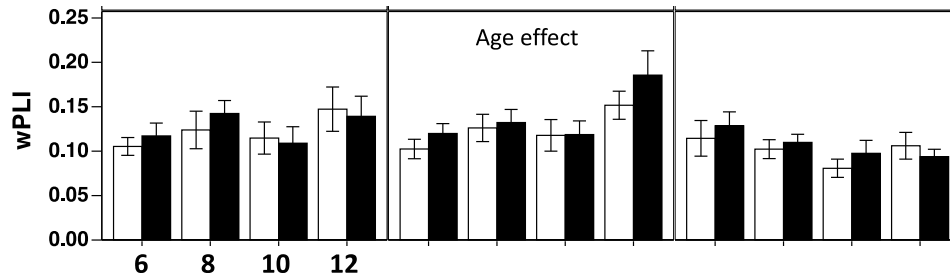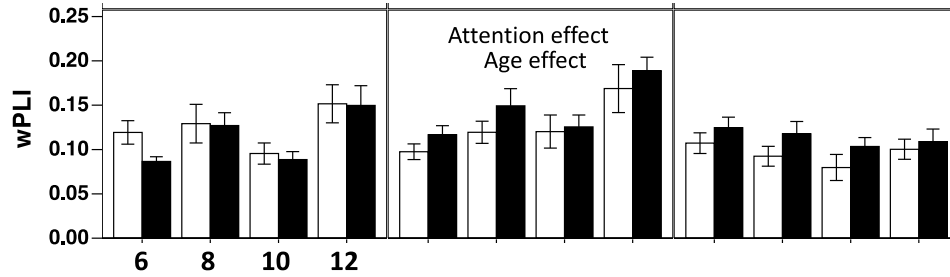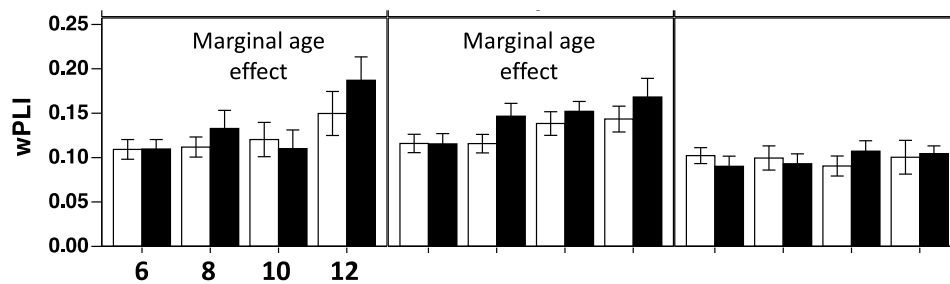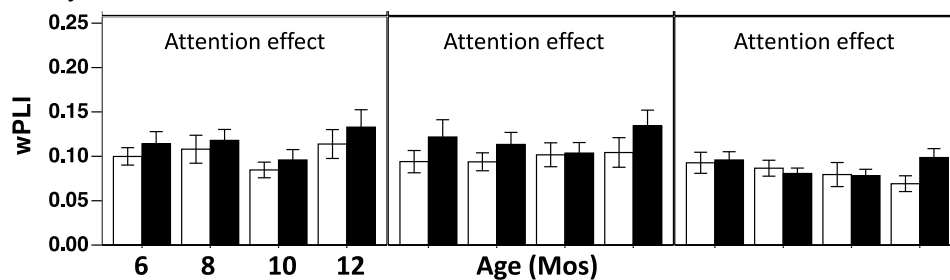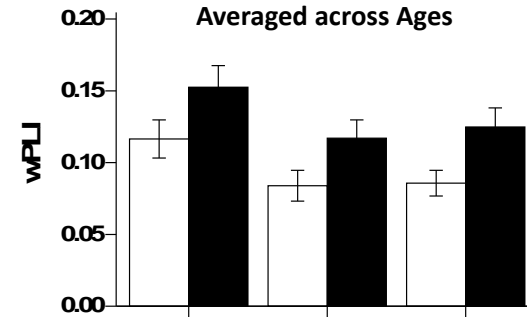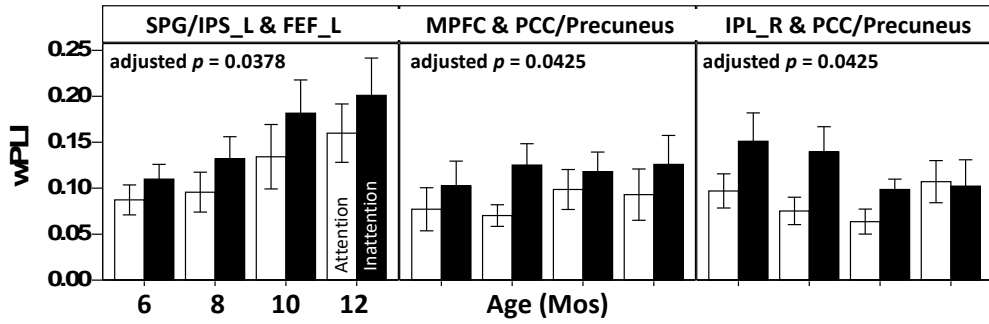
Figure 4.10 Individual bars that represent the mean connectivity (wPLI value) within the five brain networks for different attention phases, ages, and frequency bands.

Dorsal attention network The analysis for the dorsal attention network showed that the attention effect on functional connections varied across the three frequency bands. There was a significant interaction between attention phase and frequency band, $F(2, 110) = 5.78$, $p = 0.0041$. Following analyses showed that the mean wPLI value was greater during inattention than sustained attention for the alpha band only. Figure 4.10C shows the changes in the mean wPLI value within the dorsal attention network as a function of attention phase, age, and frequency band. It can be seen that the mean wPLI value was overall greater during inattention than sustained attention in the alpha band. Post-hoc comparisons ($p < 0.05$, corrected by FDR) were conducted to analyze the attention effect for individual pairs of connections between the ROIs within the dorsal attention network in the alpha band. It was found that the wPLI value between the left SPG/IPS and left FEF was significantly greater during inattention than sustained attention. Figure 4.11A includes individual bars that represent the wPLI value in the alpha band between the left SPG/IPS and the FEF across attention phases and ages. It shows that the connectivity between these two ROIs increased with age and becomes greater during inattention than sustained attention. Figure 4.11B depicts the difference in the wPLI value between sustained attention and inattention (inattention – sustained attention) for the connections between the ROIs within the dorsal attention network and the DMN in a 3D brain surface. The thickness of the lines between the ROIs represents how big the

difference is between the two attention phases, with thicker lines meaning greater difference. It can be seen that the greater connectivity in the alpha band is clearly shown between the left FEF and the left SPG/IPS. The attention effect is also shown between the

71

A.

SPG/IPS_L & FEF_L
adjusted *p* = 0.0378

MPFC & PCC/Precuneus
adjusted *p* = 0.0425

IPL_R & PCC/Precuneus
adjusted *p* = 0.0425

Age (Mos)

Averaged across Ages

B.

wPLI difference: Inattn - Attn

Dorsal attention

DMN
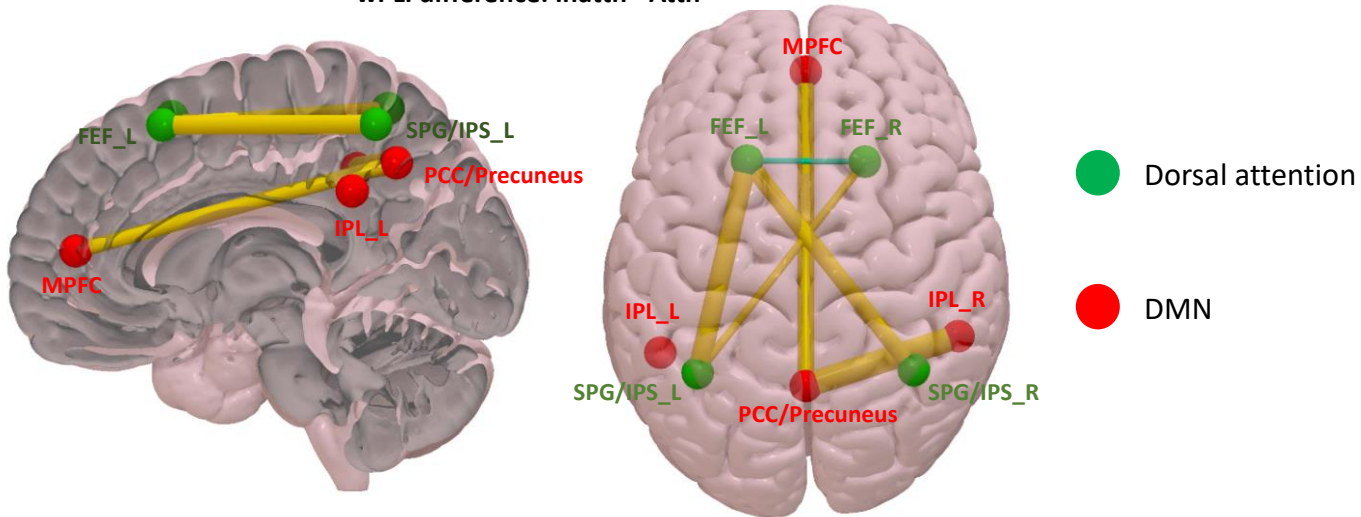
Figure 4.11 Functional connectivity in the alpha band for the dorsal attention and default mode networks. (A) The wPLI value for the three pairs of connections that showed significant difference between sustained attention and inattention in the alpha band. (B) The difference in the wPLI value between sustained attention and inattention in the alpha band. The spheres represent the nodes (ROIs) within the dorsal attention network (green) and the DMN (red). The lines represent the difference in the wPLI value between sustained attention and inattention (inattention – sustained attention) for the connections between the nodes. A threshold of 0.01 was used for the display of the connections. The thickness of the lines represents the value of the difference, with thicker lines represent greater values. *Note*: only the difference between the three pairs of connections shown in A. reached the significance level ($p < 0.05$) after FDR control.

left FEF and the right SPG/IPS, but this difference did not reach the significance level after FDR control.

The ANOVA for the dorsal attention network also revealed an interaction between age and frequency band, $F (6, 110) = 4.34$, $p = 0.00060$. This interaction was driven by an age effect found in the alpha band only, $F (3, 55) = 11.73$, $p < 0.0001$. The mean wPLI value was found to increase with age for the alpha band. Figure 4.10C shows the increase in the mean wPLI value from 6 to 12 months in the alpha band.

Ventral attention network The analysis for the ventral attention network showed marginal main effects for attention phase, $F (1, 55) = 3.84$, $p = 0.055$, and age $F (3, 55) = 2.48$, $p = 0.070$. The individual bars for the mean wPLI value within the ventral attention network are plotted in Figure 4.10D. The mean wPLI value appears to increase with age in the theta and alpha bands, although it did not reach the significance level.

Default model network The analysis for the DMN showed a significant main effect for attention phase, $F (1, 55) = 6.08$, $p = 0.0168$. The mean wPLI value was greater during inattention than sustained attention. This attention effect was not found to interact with frequency band (Figure 4.10E). Post hoc comparisons ($p < 0.05$, corrected by FDR) were conducted to analyze the attention effect for individual pairs of connections between the ROIs within the DMN. It was found that the wPLI values in the alpha band between the medial prefrontal cortex and the PCC/Precuneus and between the right inferior parietal lobule and the PCC/Precuneus were significantly greater during inattention than sustained attention. The comparisons for the connections in the theta and beta bands did not show any significance result after the FDR control. Figure 4.11A shows individual bars that represent the wPLI values for the two pairs of ROIs showing significance

attention effect in the alpha band. The wPLI values appear to be greater during inattention than sustained attention. The difference between attention and inattention in these connections also are depicted in a 3D brain surface in Figure 4.11B.

Connections between the 20 ROIs The difference between sustained attention and inattention also appeared to exist in the functional connectivity between the five brain networks. Figure 4.12 shows the difference in the wPLI value between sustained attention and inattention for all the 20 ROIs in the five networks with a network intensity of 10%. Both circular maps (top panel) and adjacency matrices are displayed in the figure. Figure 4.12A shows the difference for the theta band. It can be seen that the overall functional connectivity during inattention was greater than that during sustained attention. There was no specific pattern observed for the theta band. Figure 4.12B shows the difference for the alpha band. The circular maps demonstrate that about half of the connections that were greater for inattention involved the ROIs in the DMN, especially the PCC/Precuneus. This information also is shown by the adjacency matrix. Figure 4.12C shows the difference for the beta band. It can be seen from the circular maps and the adjacency matrices that most of the connections that were greater during inattention involved the ROIs in the visual network. No statistical analysis was conducted for these connections between networks.

Summary of the seed-based connectivity analysis for the brain networks
Functional connectivity between brain ROIs were found to change with age and attention phase. Infant sustained attention was found to have an impact on the averaged functional connectivity within the DMN and the dorsal attention network in the alpha band. In addition, the averaged functional connectivity in the alpha band within the visual,

75

Figure 4.12 Circular maps and adjacency matrices for the difference in the connectivity between sustained attention and inattention for the 20 ROIs composing the five brain networks, separately for the theta (A), alpha (B), and beta (C) frequency bands.

Figure 4.12 Circular maps and adjacency matrices for the difference in the connectivity between sustained attention and inattention for the 20 ROIs composing the five brain networks, separately for the theta (A), alpha (B), and beta (C) frequency bands.
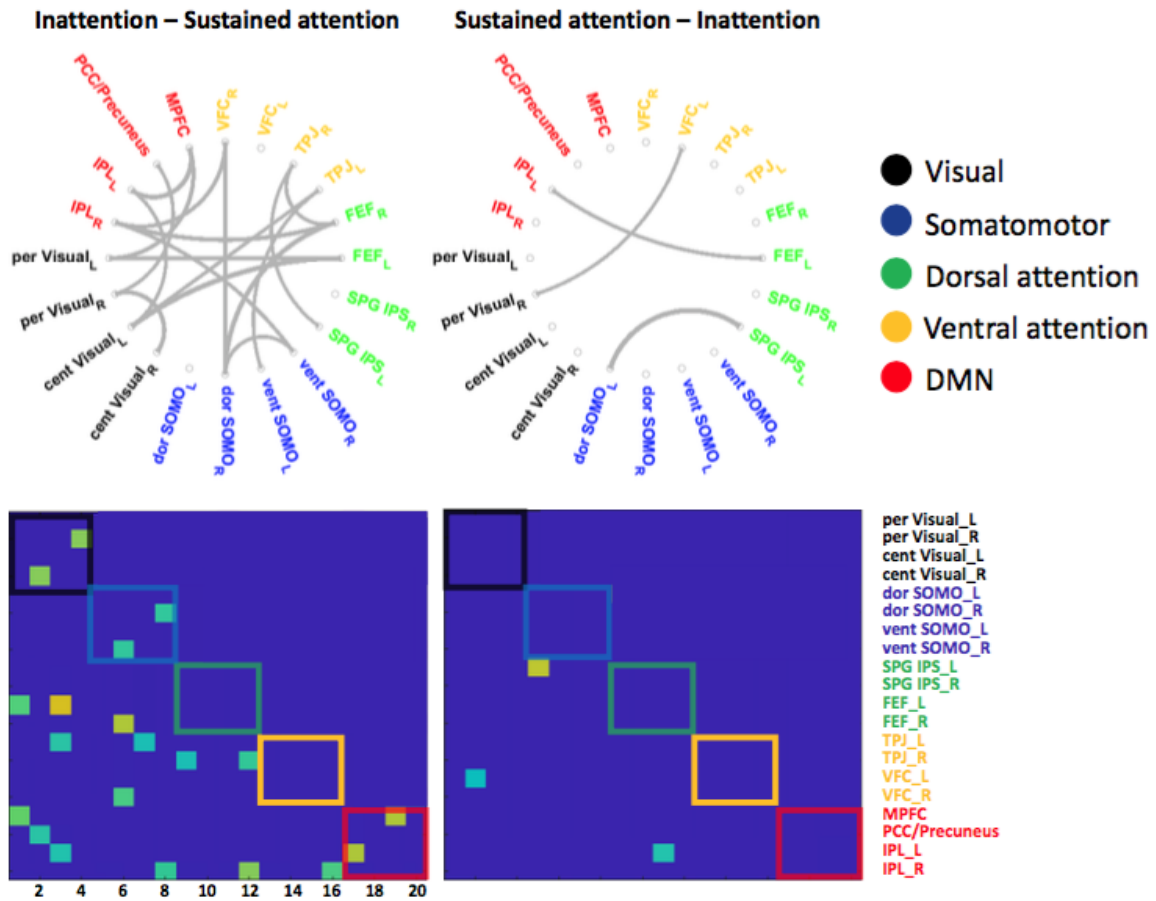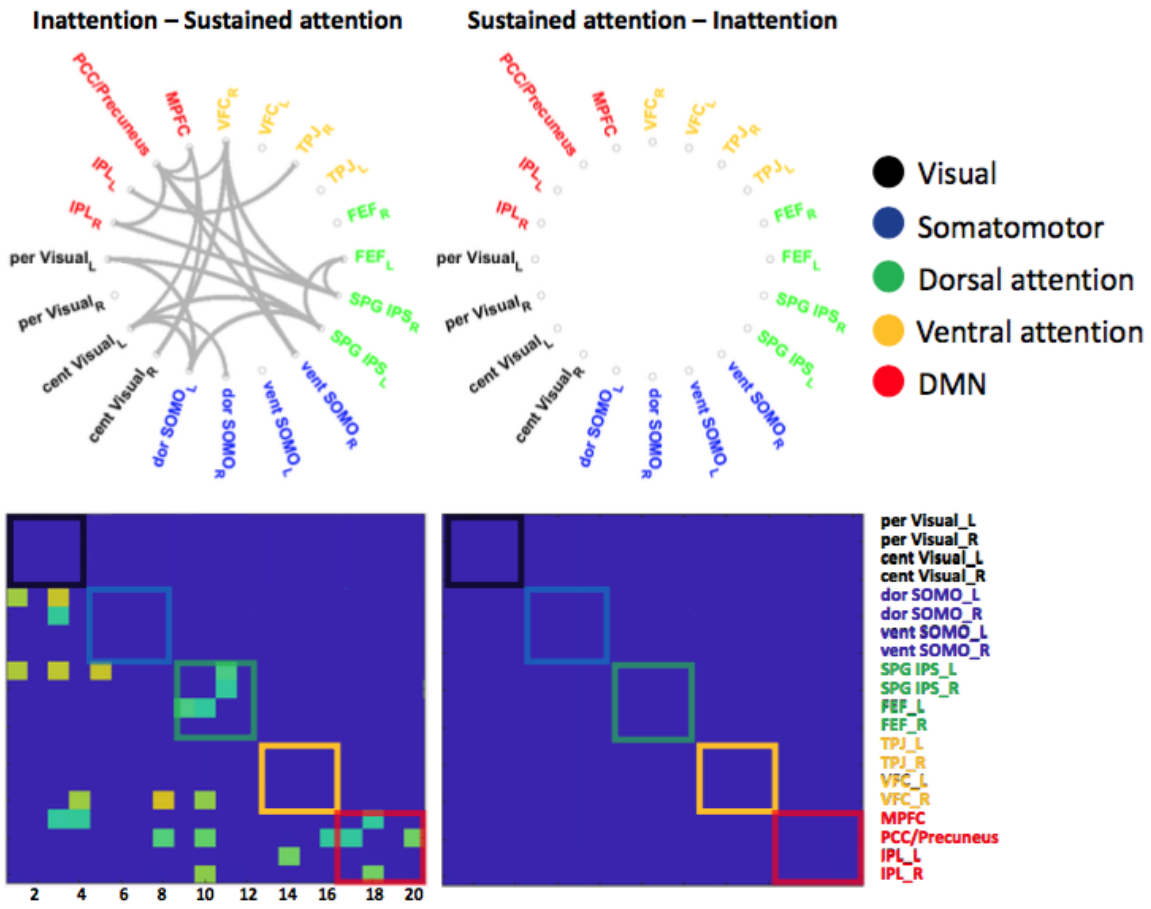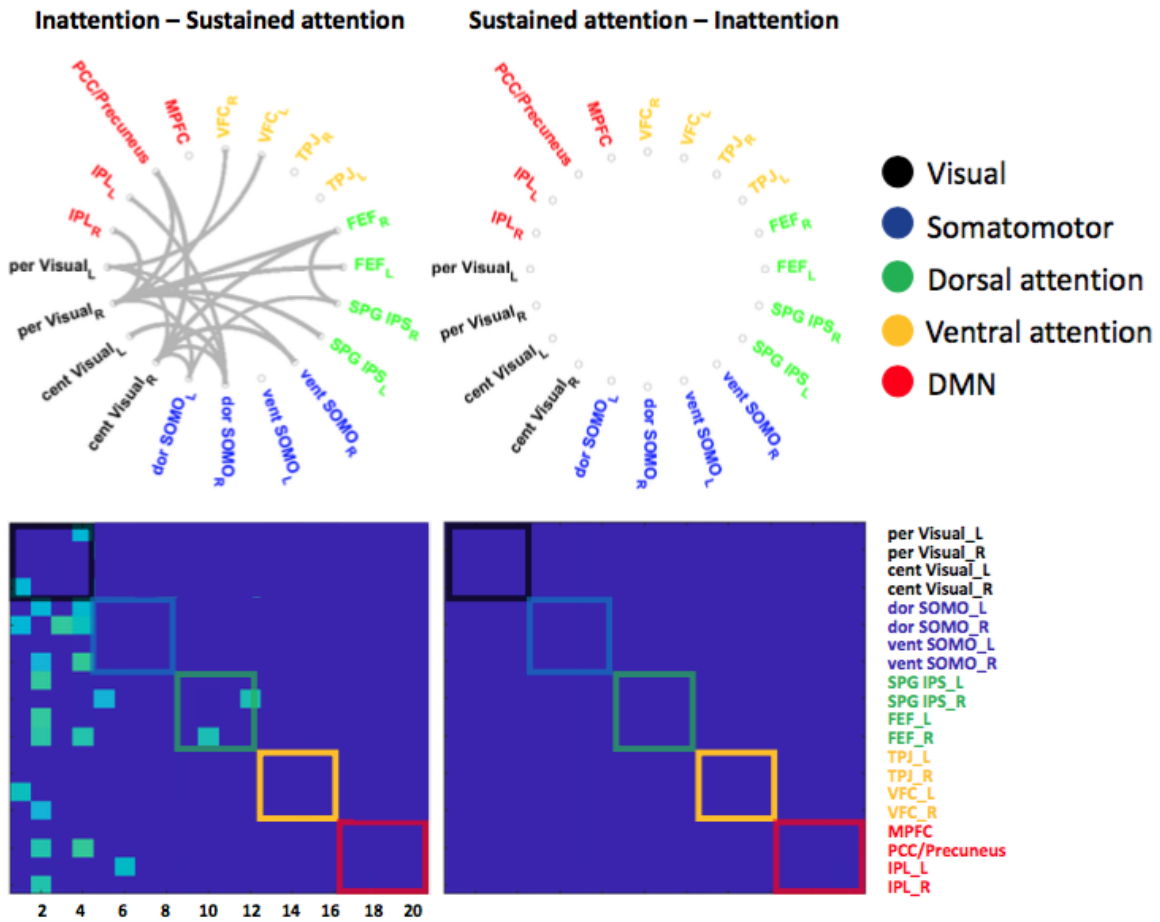
Figure 4.12 Circular maps and adjacency matrices for the difference in the connectivity between sustained attention and inattention for the 20 ROIs composing the five brain networks, separately for the theta (A), alpha (B), and beta (C) frequency bands.

somatosensory, dorsal attention, and ventral attention networks were found to increase with age. The illustration of the connections between the 20 seeds (ROIs) in circular maps and adjacency matrices indicate that the difference between sustained attention and inattention may also exist in the functional connectivity between the five networks. The detailed results are summarized in Table 5.

Connectivity Analysis for the Virtual Channel Clusters on the Sensor Level

The adjacency matrices obtained from the functional connectivity analysis for the EEG electrodes were reorganized in the order of the 10 virtual clusters. Figure 4.13A shows the reorganized adjacency matrices for the connectivity in the theta band during inattention and sustained attention (top panel). Figure 4.13A also shows the difference in connectivity between the two attention phases (bottom panel) with a network intensity of 10%. The connectivity during inattention appears to be greater than that during sustained attention in the theta band. This difference is shown in most of the clusters, except for the left temporal and frontal pole clusters. Figure 4.13B shows the adjacency matrices for the alpha band. The difference between sustained attention and inattention is mostly shown in the central and parietal clusters. There are also patterns of frontoparietal and frontocentral connections shown for the difference between sustained attention and inattention. The connectivity between the frontal clusters and the central and parietal clusters in the alpha band appears to be greater during inattention than sustained attention (Figure 4.13B). Figure 4.13C shows this kind of adjacency matrices for the beta band. The connectivity during inattention appears to be greater than that during sustained attention. However, there is no clear pattern shown in this figure.

Table 4.5 *Summary of the major results from the seed-based connectivity analyses.*

Networks	Results	Figures
	Source space	
Visual	i). The mean wPLI value was greater during inattention than sustained attention. No individual pair of ROIs showed significant greater connectivity during inattention than attention.	Figure 12A
	ii). The mean wPLI value increased with age during inattention in the alpha band.	Figure 12A
Somatomotor	i). The mean wPLI value increased with age in the alpha band.	Figure 12B
Dorsal Attention	i). The mean wPLI value was greater during inattention than sustained attention in the alpha band.	Figure 12C
	The wPLI value in the alpha band between left SPG/IPS and left FEF was significantly greater during inattention than sustained attention.	Figure 13
	ii). The mean wPLI value increased with age in the alpha band.	Figure 12C
Ventral Attention	i). Marginal age effect in the theta and alpha bands.	Figure 12D
DMN	i). The mean wPLI value was greater during inattention than sustained attention in the three frequency bands.	Figure 12E
	The wPLI values in the alpha band between MPFC and PCC/Precuneus and between right IPL and PCC/Precuneus were greater during inattention than sustained attention.	Figure 13

Figure 4.13 Adjacency matrices for the connectivity (wPLI value) between EEG electrodes for infant sustained attention, inattention, and the difference between them, separately for the theta (A), alpha (B), and beta (C) frequency bands.

B.

Alpha

Figure 4.13 Adjacency matrices for the connectivity (wPLI value) between EEG electrodes for infant sustained attention, inattention, and the difference between them, separately for the theta (A), alpha (B), and beta (C) frequency bands.
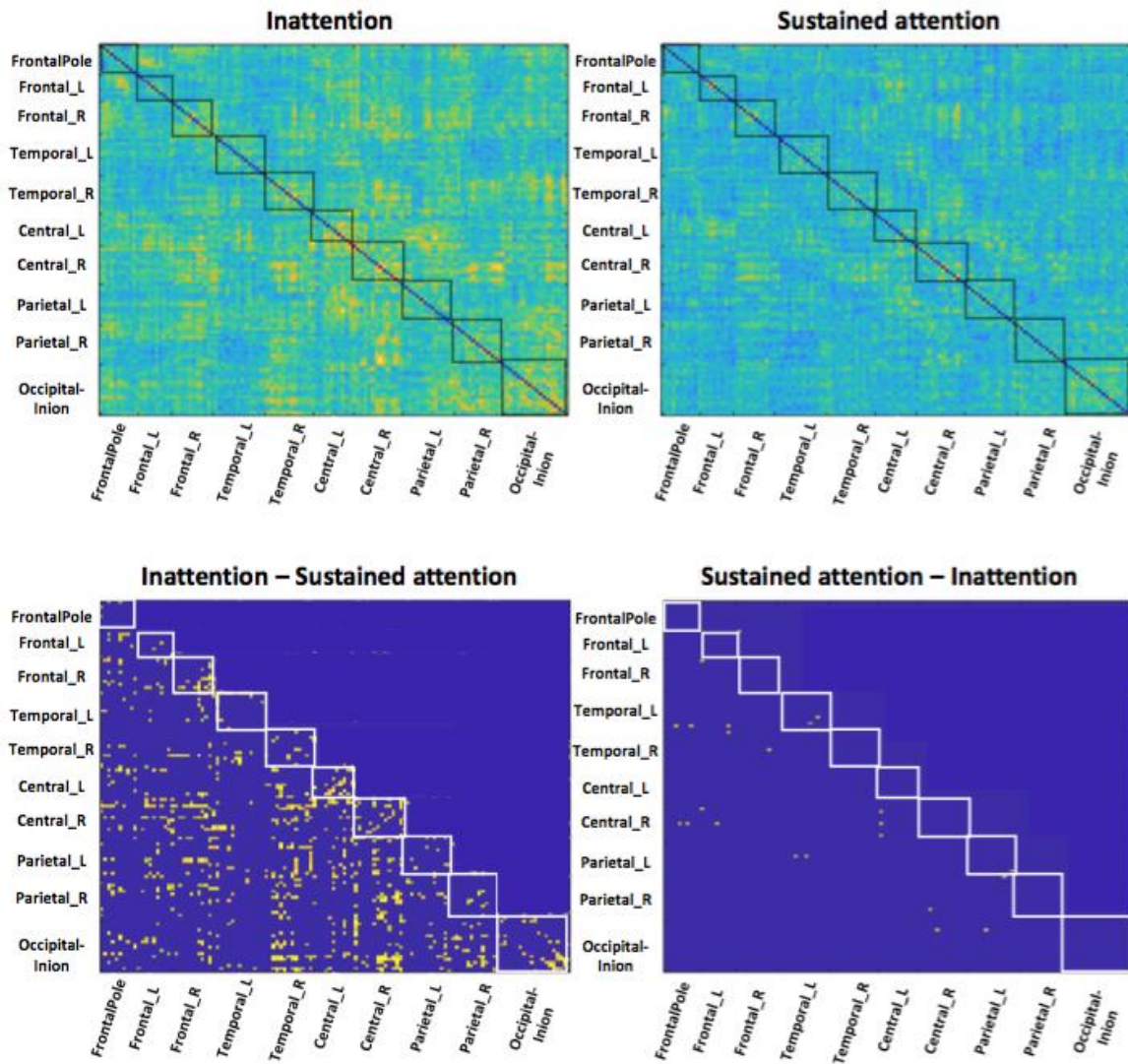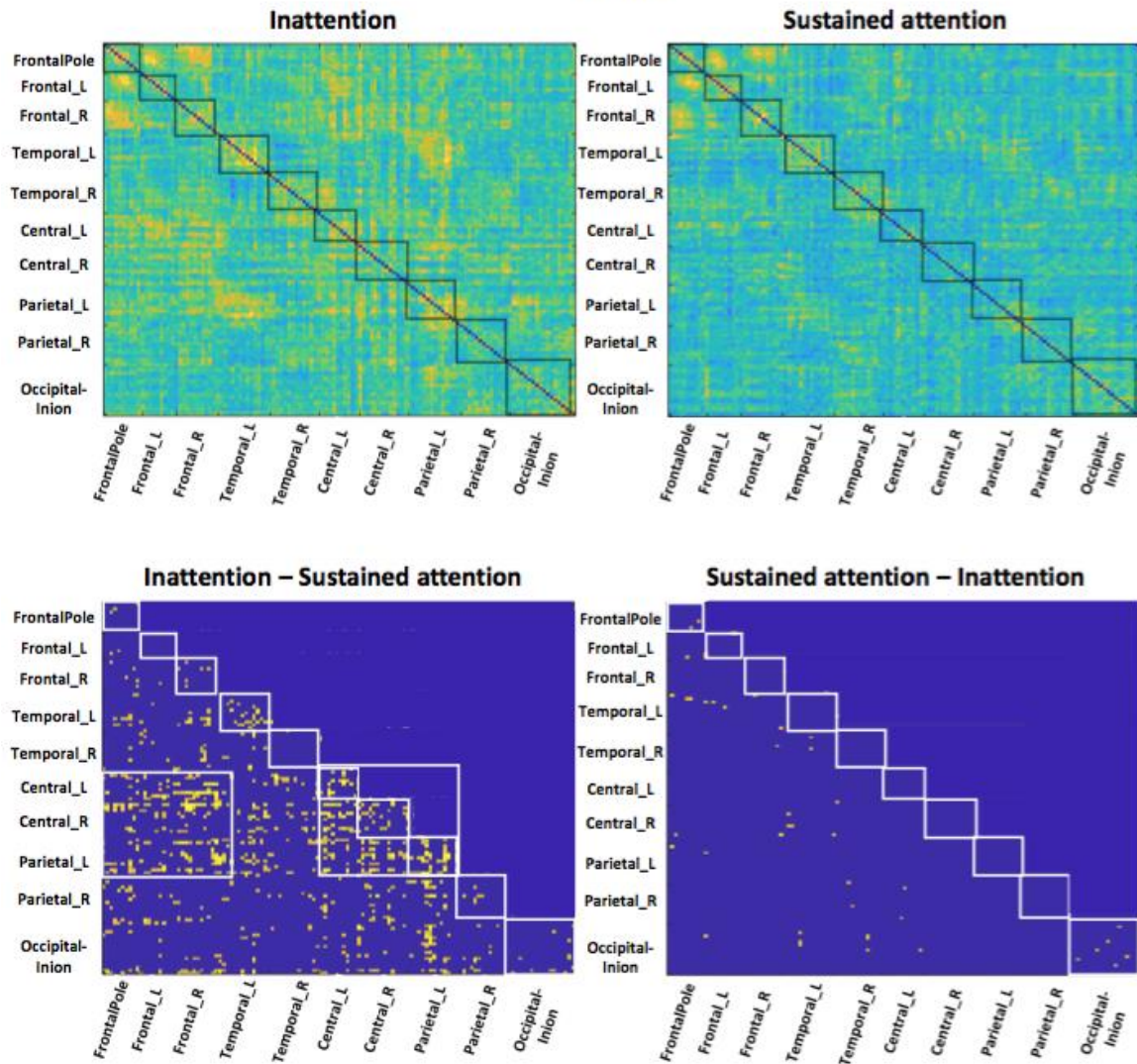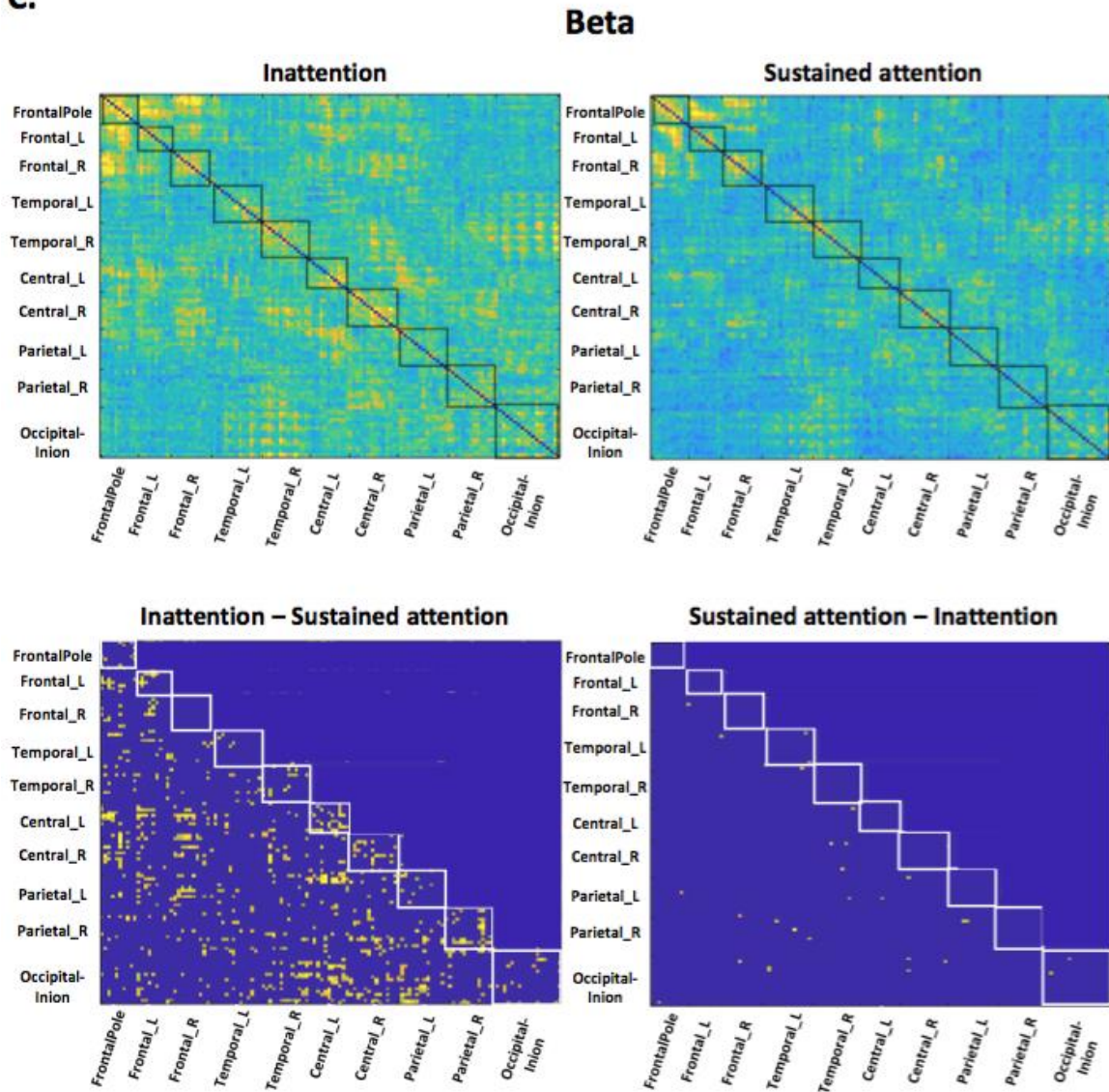
Figure 4.13 Adjacency matrices for the connectivity (wPLI value) between EEG electrodes for infant sustained attention, inattention, and the difference between them, separately for the theta (A), alpha (B), and beta (C) frequency bands.

Discussion

The present study investigated the relation between infant sustained attention and infant brain functional connectivity and its development in the second half of the first year of age. The effects of sustained attention and age were examined in three frequently studied infant EEG rhythms that were the theta (2 – 6 Hz), alpha (6 – 9 Hz), and beta (9 – 13 Hz) rhythms. The primary goal of the dissertation project was to investigate the functional connectivity during infant sustained attention. It was hypothesized that infants would show distinct patterns of brain network topology during sustained attention reflected by graph theory measures, such as the path length, clustering coefficient, and small-worldness. It was also expected to find weaker functional connectivity within the five brain networks in the alpha band and stronger connectivity in the theta band during sustained attention. Our results lent support to part of these hypotheses. Distinct patterns of brain network topology were found with graph theory measures for sustained attention. The path length was longer and the clustering coefficient was lower during sustained attention than inattention. However, there was no difference in the small-worldness between the two attention phases. Seed-based connectivity analysis showed that the connectivity within the DMN and the dorsal attention network was weaker in the alpha band during sustained attention than inattention. The connectivity between the networks also appeared to be weaker during sustained attention in the alpha band. However, no theta effect was found in terms of the connectivity within the networks. The overall connectivity between the networks appeared to be weaker in the theta and beta bands during sustained attention.

The second goal of this study was to investigate the development of brain functional connectivity from 6 to 12 months of age using EEG measures. The path length was expected to decrease with age, while the clustering coefficient and small-worldness were expected to increase with age. The functional connectivity between ROIs within the five brain networks was hypothesized to increase with age. The current results supported the majority of these hypotheses. The path length was found to decrease with age and the clustering coefficient was found to increase with age in the theta and alpha bands. These results were shown in both source space and sensor level analyses. Infants at 6 and 8 months showed the feature of small-worldness in their brain networks with low network intensity. However, the feature of small-worldness was not found at the two older ages. The functional connectivity within the visual, somatosensory, and dorsal attention networks were found to increase with age in the alpha band. However, no change of connectivity within the networks with age was found for the theta and beta bands.

Functional Connectivity in Major Brain Networks during Infant Sustained Attention

The finding of the weaker functional connectivity in the alpha band during sustained attention in the DMN indicates the important role that the DMN plays in infant attention. Attenuated alpha power during infant sustained attention has been shown by previous EEG research (Orekhova, Stroganova, & Posikera, 2001; Xie et al., 2017). Xie and colleagues localized the attenuated alpha activity to the brain regions composing the DMN using the technique of EEG source analysis. It should be noted that the current project and Xie et al. (2017) used the same data but for different analyses and research goals. The finding in the current study suggests that the functional connectivity in the

alpha band between the components of the DMN also is attenuated during sustained attention (Figure 4.10E, 13). This finding supports the idea that enhanced brain alertness and attention allocation during infant sustained attention might be caused by attenuated activity in the DMN. The attention effect on the connectivity within the DMN was primarily shown at 12 months (Figure 4.10E). This is consistent with the finding from the power analysis that the attention effect on the alpha power within the DMN did not appear until 12 months of age (Xie et al., 2017).

The changes in functional connectivity observed here should not be simply caused by the changes in EEG power. The wPLI technique used in the current study was designed to diminish the effect of the amplitude on the connectivity between two electrodes or ROIs. In addition, many impacts of attention on EEG power found by Xie et al. (2017) were not shown here for the functional brain connectivity.

Infant sustained attention is also associated with a decrease of functional connectivity in the alpha band in the dorsal attention network. The current study uses a paradigm including dancing Sesame Street characters presented in different locations. The areas included in the dorsal attention network (e.g., the FEF and SPG/IPS) are crucial for spatial attention orienting, goal-directed selection for stimuli, and planning for eye-movements (Corbetta & Shulman, 2002; Peterson & Posner, 2012). Therefore, this network is very likely to be active during the presentation in this experiment, although the trials with eye movements have been excluded from the analyses. The finding of the decreased connectivity in the alpha band might suggest the releasing of the dorsal attention system (i.e., task-relevant areas) from inhibition (Klimesch, Sauseng, & Hanslmayr, 2007).

An alternative explanation of the findings in the two attention-related networks is that the connectivity over the entire brain decreased during infant sustained attention. The connections between ROIs within the other three networks did not reach the significance level when they were analyzed individually with control for multiple comparisons. However, the connections between these ROIs still appeared to be attenuated during infant sustained attention (Figure 4.12). The overall decreased functional connectivity in the brain also was shown by the graph theory measures, which will be discussed in the next section. Therefore, the weaker connectivity within the dorsal attention and the DMN might also be due to the overall decreased connectivity during sustained attention.

The weakened connectivity in the alpha band found for the frontal, central, and parietal sensor clusters might be underlain by the decreased connectivity in the DMN and the dorsal attention network. The connectivity between the frontal cluster and the central and parietal clusters appeared to be weakened for the alpha band during infant sustained attention (Figure 4.13B). This finding suggests the changes occurred in underlying neural mechanisms during infant sustained attention. The cortical source analysis conducted in the current study provides a link between the finding on the scalp and the changes in the brain. The attenuated frontoparietal connectivity between the components in the DMN (the MPFC and PCC/Precuneus) and the dorsal attention network (the FEF and the SPG/IPS) might cause the distinct patterns observed on the sensor level.

The effect of sustained attention on the functional connectivity in the beta band indicates a delayed development of the beta rhythm during infancy. Differentiated functional connectivity was found within the visual network and the DMN for the beta band during sustained attention. However, this pattern was only shown at 12 months.

This finding suggests that it might be difficult to identify the functional role of the beta rhythm in infant cognition until the end of the first year. A previous study did not find difference in beta power between sustained attention and inattention at 12 months with the same experimental design (Xie et al., 2017). These findings suggest a much delayed development of the beta rhythm. Future studies need to be conducted to determine the developmental trajectory of the beta rhythm and its relation to infant cognition.

Distinct Network Topology during Infant Sustained Attention

Infant sustained attention is accompanied by an attenuation of brain network integration and segregation. The finding of shorter path length and higher clustering coefficient during inattention than sustained attention suggests that the long-distance (integration) and local (segregation) communications between cortical regions are weakened during sustained attention (Figure 4.7, 4.8, 4.10, and 4.11). This distinct pattern of brain network topology was revealed by the analyses in the source space and those on the sensor level. This finding is inconsistent with my hypothesis that was made based on the improved information processing found during sustained attention by previous research (e.g., Richards, 2008, Xie et al., 2017, Xie & Richards, 2016a).

One explanation of this finding is that infant brain networks become more randomized with higher cost for local and global communications during inattention. This explanation is consistent with the findings by studies on the attention deficit hyperactivity disorder (ADHD). Decreased path length and increased clustering coefficient have been found in children with ADHD using EEG measures (Ahmadlou, Adeli, & Adeli, 2012), although fMRI research has shown a different pattern of increased clustering coefficient and path length in ADHD children (Cao, Shu, Cao, Wang, & He,

88

2014). The atypical network topology found in these studies with ADHD children has been seen as a reflection of a more random network organization with higher cost for connections. Therefore, it is plausible that the brain network topology during infant inattention is comparable to that shown in ADHD children with stronger but high-cost connections between brain regions.

The distinct patterns of network topology found during infant inattention might also be analogous to the compensation effect after sleep deprivation. Decreased path length and increased clustering coefficient have been found in participants after sleep deprivation (Liu, Li, Wang, & Lei, 2014). This pattern of enhanced network integration and segregation could be a reflection of the adaptive mechanisms in the brain under conditions of diminished attention resources due to insufficient sleep (Liu et al., 2014). Similar adaptive mechanisms might occur during infant inattention when the attention resources are limited and the information processing is less efficient compared to sustained attention.

The current study suggests novel neural correlates of infant sustained attention with respect to graph theory measures. Infant sustained attention has been associated with amplified ERP responses (Guy et al., 2016; Xie & Richards, 2016a, b) and attenuated alpha power (Xie et al., 2017). The current study suggests that infant sustained attention is also associated with longer path length and lower clustering coefficient. These features of network topology indicate a less randomized and overall more cost-effective organization of brain networks during sustained attention. Infant sustained inattention is characterized by a deceleration of HR caused by an increase of the function of the parasympathetic system (Richards, 2008). This is accompanied by an increase of the

function of the tonic alerting system (Richards, 2008; Xie et al., 2017). The changes in the neurotransmitter system and the alerting network should have an impact on the communication between subcortical (e.g., the thalamus) and cortical regions. This in turn might result in the distinct patterns of brain network topology found during infant sustained attention in different frequency bands. This possibility needs to be further investigated with different functional connectivity and graph theory measures, such as measuring the correlation between hemodynamic signals and using binary brain networks.

The Functional Connectivity in Major Brain Networks Increases with Age

The current study suggests a rapid change in the strength of functional connectivity within the major brain networks during the first year of age. An increase of the strength of functional connectivity was found in the alpha band for the visual, somatosensory, dorsal attention, and ventral attention networks (Figure 4.10). This dramatic development from 6 to 12 months is consistent with the increase of the overall brain functional connectivity shown by the graph theory measures discussed in the next section. Only the DMN did not show an increase of functional connectivity within the network. The absence of the age effect for the DMN is in line with previous fMRI research showing that the functional connectivity in the DMN is not exhibited until 12 months of age (Gao et al., 2009; 2011).

The development of brain functional connectivity in these networks varies across the frequency bands. The age effect was predominately found in the alpha band with only a marginal effect shown for the theta band and no effect shown for the beta band. The finding of no change in the beta band connectivity is consistent with a previous study

showing no age effect on the beta power from 6 to 12 months (Xie et al., 2017). However, the finding of no change in the theta band connectivity is inconsistent with my hypothesis nor with the graph theory findings discussed later. Previous studies have shown that the relation between the theta rhythm and infant attention is well established by 8 months of age (Orekhova et al., 1999; Xie et al., 2017). It is possible that the theta band connectivity in these brain networks develops dramatically in the first few months of life but with a much slower pace in the second half of the first year. Studies have shown that the peak of the infant theta and alpha rhythms changes over infancy (Marshall et al., 2002; Xie et al., 2017). The choice of the range of the frequency bands in the current study was based on past infant research (e.g., Marshall et al., 2002; Orekhova et al., 1999). Another possibility for finding no age effect in the theta rhythm could be that the band (2 – 6 Hz) used to define the theta rhythm may not cover the most dramatic connectivity changes for some subjects. Future research may identify the peak frequency for each infant rhythm sot that the connectivity changes can be better examined.

Development of Brain Network Topology in the Second Half of the First Year

There is an increase of functional integration and segregation of information processing over the development from 6 to 12 months of life from a graph theory perspective. The finding of the decrease of path length and increase of clustering coefficient in the theta and alpha bands indicates the changes in the global and local efficiency of information processing in brain networks. This finding is parallel to the existing EEG literature that has shown the development of functional integration and segregation of brain networks from early childhood (e.g., 2 to 4 years) to adolescence (Bathelt et al., 2013; Boersma et al., 2011; Miskovic et al., 2015; Smit et al., 2012). The

91

current study extends our understanding of the development of functional networks in different frequency rhythms from childhood (over 2 years of age) to infancy.

The changes in these graph theory measures primarily occur in the theta and alpha frequency bands during infancy. No dramatic change in path length, clustering coefficient, or small-worldness was found for the beta band in the source space analysis. This finding suggests that the communication of information between brain regions might rely more on the oscillatory signals in the infant theta and alpha bands than the oscillations in the beta band. The delayed development of functional connectivity in the beta band is compatible with the fact that the functional significance of the beta band oscillations is still not clear during infancy (Cuevas et al., 2014; Xie et al., 2017). Prior EEG studies have shown changes in brain network topology in the beta band during childhood and adolescence (e.g., Bathelt et al., 2013; Boersma et al., 2011). Future research may examine the brain functional connectivity in the beta band with infants older than a year of age.

It should be noted that there were also inconsistent findings among these EEG studies. For example, some studies have found an increase of path length in the alpha band over childhood and adolescence (Boersma et al., 2011; Smit et al., 2012), while the current study and others have shown a decrease of path length in the alpha band with age (Bathelt et al., 2013; Miskovic et al., 2015). The different techniques (e.g., Pearson correlation, imaginary part of the coherency, wPLI, and SL) used to measure the functional connectivity between EEG signals might have contributed to these inconsistent findings (Bastos & Schoffelen, 2016; Vinck et al., 2011). A recent study has shown that the choice of the inverse solution (e.g., beamformer solutions vs. eLORETA distributed

solutions) and the software package (e.g., Fieldtrip vs. Brainstorm) also has an impact on the connectivity results (Mahjoory et al., 2017). Future research should be conducted to investigate the potential difference caused by using different connectivity measures and techniques in the study of brain networks with pediatric populations.

The current study provides convergent evidence for the development of brain network topology during infancy that has been shown by resting-state fMRI research. A prior fMRI study has found rapid changes in the global and local reconfigurations in brain networks during the first year of life (Gao et al., 2011). The findings in the current study also indicate rapid changes in the efficiency of global and local communication of information between brain regions. The small-world connectional architecture for brain networks was observed in the alpha and beta bands at 6 and 8 months with low network intensities. This finding is consistent with previous fMRI studies showing an early presence of the small-worldness for brain networks in newborn (Fransson et al., 2011) and preterm infants (Cao et al., 2017; van den Heuvel et al., 2015). However, the absence of the small-worldness at 10 and 12 months is inconsistent with the fMRI literature that has suggested a continued development of the small-worldness throughout the first few years of life (Cao et al., 2016; Fair et al., 2009; Power et al., 2010). The experimental paradigm used by the current study was not resting-state because infants were watching Sesame Street videos. This kind of dynamic stimuli becomes more attractive with age from 6 to 12 months (Courage et al., 2006). The enhanced engagement in the "task" among the older infants might result in the finding of no small-worldness for brain networks at 10 and 12 months. Future study should consider testing the

development of brain network topology using graph theory measures and EEG recordings with a resting-state paradigm.

The Study of Functional Connectivity in the Source Space and on the Sensor Level

The study of the network topology with graph theory measures in the source space and on the sensor level might show both similar and inconsistent findings. The sustained attention effect was found for infants across ages using graph theory measures with the 48 LPBA cortical ROIs, as well as the 126 GSN/HGSN electrodes. In addition, both types of analyses showed the development of clustering coefficient in the alpha band and the small-worldness at younger ages with low network intensities. However, there were also inconsistent findings of the graph theory measures between the analyses in the source space and those on the sensor level. For example, the development of path length across ages was only found in the source space. The development of path length and clustering coefficient in the theta and alpha bands was consistently shown by the analyses in the source space, while the sensor level analyses only showed changes of the clustering coefficient in the alpha and beta bands. The difference in the number of nodes (48 vs. 126) and the spurious connections between EEG electrodes caused by the volume conduction issue may contribute to the inconsistent findings between the analyses in the source space and those on the sensor level.

The information about the seed-based functional connectivity between brain ROIs might only be obtained by conducting the analyses in the source space. The measurement of the connectivity between EEG electrodes suggests that the communication between the underlying neural networks varies with infant attention state and develops with age. However, it is difficult to link the changes in the electrodes to the changes in specific

94

brain ROIs. The current study solves this issue by measuring the connectivity between reconstructed source activities in brain ROIs.

Conclusion

The current study advances our understanding of infant sustained attention and its development. The current findings extend the Richards' heart rate model of infant sustained attention (Richards & Casey, 1992) by establishing a connection between sustained attention and brain functional connectivity. The work here also sheds light on the development of infant sustained attention. The attenuated within network connectivity in the alpha band was observed at 6 months for the dorsal attention network. The attention effect on the overall network topology in a graph theory perspective also was found from 6 months of age. However, the attention effect for the DMN was not observed until 12 months of age. The interaction between sustained attention, age, and brain networks suggests that changes in infant sustained attention still occur from 6 to 12 months and the relation between attention and age might vary across brain networks.

The current study also suggests that cortical source analysis with EEG data can be used with infant participants to study the functional connectivity in brain networks. The usage of age-appropriate average MRI templates for source analysis should minimize the errors that would be caused by using an adult MRI given the differences in the anatomical features between infants' and adults' brain. The method used in the current study suggests an alternative way to examine the development of brain networks. This method should be particularly useful for infant studies because of the easy application of EEG and its tolerance to movement compared to fMRI with infants. Similar findings on the development of brain networks have been shown by the current study in comparison

to previous infant MRI research. These findings might serve as a reference that allows us to identify the disruptions in the brain networks of children with neurodevelopmental disorders (e.g., ASD and ADHD).

REFERENCES

Ahmadlou, M., Adeli, H., & Adeli, A. (2012). Graph theoretical analysis of organization of functional brain networks in ADHD. *Clin EEG Neurosci, 43*(1), 5-13. doi:10.1177/1550059411428555

Babiloni, F., Cincotti, F., Babiloni, C., Carducci, F., Mattia, D., Astolfi, L., . . . He, B. (2005). Estimation of the cortical functional connectivity with the multimodal integration of high-resolution EEG and fMRI data by directed transfer function. *Neuroimage, 24*(1), 118-131. doi:10.1016/j.neuroimage.2004.09.036

Bastos, A. M., & Schoffelen, J. M. (2016). A Tutorial Review of Functional Connectivity Analysis Methods and Their Interpretational Pitfalls. *Front Syst Neurosci, 9*. doi:Artn 175

10.3389/Fnsys.2015.00175

Bathelt, J., O'Reilly, H., Clayden, J. D., Cross, J. H., & de Haan, M. (2013). Functional brain network organisation of children between 2 and 5 years derived from reconstructed activity of cortical sources of high-density EEG recordings. *Neuroimage, 82*, 595-604. doi:10.1016/j.neuroimage.2013.06.003

Berg, W. K., & Berg, K. M. (1979). Psychophysiological development in infancy: state, sensory function, and attention. In J. D. Osofsky (Ed.), *Handbook of Infant Development* (pp. 243-283). New York: Wiley

Boersma, M., Smit, D. J., Boomsma, D. I., De Geus, E. J., Delemarre-van de Waal, H. A., & Stam, C. J. (2013). Growing trees in child brains: graph theoretical analysis of electroencephalography-derived minimum spanning tree in 5- and 7-year-old children reflects brain maturation. *Brain Connect, 3*(1), 50-60. doi:10.1089/brain.2012.0106

Boersma, M., Smit, D. J., de Bie, H. M., Van Baal, G. C., Boomsma, D. I., de Geus, E. J., . . . Stam, C. J. (2011). Network analysis of resting state EEG in the developing young brain: structure comes with maturation. *Hum Brain Mapp, 32*(3), 413-425. doi:10.1002/hbm.21030

Bullmore, E., & Sporns, O. (2009). Complex brain networks: graph theoretical analysis of structural and functional systems. *Nat Rev Neurosci, 10*(3), 186-198. doi:10.1038/nrn2575

Cao, M., He, Y., Dai, Z. J., Liao, X. H., Jeon, T. N., Ouyang, M. H., . . . Huang, H. (2017). Early Development of Functional Network Segregation Revealed by Connectomic Analysis of the Preterm Human Brain. *Cereb Cortex, 27*(3), 1949-1963. doi:10.1093/cercor/bhw038

Cao, M., Huang, H., Peng, Y., Dong, Q., & He, Y. (2016). Toward Developmental Connectomics of the Human Brain. *Frontiers in Neuroanatomy, 10*. doi:ARTN 25 10.3389/fnana.2016.00025

Cao, M., Shu, N., Cao, Q., Wang, Y., & He, Y. (2014). Imaging functional and structural brain connectomics in attention-deficit/hyperactivity disorder. *Molecular Neurobiology, 50*(3), 1111-1123. doi:10.1007/s12035-014-8685-x

Casey, B. J., & Richards, J. E. (1988). Sustained Visual-Attention In Young Infants

    Measured with an Adapted Version Of the Visual Preference Paradigm. *Child Dev,*

    59(6), 1514-1521. doi:DOI 10.1111/j.1467-8624.1988.tb03679.x

Chu-Shore, C. J., Kramer, M. A., Bianchi, M. T., Caviness, V. S., & Cash, S. S. (2011).

    Network analysis: applications for the developing brain. *J Child Neurol, 26*(4), 488-

    500. doi:10.1177/0883073810385345

Corbetta, M., & Shulman, G. L. (2002). Control of goal-directed and stimulus-driven

    attention in the brain. *Nat Rev Neurosci, 3*(3), 201-215. doi:10.1038/nrn755

Colombo, J. (2001). The development of visual attention in infancy. *Annual Review of*

    Psychology, 52, 337-367. doi:DOI 10.1146/annurev.psych.52.1.337

Colombo, J. (2002). Infant attention grows up: The emergence of a developmental

    cognitive neuroscience perspective. *Curr Dir Psychol Sci, 11*(6), 196-200. doi:Doi

    10.1111/1467-8721.00199

Courage, M. L., Reynolds, G. D., & Richards, J. E. (2006). Infants' attention to patterned

    stimuli: Developmental change from 3 to 12 months of age. *Child Dev, 77*(3), 680-

    695. doi:DOI 10.1111/j.1467-8624.2006.00897.x

Courchesne, E., Ganz, L., & Norcia, A. M. (1981). Event-Related Brain Potentials To

    Human Faces In Infants. *Child Dev, 52*(3), 804-811. doi:DOI 10.1111/j.1467-

    8624.1981.tb03117.x

Cuevas, K., Cannon, E. N., Yoo, K., & Fox, N. A. (2014). The Infant EEG Mu Rhythm:

    Methodological Considerations and Best Practices. *Developmental Review, 34*(1),

    26-43. doi:10.1016/j.dr.2013.12.001

Cuevas, K., Swingler, M. M., Bell, M. A., Marcovitch, S., & Calkins, S. D. (2012). Measures of frontal functioning and the emergence of inhibitory control processes at 10 months of age. *Dev Cogn Neurosci, 2*(2), 235-243. doi:10.1016/j.dcn.2012.01.002

Dai, Z. X., de Souza, J., Lim, J. L., Ho, P. M., Chen, Y., Li, J. H., . . . Sun, Y. (2017). EEG Cortical Connectivity Analysis of Working Memory Reveals Topological Reorganization in Theta and Alpha Bands. *Front Hum Neurosci, 11*. doi:ARTN 237 10.3339/fnhum.2017.00237

Damoiseaux, J. S., Rombouts, S. A., Barkhof, F., Scheltens, P., Stam, C. J., Smith, S. M., & Beckmann, C. F. (2006). Consistent resting-state networks across healthy subjects. *Proc Natl Acad Sci U S A, 103*(37), 13848-13853. doi:10.1073/pnas.0601417103

de Haan, M. (Ed.) (2007). *Infant EEG and Event-related Potentials*. New York: Psychological Press.

De Vico Fallani, F., Astolfi, L., Cincotti, F., Mattia, D., Tocci, A., Marciani, M. G., . . . Babiloni, F. (2007). Extracting information from cortical connectivity patterns estimated from high resolution EEG recordings: a theoretical graph approach. *Brain Topogr, 19*(3), 125-136. doi:10.1007/s10548-007-0019-0

Deboer, T., Scott, L. S., & Nelson, C. A. (2007). Methods for acquiring and analysing infant event-related potentials. In M. De Haan (Ed.), *Infant EEG and Event-related Potentials* (pp. 5-37). London: Psychology Press.

Delorme, A., & Makeig, S. (2004). EEGLAB: an open source toolbox for analysis of single-trial EEG dynamics including independent component analysis. *Journal of Neuroscience Methods, 134*(1), 9-21. doi:DOI 10.1016/j.jneumeth.2003.10.009

Ergenoglu, T., Demiralp, T., Bayraktaroglu, Z., Ergen, M., Beydagi, H., & Uresin, Y. (2004). Alpha rhythm of the EEG modulates visual detection performance in humans. *Cognitive Brain Research, 20*(3), 376-383. doi:10.1016/j.cogbrainres.2004.03.009

Fair, D. A., Cohen, A. L., Dosenbach, N. U. F., Church, J. A., Miezin, F. M., Barch, D. M., . . . Schlaggar, B. L. (2008). The maturing architecture of the brain's default network. *Proceedings of the National Academy of Sciences of the United States of America, 105*(10), 4028-4032. doi:10.1073/pnas.0800376105

Fair, D. A., Cohen, A. L., Power, J. D., Dosenbach, N. U. F., Church, J. A., Miezin, F. M., . . . Petersen, S. E. (2009). Functional Brain Networks Develop from a "Local to Distributed" Organization. *Plos Computational Biology, 5*(5). doi:ARTN e1000381 10.1371/journal.pcbi.1000381

Fair, D. A., Dosenbach, N. U. F., Church, J. A., Cohen, A. L., Brahmbhatt, S., Miezin, F. M., . . . Schlaggar, B. L. (2007). Development of distinct control networks through segregation and integration. *Proceedings of the National Academy of Sciences of the United States of America, 104*(33), 13507-13512. doi:10.1073/pnas.0705843104

Fox, N. A., Bakermans-Kranenburg, M. J., Yoo, K. H., Bowman, L. C., Cannon, E. N., Vanderwert, R. E., . . . van, I. M. H. (2016). Assessing human mirror activity with EEG mu rhythm: A meta-analysis. *Psychol Bull, 142*(3), 291-313. doi:10.1037/bul0000031

Frick, J. E., & Richards, J. E. (2001). Individual differences in infants' recognition of briefly presented visual stimuli. *Infancy, 2*(3), 331-352.

Gao, W., Gilmore, J. H., Giovanello, K. S., Smith, J. K., Shen, D., Zhu, H., & Lin, W. (2011). Temporal and spatial evolution of brain network topology during the first two years of life. *PLoS One, 6*(9), e25278. doi:10.1371/journal.pone.0025278

Gao, W., Zhu, H., Giovanello, K. S., Smith, J. K., Shen, D., Gilmore, J. H., & Lin, W. (2009). Evidence on the emergence of the brain's default network from 2-week-old to 2-year-old healthy pediatric subjects. *Proc Natl Acad Sci U S A, 106*(16), 6790-6795. doi:10.1073/pnas.0811221106

Giedd, J. N., Blumenthal, J., Jeffries, N. O., Castellanos, F. X., Liu, H., Zijdenbos, A., . . . Rapoport, J. L. (1999). Brain development during childhood and adolescence: a longitudinal MRI study. *Nat Neurosci, 2*(10), 861-863. doi:10.1038/13158

Goldenberg, D., & Galvan, A. (2015). The use of functional and effective connectivity techniques to understand the developing brain. *Dev Cogn Neurosci, 12*, 155-164. doi:10.1016/j.dcn.2015.01.011

Guy, M. W., Zieber, N., & Richards, J. E. (2016). The Cortical Development of Specialized Face Processing in Infancy. *Child Dev*. doi:10.1111/cdev.12543

Hammers, A., Allom, R., Koepp, M. J., Free, S. L., Myers, R., Lemieux, L., . . . Duncan, J. S. (2003). Three-dimensional maximum probability atlas of the human brain, with particular reference to the temporal lobe. *Hum Brain Mapp, 19*(4), 224-247. doi:10.1002/hbm.10123

Hicks, J. M., & Richards, J. E. (1998). The effects of stimulus movement and attention on peripheral stimulus localization by 8-to 26-week-old infants. *Infant Behavior & Development, 21*(571-589).

Hillebrand, A., Barnes, G. R., Bosboom, J. L., Berendse, H. W., & Stam, C. J. (2012). Frequency-dependent functional connectivity within resting-state networks: An atlas-based MEG beamformer solution. *Neuroimage, 59*(4), 3909-3921. doi:10.1016/j.neuroimage.2011.11.005

Hunter, S. K., & Richards, J. E. (2003). Peripheral Stimulus Localization by 5- to 14-Week-Old Infants During Phases of Attention. *Infancy, 4*(1), 1-25. doi:10.1207/S15327078IN0401_1

Jackson, J. C., Kantowit.Sr, & Graham, F. K. (1971). Can Newborns Show Cardiac Orienting. *Child Dev, 42*(1), 107-&. doi:DOI 10.1111/j.1467-8624.1971.tb03622.x

Klimesch, W., Sauseng, P., & Hanslmayr, S. (2007). EEG alpha oscillations: the inhibition-timing hypothesis. *Brain Research Reviews, 53*(1), 63-88. doi:10.1016/j.brainresrev.2006.06.003

Knickmeyer, R. C., Gouttard, S., Kang, C., Evans, D., Wilber, K., Smith, J. K., . . . Gilmore, J. H. (2008). A structural MRI study of human brain development from birth to 2 years. *J Neurosci, 28*(47), 12176-12182. doi:10.1523/JNEUROSCI.3479-08.2008

Lansink, J. M., Mintz, S., & Richards, J. E. (2000). The distribution of infant attention during object examination. *Developmental Science, 3*(2), 163-170. doi:10.1111/1467-7687.00109

Lansink, J. M., & Richards, J. E. (1997). Heart rate and behavioral measures of attention in six-, nine-, and twelve-month-old infants during object exploration. *Child Dev, 68*(4), 610-620. doi:Doi 10.2307/1132113

Liao, Y., Acar, Z. A., Makeig, S., & Deak, G. (2015). EEG imaging of toddlers during dyadic turn-taking: Mu-rhythm modulation while producing or observing social actions. *Neuroimage, 112*, 52-60. doi:10.1016/j.neuroimage.2015.02.055

Liu, H., Li, H., Wang, Y., & Lei, X. (2014). Enhanced brain small-worldness after sleep deprivation: a compensatory effect. *Journal of Sleep Research, 23*(5), 554-563. doi:10.1111/jsr.12147

Lowe, M. J., Mock, B. J., & Sorenson, J. A. (1998). Functional connectivity in single and multislice echoplanar imaging using resting-state fluctuations. *Neuroimage, 7*(2), 119-132. doi:DOI 10.1006/nimg.1997.0315

Mahjoory, K., Nikulin, V. V., Botrel, L., Linkenkaer-Hansen, K., Fato, M. M., & Haufe, S. (2017). Consistency of EEG source localization and connectivity estimates. *NeuroImage*, *152*, 590-601.

Mallin, B. M., & Richards, J. E. (2012). Peripheral Stimulus Localization by Infants of Moving Stimuli on Complex Backgrounds. *Infancy, 17*(6), 692-714. doi:10.1111/j.1532-7078.2011.00109.x

Marshall, P. J., Bar-Haim, Y., & Fox, N. A. (2002). Development of the EEG from 5 months to 4 years of age. *Clin Neurophysiol, 113*(8), 1199-1208.

Marshall, P. J., & Meltzoff, A. N. (2011). Neural mirroring systems: Exploring the EEG mu rhythm in human infancy. *Developmental Cognitive Neuroscience, 1*(2), 110-123. doi:10.1016/j.dcn.2010.09.001

Marshall, P. J., Young, T., & Meltzoff, A. N. (2011). Neural correlates of action

   observation and execution in 14-month-old infants: an event-related EEG

   desynchronization study. *Developmental Science, 14*(3), 474-480.

   doi:10.1111/j.1467-7687.2010.00991.x

Maslov, S., & Sneppen, K. (2002). Specificity and stability in topology of protein

   networks. *Science, 296*(5569), 910-913. doi:10.1126/science.1065103

Michel, C. M., & Murray, M. M. (2012). Towards the utilization of EEG as a brain

   imaging tool. *Neuroimage, 61*(2), 371-385. doi:10.1016/j.neuroimage.2011.12.039

Michel, C. M., Murray, M. M., Lantz, G., Gonzalez, S., Spinelli, L., & Grave de Peralta,

   R. (2004). EEG source imaging. *Clin Neurophysiol, 115*(10), 2195-2222.

   doi:10.1016/j.clinph.2004.06.001

Miskovic, V., Ma, X., Chou, C. A., Fan, M., Owens, M., Sayama, H., & Gibb, B. E.

   (2015). Developmental changes in spontaneous electrocortical activity and network

   organization from early to late childhood. *Neuroimage, 118*, 237-247.

   doi:10.1016/j.neuroimage.2015.06.013

Mognon, A., Jovicich, J., Bruzzone, L., & Buiatti, M. (2011). ADJUST: An automatic

   EEG artifact detector based on the joint use of spatial and temporal features.

   Psychophysiology, 48(2), 229-240. doi:10.1111/j.1469-8986.2010.01061.x

Nelson, C. A., & Collins, P. F. (1991). Event-Related Potential And Looking-Time

   Analysis Of Infants Responses To Familiar And Novel Events - Implications for

   Visual Recognition Memory. *Dev Psychol, 27*(1), 50-58. doi:Doi 10.1037//0012-

   1649.27.1.50

Nolte, G., Bai, O., Wheaton, L., Mari, Z., Vorbach, S., & Hallett, M. (2004). Identifying true brain interaction from EEG data using the imaginary part of coherency. *Clinical Neurophysiology, 115*(10), 2292-2307. doi:10.1016/j.clinph.2004.04.029

Nunez, P. L., Srinivasan, R., Westdorp, A. F., Wijesinghe, R. S., Tucker, D. M., Silberstein, R. B., & Cadusch, P. J. (1997). EEG coherency .1. Statistics, reference trode, volume conduction, Laplacians, cortical imaging, and interpretation at multiple scales. *Electroencephalogr Clin Neurophysiol, 103*(5), 499-515. doi:Doi 10.1016/S0013-4694(97)00066-7

Nystrom, P. (2008). The infant mirror neuron system studied with high density EEG. *Soc Neurosci, 3*(3-4), 334-347. doi:10.1080/17470910701563665

Oakes, L. M., Madole, K. L., & Cohen, L. B. (1991). Infants Object Examining - Habituation And Categorization. *Cognitive Development, 6*(4), 377-392. doi:Doi 10.1016/0885-2014(91)90045-F

Oakes, L. M., & Tellinghuisen, D. J. (1994). Examining In Infancy - Does It Reflect Active Processing. *Dev Psychol, 30*(5), 748-756. doi:Doi 10.1037//0012-1649.30.5.748

Oostenveld, R., Fries, P., Maris, E., & Schoffelen, J. M. (2011). FieldTrip: Open source software for advanced analysis of MEG, EEG, and invasive electrophysiological data. *Comput Intell Neurosci, 2011*, 156869. doi:10.1155/2011/156869

Orekhova, E. V., Stroganova, T. A., & Posikera, I. N. (1999). Theta synchronization during sustained anticipatory attention in infants over the second half of the first year of life. *International Journal of Psychophysiology, 32*(2), 151-172. doi:Doi 10.1016/S0167-8760(99)00011-2

Orekhova, E. V., Stroganova, T. A., & Posikera, I. N. (2001). Alpha activity as an index of cortical inhibition during sustained internally controlled attention in infants. *Clin Neurophysiol, 112*(5), 740-749.

Pascual-Marqui, R. D., Lehmann, D., Koukkou, M., Kochi, K., Anderer, P., Saletu, B., . . . Kinoshita, T. (2011). Assessing interactions in the brain with exact low-resolution electromagnetic tomography. *Philos Trans A Math Phys Eng Sci, 369*(1952), 3768-3784. doi:10.1098/rsta.2011.0081

Paus, T. (2010). Growth of white matter in the adolescent brain: myelin or axon? *Brain Cogn, 72*(1), 26-35. doi:10.1016/j.bandc.2009.06.002

Pempek, T. A., Kirkorian, H. L., Richards, J. E., Anderson, D. R., Lund, A. F., & Stevens, M. (2010). Video comprehensibility and attention in very young children. *Dev Psychol, 46*(5), 1283-1293. doi:10.1037/a0020614

Perez-Edgar, K., McDermott, J. N., Korelitz, K., Degnan, K. A., Curby, T. W., Pine, D. S., & Fox, N. A. (2010). Patterns of sustained attention in infancy shape the developmental trajectory of social behavior from toddlerhood through adolescence. *Dev Psychol, 46*(6), 1723-1730. doi:10.1037/a0021064

Petersen, S. E., & Posner, M. I. (2012). The Attention System of the Human Brain: 20 Years After. *Annual Review of Neuroscience, Vol 35, 35*, 73-89. doi:10.1146/annurev-neuro-062111-150525

Power, J. D., Fair, D. A., Schlaggar, B. L., & Petersen, S. E. (2010). The development of human functional brain networks. *Neuron, 67*(5), 735-748. doi:10.1016/j.neuron.2010.08.017

Reynolds, G. D., Courage, M. L., & Richards, J. E. (2010). Infant attention and visual preferences: converging evidence from behavior, event-related potentials, and cortical source localization. *Dev Psychol, 46*(4), 886-904. doi:10.1037/a0019670

Reynolds, G. D., & Richards, J. E. (2005). Familiarization, attention, and recognition memory in infancy: an event-related potential and cortical source localization study. *Dev Psychol, 41*(4), 598-615. doi:10.1037/0012-1649.41.4.598

Reynolds, G. D., & Richards, J. E. (2009). Cortical Source Localization of Infant Cognition. *Developmental Neuropsychology, 34*(3), 312-329. doi:Pii 910996962 10.1080/87565640902801890

Reynolds, G. D. R., J.E. (2008). Infant heart rate: A developmental psychophysiological perspective. In L. A. S. S. J. Segalowitz (Ed.), *Developmental Psychophysiology* (pp. 173-210). Cambridge, UK: Cambridge Press.

Richards, J. E. (1989). Sustained Visual-Attention In 8-Week-Old Infants. *Infant Behavior & Development, 12*(4), 425-436. doi:Doi 10.1016/0163-6383(89)90024-6

Richards, J. E. (1989). Development And Stability In Visual Sustained Attention In 14, 20, And 26 Week Old Infants. *Psychophysiology, 26*(4), 422-430. doi:DOI 10.1111/j.1469-8986.1989.tb01944.x

Richards, J. E. (1997). Peripheral stimulus localization by infants: attention, age, and individual differences in heart rate variability. *J Exp Psychol Hum Percept Perform, 23*(3), 667-680.

Richards, J. E. (1997). Effects of attention on infants' preference for briefly exposed visual stimuli in the paired-comparison recognition-memory paradigm. *Dev Psychol, 33*(1), 22-31.

Richards, J. E. (2000). Localizing the development of covert attention in infants with scalp event-related potentials. *Dev Psychol, 36*(1), 91-108.

Richards, J. E. (2001). Cortical Indexes of Saccade Planning Following Covert Orienting in 20-Week-Old Infants. *Infancy, 2*(2), 135-157. doi:Doi 10.1207/S15327078in0202_2

Richards, J. E. (2003). Attention affects the recognition of briefly presented visual stimuli in infants: an ERP study. *Dev Sci, 6*(3), 312-328. doi:10.1111/1467-7687.00287

Richards, J. E. (2004). Development of covert orienting in young infants. In L. Itti, G. Rees, & J. Tsotsos (Eds.), *Neurobiology of attention* (pp. 82 - 88): Academic Press / Elsevier.

Richards, J. E. (2008). Attention in young infants: A developmental psychophysiological perspective. In C. A. Nelson & M. Luciana (Eds.), *Handbook of developmental cognitive neuroscience (2nd ed.).* (pp. 479-497). Cambridge, MA, US: MIT Press.

Richards, J. E. (2009). Attention in the brain and early infancy. In S. P. Johnson (Ed.), *Neoconstructivism: The new science of cognitive development* (Vol. 1). New York, NY: Oxford University Press.

Richards, J. E. (2010). The development of attention to simple and complex visual stimuli in infants: Behavioral and psychophysiological measures. *Developmental Review, 30*(2), 203-219. doi:10.1016/j.dr.2010.03.005

Richards, J. E., Boswell, C., Stevens, M., & Vendemia, J. M. (2015). Evaluating methods for constructing average high-density electrode positions. *Brain Topogr, 28*(1), 70-86. doi:10.1007/s10548-014-0400-8

Richards, J. E., & Casey, B. J. (1991). Heart-Rate-Variability during Attention Phases In Young Infants. *Psychophysiology, 28*(1), 43-53. doi:DOI 10.1111/j.1469-8986.1991.tb03385.x

Richards, J. E., & Casey, B. J. (1992). Development Of Sustained Visual-Attention In the Human Infant. *Attention And Information Processing In Infants And Adults*, 30-60.

Richards, J. E., & Cronise, K. (2000). Extended visual fixation in the early preschool years: look duration, heart rate changes, and attentional inertia. *Child Dev, 71*(3), 602-620.

Richards, J. E., & Holley, F. B. (1999). Infant attention and the development of smooth pursuit tracking. *Dev Psychol, 35*(3), 856-867.

Richards, J. E., & Hunter, S. K. (1997). Peripheral stimulus localization by infants with eye and head movements during visual attention. *Vision Research, 37*(21), 3021-3035. doi:Doi 10.1016/S0042-6989(97)00082-5

Richards, J. E., Sanchez, C., Phillips-Meek, M., & Xie, W. (2016). A database of age-appropriate average MRI templates. *Neuroimage, 124*, 1254-1259. doi:10.1016/j.neuroimage.2015.04.055

Richards, J. E., & Turner, E. D. (2001). Extended visual fixation and distractibility in children from six to twenty-four months of age. *Child Dev, 72*(4), 963-972.

Richards, J. E. X., W. (2015). Brains for all the ages: Structural neurodevelopment in infants and children from a life-span perspective. In J. Benson (Ed.), *Advances in Child Development and Behavior* (Vol. 48, pp. 1-52). Philadephia, PA: Elsevier.

Rubinov, M., & Sporns, O. (2010). Complex network measures of brain connectivity: uses and interpretations. *Neuroimage, 52*(3), 1059-1069. doi:10.1016/j.neuroimage.2009.10.003

Ruff, H. A. (1986). Components Of Attention during Infants Manipulative Exploration. *Child Dev, 57*(1), 105-114.

Ruff, H. A., & Lawson, K. R. (1990). Development Of Sustained, Focused Attention In Young-Children during Free Play. *Dev Psychol, 26*(1), 85-93. doi:Doi 10.1037//0012-1649.26.1.85

Sauseng, P., Hoppe, J., Klimesch, W., Gerloff, C., & Hummel, F. C. (2007). Dissociation of sustained attention from central executive functions: local activity and interregional connectivity in the theta range. *Eur J Neurosci, 25*(2), 587-593. doi:10.1111/j.1460-9568.2006.05286.x

Sauseng, P., Klimesch, W., Stadler, W., Schabus, M., Doppelmayr, M., Hanslmayr, S., . . . Birbaumer, N. (2005). A shift of visual spatial attention is selectively associated with human EEG alpha activity. *European Journal of Neuroscience, 22*(11), 2917-2926. doi:10.1111/j.1460-9568.2005.04482.x

Schoffelen, J. M., & Gross, J. (2009). Source connectivity analysis with MEG and EEG. *Hum Brain Mapp, 30*(6), 1857-1865. doi:10.1002/hbm.20745

Shattuck, D. W., Mirza, M., Adisetiyo, V., Hojatkashani, C., Salamon, G., Narr, K. L., . . . Toga, A. W. (2008). Construction of a 3D probabilistic atlas of human cortical structures. *Neuroimage, 39*(3), 1064-1080. doi:10.1016/j.neuroimage.2007.09.031

Smit, D. J., Boersma, M., Schnack, H. G., Micheloyannis, S., Boomsma, D. I., Hulshoff Pol, H. E., . . . de Geus, E. J. (2012). The brain matures with stronger functional connectivity and decreased randomness of its network. *PLoS One, 7*(5), e36896. doi:10.1371/journal.pone.0036896

Smit, D. J., de Geus, E. J., van de Nieuwenhuijzen, M. E., van Beijsterveldt, C. E., van Baal, G. C., Mansvelder, H. D., . . . Linkenkaer-Hansen, K. (2011). Scale-free modulation of resting-state neuronal oscillations reflects prolonged brain maturation in humans. *J Neurosci, 31*(37), 13128-13136. doi:10.1523/JNEUROSCI.1678-11.2011

Smith, S. M., Jenkinson, M., Woolrich, M. W., Beckmann, C. F., Behrens, T. E. J., Johansen-Berg, H., . . . Matthews, P. M. (2004). Advances in functional and structural MR image analysis and implementation as FSL. *Neuroimage, 23*, S208-S219. doi:10.1016/j.neuroimage.2004.07.051

Sporns, O., & Zwi, J. D. (2004). The small world of the cerebral cortex. *Neuroinformatics, 2*(2), 145-162. doi:10.1385/NI:2:2:145

Stam, C. J., de Haan, W., Daffertshofer, A., Jones, B. F., Manshanden, I., van Walsum, A. M. V., . . . Scheltens, P. (2009). Graph theoretical analysis of magnetoencephalographic functional connectivity in Alzheimers disease. *Brain, 132*, 213-224. doi:10.1093/brain/awn262

Stam, C. J., Nolte, G., & Daffertshofer, A. (2007). Phase lag index: Assessment of functional connectivity from multi channel EEG and MEG with diminished bias from common sources. *Human Brain Mapping, 28*(11), 1178-1193. doi:10.1002/hbm.20346

Thatcher, R. W., Walker, R. A., & Giudice, S. (1987). Human cerebral hemispheres develop at different rates and ages. *Science, 236*(4805), 1110-1113.

Thorpe, S. G., Cannon, E. N., & Fox, N. A. (2016). Spectral and source structural development of mu and alpha rhythms from infancy through adulthood. *Clinical Neurophysiology, 127*(1), 254-269. doi:10.1016/j.clinph.2015.03.004

Tzourio-Mazoyer, N., Landeau, B., Papathanassiou, D., Crivello, F., Etard, O., Delcroix, N., . . . Joliot, M. (2002). Automated anatomical labeling of activations in SPM using a macroscopic anatomical parcellation of the MNI MRI single-subject brain. *Neuroimage, 15*(1), 273-289. doi:10.1006/nimg.2001.0978

van den Heuvel, M. P., Kersbergen, K. J., de Reus, M. A., Keunen, K., Kahn, R. S., Groenendaal, F., . . . Benders, M. J. N. L. (2015). The Neonatal Connectome During Preterm Brain Development. *Cereb Cortex, 25*(9), 3000-3013. doi:10.1093/cercor/bhu095

Vertes, P. E., & Bullmore, E. T. (2015). Annual research review: Growth connectomics-- the organization and reorganization of brain networks during normal and abnormal development. *J Child Psychol Psychiatry, 56*(3), 299-320. doi:10.1111/jcpp.12365

Vinck, M., Oostenveld, R., van Wingerden, M., Battaglia, F., & Pennartz, C. M. (2011). An improved index of phase-synchronization for electrophysiological data in the presence of volume-conduction, noise and sample-size bias. *Neuroimage, 55*(4), 1548-1565. doi:10.1016/j.neuroimage.2011.01.055

Wang, J., Wang, X., Xia, M., Liao, X., Evans, A., & He, Y. (2015). GRETNA: a graph theoretical network analysis toolbox for imaging connectomics. *Front Hum Neurosci, 9*, 386. doi:10.3389/fnhum.2015.00386

Wang, J. H., Zuo, X. N., Gohel, S., Milham, M. P., Biswal, B. B., & He, Y. (2011). Graph Theoretical Analysis of Functional Brain Networks: Test-Retest Evaluation on Short- and Long-Term Resting-State Functional MRI Data. *PLoS One, 6*(7). doi:ARTN e21976

10.1371/journal.pone.0021976

Watts, D. J., & Strogatz, S. H. (1998). Collective dynamics of 'small-world' networks. *Nature, 393*(6684), 440-442. doi:Doi 10.1038/30918

Webb, S. J., Long, J. D., & Nelson, C. A. (2005). A longitudinal investigation of visual event-related potentials in the first year of life. *Developmental Science, 8*(6), 605-616. doi:DOI 10.1111/j.1467-7687.2005.00452.x

Welch, P. (1967). The use of fast Fourier transform for the estimation of power spectra: a method based on time averaging over short, modified periodograms. *IEEE Transactions on audio and electroacoustics, 15*(2), 70-73.

Westlye, L. T., Walhovd, K. B., Dale, A. M., Bjornerud, A., Due-Tonnessen, P., Engvig, A., . . . Fjell, A. M. (2010). Life-Span Changes of the Human Brain White Matter: Diffusion Tensor Imaging (DTI) and Volumetry. *Cereb Cortex, 20*(9), 2055-2068. doi:10.1093/cercor/bhp280

Wolff, J. J., Gu, H., Gerig, G., Elison, J. T., Styner, M., Gouttard, S., . . . Network, I. (2012). Differences in white matter fiber tract development present from 6 to 24 months in infants with autism. *American Journal of Psychiatry, 169*(6), 589-600. doi:10.1176/appi.ajp.2011.11091447

Xie, W., Mallin, B. M., & Richards, J. E. (2017). Development of infant sustained attention and its relation to EEG oscillations: an EEG and cortical source analysis study. *Dev Sci*. doi:10.1111/desc.12562

Xie, W., & Richards, J. E. (2016). The Relation between Infant Covert Orienting, Sustained Attention and Brain Activity. *Brain Topography, 1*, 1-22. doi:10.1007/s10548-016-0505-3

Xie, W., & Richards, J. E. (2016). Effects of interstimulus intervals on behavioral, heart rate, and event-related potential indices of infant engagement and sustained attention. *Psychophysiology, 53*(8), 1128-1142. doi:10.1111/psyp.12670

Yeo, B. T. T., Krienen, F. M., Sepulcre, J., Sabuncu, M. R., Lashkari, D., Hollinshead, M., . . . Buckner, R. L. (2011). The organization of the human cerebral cortex estimated by intrinsic functional connectivity. *J Neurophysiol, 106*(3), 1125-1165. doi:10.1152/jn.00338.2011

Zhang, Z. Q., Liao, W., Chen, H. F., Mantini, D., Ding, J. R., Xu, Q., . . . Lu, G. M. (2011). Altered functional-structural coupling of large-scale brain networks in idiopathic generalized epilepsy. *Brain, 134*, 2912-2928. doi:10.1093/brain/awr223